UNIVERSITY OF OKLAHOMA

GRADUATE COLLEGE

INVESTIGATION OF THE EFFECTS OF END REGION DETERIORATION IN

PRECAST, PRESTRESSED CONCRETE BRIDGE GIRDERS

A THESIS

SUBMITTED TO THE GRADUATE FACULTY

in partial fulfillment of the requirements for the

Degree of

MASTER OF SCIENCE

By

DARION MAYHORN
Norman, Oklahoma
2016

INVESTIGATION OF THE EFFECTS OF END REGION DETERIORATION IN
PRECAST, PRESTRESSED CONCRETE BRIDGE GIRDERS

A THESIS APPROVED FOR THE
SCHOOL OF CIVIL ENGINEERING AND ENVIRONMENTAL SCIENCE

BY

_____
Dr. Royce Floyd, Chair

_____
Dr. Chris Ramseyer

_____
Dr. Jeffery Volz

Dedication

This thesis is dedicated to my mom for establishing a love for learning within me, and for proving that slow and steady wins the race.

I also dedicate this thesis to my family and friends who've provided encouragement and support on this journey.

Acknowledgements

First, I would like to express my gratitude to my advisor Dr. Royce Floyd for the continuous support throughout this research effort. I appreciate the guidance, patience, and knowledge provided during this undertaking. I aspire to be as well rounded, and hard-working while managing to always seem at ease.

I would also like to thank the rest of my thesis committee: Dr. Chris Ramseyer and Dr. Jeffery Volz. I'd also like to thank Dr. Jinsong Pei for encouraging me to pursue a thesis while working on my graduate coursework here at OU.

I'm forever grateful for my initial research opportunities at Saint Louis University under Dr. Hindi, and Argonne National Laboratory under Dr. Ben O'Connor & Dr. Dave Murphy.

I'm truly appreciative of the financial support from my employer, the Bureau of Reclamation. As well as the emotional support from my supervisors and coworkers.

I would like to thank the Southern Plains Transportation Center for funding the larger project from which this thesis evolved.

Last but not least, I'd like to thank my family and friends for being nothing short of amazing, for always encouraging me to strive for my very best, and for always expecting me to live to my full potential.

Table of Contents

List of Tables

List of Figures

ix

xiii

Abstract

An important factor in life expectancy of concrete bridges is the effect of corrosion of reinforcing steel on concrete and appurtenant embedded materials. New bridges, though continuously exposed to the elements, are expected to last roughly 75 years. Particularly important for aging infrastructure is determining methods to rehabilitate a structure where complete replacement may not be a feasible option. This research is intended to build on the current body of knowledge surrounding corrosion related deterioration of prestressed concrete girders due to extreme environments. Nine prestressed half-scale AASHTO Type II girders were constructed that replicated girders from a bridge recently taken out of service (from I-244 in Tulsa County), which was representative of a large number of aging bridges in the state of Oklahoma. Two different girder designs, corresponding to the different prestressing strand configurations used in the original bridge were utilized. One end region of each girder was exposed to a corrosion accelerant process, and three different exposures were used to illustrate varying environmental conditions. The end regions of six girders were shear tested, after damage by corrosion, to provide an understanding of the effects of end region deterioration on strand anchorage and shear capacity. Measured shear values were less than the nominal design shear capacity (ACI and AASHTO LFRD 2007 methods) for each girder. All of the girder ends that had been exposed to the corrosive environment had a larger measured shear than the control end, except for one girder (C2). Of the six shear tests on the corroded end of the girders, four resulted in slip of the prestressing strands prior to the initial crack of the beam. For the control end of the girders, all six shear tests illustrated cracking of the girder prior to the initiation of slip.

Concurrently with the lab experiments, this research included visiting and inspecting similar bridges as those used in the design for the lab experiment (prestressed concrete bridges with AASHTO Type II girders) to identify varying levels of deterioration due to corrosion. Over the course of 19 site visits, the following deterioration characteristics were identified: corroded bearing plates; corroded anchor bolts and nuts; spalling above the support; exposed rebar and prestressing strands; diagonal cracking of the back corner of the girder; vertical cracking along the girder and diaphragm interface; diagonal cracking from the top flange and web interface; and diaphragm deterioration. Together, the observations from the field inspections and the lab experiments were used to analyze existing retrofit methods and determine recommendations for in-situ rehabilitation for varying levels of deterioration.

While the research does not provide a final solution, the results are expected to provide more breadth in our understanding of prestressed concrete, shear design, effects of corrosion and methods to rehabilitate aging infrastructure.

1 Introduction

1.1 Prestressed Concrete

Prestressed concrete can be traced back to the late 1800s, when P.H. Jackson received the very first patent in the United States for his prestressed concrete design (Dinges, 2009). Five thousand miles away, also in the late 1800s, C.W. Doehring in Germany obtained a patent for prestressing slabs with metal wires (Nawy, 2010). Then in the 1920s and 1930s, Eugene Freyssinet introduced the concept of utilizing high-strength steels for prestressed concrete design. In 1948, Gustave Magnel wrote the first book on prestressed concrete design (Dinges, 2009), and in the 20th century, American engineer T.Y. Lin greatly simplified the prestressed concrete design with his load-balancing method (Nawy, 2010). A number of other innovations were made in prestressed concrete construction throughout the 20th century and prestressed concrete girders are currently widely used for bridge construction in the United States.

1.1.1 Differences between Prestressed Concrete and Reinforced Concrete

Traditional reinforced concrete utilizes the best properties of both steel (tension) and concrete (compression) in structural systems to resist loading. The compressive strength of the concrete resists compressive stresses due to bending at the top of the component if the member is subjected to positive bending as shown in Figure 1. By itself, concrete's low tensile strength causes the component (e.g., beam or slab) to crack when the tensile stresses introduced due to bending exceed the tensile capacity of the concrete, which can lead to sudden failure. To help the component resist tensile stress and cracking, reinforcing steel is placed at the bottom of the component as Figure 1 illustrates in a theoretical interpretation of reinforced concrete beam design.

1
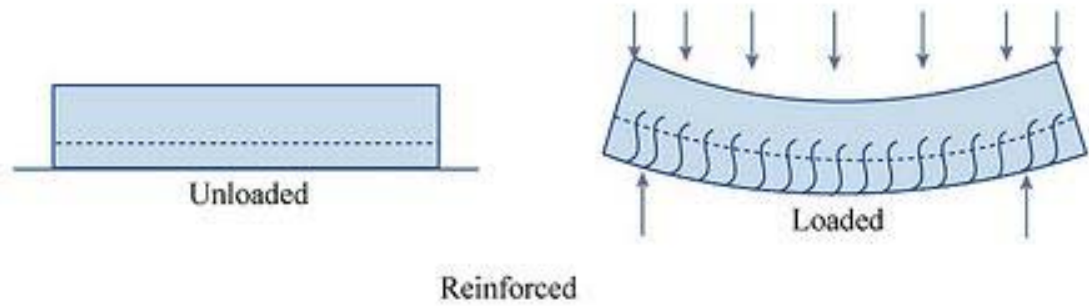
Figure 1. Typical reinforced concrete beam schematic (MIT OpenCourseWare, 2008)

Prestressed concrete takes a more direct approach to resist loading. The theory of prestressed concrete relies on providing an internal bending counteractive to the bending caused by external loads. A prestressing force is created using high tensile strength strands in the longitudinal direction that are tensioned and then released to the concrete, thereby inducing a bending stress and curvature that counteracts bending from external loads. Prestressed concrete can be pre-tensioned (tensioning of the strands before the concrete sets) or post-tensioned (tensioning after the concrete sets) to create the required prestressing force. When the component is loaded, the component theoretically returns to a straighter shape. The induced compressive stress from the prestressing force also contributes to the beam's shear capacity. Figure 2 illustrates a theoretical interpretation of prestressed concrete beam design.
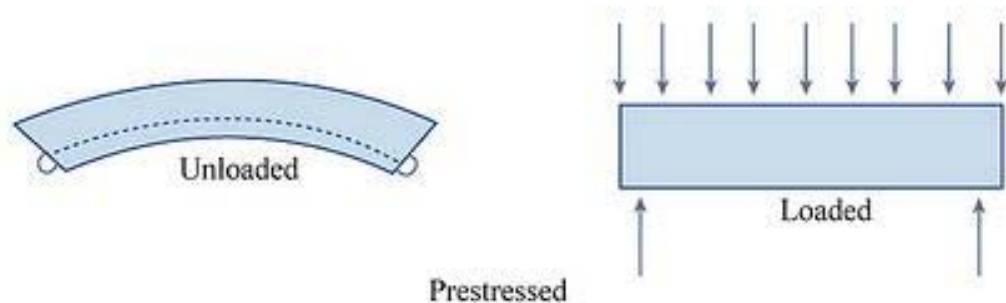
Figure 2. Typical prestressed concrete beam schematic (MIT OpenCourseWare, 2008)

In principle, prestressed concrete differs from reinforced concrete in its ability to influence a system's properties (e.g., flexible/rigid) without altering its strength. A prestressed member requires roughly 20% less depth and reinforcement than a comparably designed reinforced concrete member with the same design strength (Nawy, 2010). The reduction in size of members reduces the weight of the structure and the required size of foundations. Prestressed concrete has also been found to have a lower lifetime cost due to reduced maintenance costs (e.g., fewer joints) (Nawy, 2010).

The advancement in high strength steel strands has led to a substantial growth in the field of prestressed concrete. Prestressed concrete is used in buildings, tanks, oil drilling platforms, power stations, and bridges. The lighter foundations and longer spans associated with prestressed concrete provide more flexibility in design when compared to typical reinforced concrete. Nawy (2010) states that "very large spans such as segmental bridges or cable-stayed bridges can *only* be constructed [with concrete] through the use of prestressing."

1.2 Relevance of Research

For prestressed concrete girders, the end zones play an integral part in the overall function of the design. In the end zones of pretensioned girders, the load is transferred to the beam through bond between the prestressing strands and the concrete. This force distribution process, coined the prestress transfer, requires higher concentrations of mild steel reinforcement in the end zone region to resist bursting stresses resulting from the prestress transfer as well as high shear loading. Along with being important for the prestress transfer process, the end zone region is subjected to the largest shear demand. Finally, the end zone regions are subjected to high compressive stress resulting from the

3

prestressing force, specifically areas past the transfer length where the full prestress is applied, since the moments due to dead load in these regions are small.

Bridges designed 30-50 years ago typically used the American Association of State Highway and Transportation Officials (AASHTO) Standard Specifications to design prestressed girders. In the past, AASHTO recommended a "quarter-point rule" for shear design, which often produced a less conservative design than the current specifications. The "quarter point rule" considered the critical section for shear to be at a quarter (1/4) of the span length, and all sections between the end and the quarter point were designed using the applied shear from the quarter point. The current AASHTO Load and Resistance Factor Design (LRFD) Specifications are more conservative and specify that the critical section for shear be closer to the supports than the quarter-point of the span (e.g., h/2, h/8). This change in design codes has a large impact on shear demand from the quarter span point to the nearest end. Thus the shear capacity in the end zone regions of older bridges are influenced by the previous, less conservative design code. Figure 3 illustrates an example of the shear diagram for a simply supported beam with an applied distributed load; the span points h/2 and L/4 are highlighted to illustrate the difference in applied shear at critical locations for shear design.
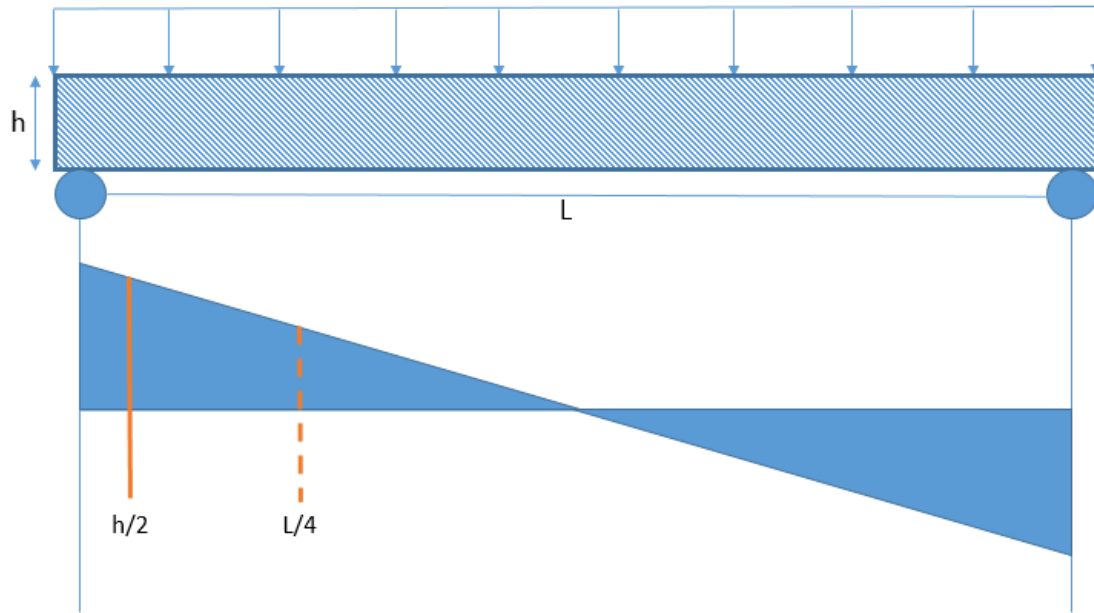
Figure 3. Shear diagram of distributed load on a simply, supported beam

Practicing engineers should be extremely mindful of the operation and maintenance of a structure when designing. Prestressed concrete girders require high percentages of mild steel reinforcement in girder end zones to resist shear loading and bursting stresses from the prestress transfer. These regions are particularly important because any damage in this region could have a lasting impact on the girder's overall strength as well as shear capacity. The girder end zone region's high percentage of steel provides more susceptibility to corrosion since this region is often near the joints of the bridge deck which provides a path for seepage and chlorides from deicing salts to reach the girder ends.

As our population increases, city planners and engineers are tasked with creating and maintaining infrastructure capable of withstanding the increase. Naturally, one can engineer for capacity or human-induced actions. It is more difficult to properly plan and engineer for the natural environment and human-actions taken as a result of the

5

environment. New bridges, though continuously exposed to the elements, are expected to last approximately 75 years. An important factor in life expectancy of concrete bridges is the effect of corrosion on concrete and appurtenant embedded materials. Corrosion can quickly deteriorate a structure, causing it to lose its strength and designed purpose. Corrosion in the aforementioned end zone regions has the potential to affect shear capacity through deterioration of the concrete and affecting the transfer of prestress by decreased bonding between the strands and the concrete.

Corrosion is the natural process by which metals are drawn to exist in their more-natural metallic compound state (e.g., oxide). In order for corrosion to take place there are three necessary components: an electrolyte, oxygen, and a material capable of supplying electrons. The reaction typically starts at the surface of the metal; there is a visible aspect of corrosion typically described as rusting. Once the steel embedded in concrete begins to corrode, and deteriorate, it typically expands since the corrosion products occupy a larger volume than the original metal. That expansion causes cracking which allows the steel to be exposed to even more elements (e.g., air, water) to further accelerate the corrosion process. Corrosion impacts the concrete member in many ways, with one being the loss of strength of the steel embedded in the concrete as it deteriorates. It is important to note that corrosion of steel occurs fastest in steel that is stressed (i.e., has a load on it). In order to prevent corrosion, many structures are now coated with materials to prevent/delay the ability of the corrosion process to occur. In the mid-1900s, an epoxy was not applied to reinforced steel, and almost certainly never applied to prestressed strands.

Along with natural impacts to our infrastructure, nationwide, it is simply aging. Much of the infrastructure was constructed over 65 years ago, and is now nearing the end of its expected design life. Increased scrutiny on public spending, along with the magnitude of concerns (i.e., deterioration of, and increased demand on infrastructure), creates a disastrous recipe when considering replacement of much of the aging infrastructure. In order to still be effective, planners are looking at rehabilitation as the best option, especially in a climate not very supportive of large-scale, large-dollar replacement projects.

The ability to better design structures to mitigate the effects of corrosion is important. However, in order to do so, more research is necessary on prestressed concrete and corrosion, and opportunities are needed to perform in-situ rehabilitation. The research described in this thesis is intended to expand on the current body of knowledge surrounding corrosion of prestressed concrete girders due to extreme environments, with particular focus on how end zone deterioration ultimately affects the girder's shear capacity.

2 Literature Review

2.1 Corrosion and Concrete

For decades, engineering researchers have been developing methods to mitigate the occurrence and effects of corrosion in prestressed concrete structures. As defined by Fasl et al. (2016), "corrosion is an electrochemical process that causes localized or uniform section loss in a metallic element, reducing the element's cross-sectional area and overall strength." Corrosion of steel in concrete, as discussed, can cause many concerns including cracking, delamination, and spalling of the concrete. In perfect conditions, the steel embedded in concrete is protected from elements causing corrosion by the alkalinity of the surrounding concrete. However, the following are major factors that influence the susceptibility of steel to corrosion: permeability of the concrete, degree of cracking, drainage, environmental conditions, surface treatment, structural geometry, concrete quality, and concrete cover (Basham, 2015; Coggins & French, 1990). According to Chou and Hover (1987), industry and governing bodies in building codes and specifications reflect this concern by requiring concrete cover and chloride control. One major consequence of corrosion in concrete is the potential for reduction of the live load capacity. This capacity is impacted by both the reduction of the steel cross-section and loss of bonding between the concrete and steel. In a study focused on deterioration of prestressed concrete bridge beams, Bruce et al. (2008) concluded that corrosion in prestressing strands reduces the structural performance of a beam faster than corrosion exhibited in conventional reinforced beams because a larger proportion of the steel cross-section is lost. Szilard (1969) emphasized that prestressing steel is also subjected to significantly higher stresses with smaller diameters in relation to conventional reinforcement.

8

Vu et al. (2005) found that concrete cover and w/c were good predictors for performance of chloride contaminated concrete related to cracking. The researchers found that generally "the rate of crack propagation decreases as concrete quality increases."

2.2   Susceptibility of Bridges to Corrosion

Chlorides are particularly damaging for concrete and appurtenant embedded materials. Mukherjee and Rai (2009) state that "corrosion of steel reinforcement, both prestressing tendons and non-prestressed rebars, caused by infiltration of de-icing agents, is one of the primary sources of a structure's deterioration." Song and Shayan (1998) hypothesized that chlorides could be introduced to concrete through some of the following methods: use of chloride as an accelerant; use of water containing chloride, contaminated aggregates, sea salt spray; and use of chemicals and de-icing salts. A survey of bridges used in salt de-icing environments illustrated that the majority of chloride-induced corrosion over time was due to "chloride-laden water" from the bridge deck that trickled through expansion joints, cracks in the deck concrete overlay, and inadequately designed concrete cover (Novokshchenov, 1989). Smith and Virmani (2000) of the Federal Highway Administration noted the ability to minimize the number of deck joints as a means to reduce the availability of seepage paths for chlorides to reach a bridge's superstructure and substructure. The report notes that "bridges as long as 850 m (2800 ft) have been constructed without joints except at the abutments" (Smith & Virmani, 2000). This provides evidence that the 21st century design engineer must take care to not only create a beautiful system, but one that will also stand the test of time and the environment.

While researching chloride ion distribution in 20-year-old prestressed concrete girders in Minnesota, Coggins and French (1990) found that the only evidence of strand corrosion was observed at the ends of the beams. In these cases, "the mortar coating had spalled from the strand ends due to weathering or drainage at the deck joints." They also found that chloride levels were higher on the side of interior beams facing oncoming traffic than exterior beams of the same direction through a detailed examination and performing a chloride ion penetration analysis on samples from girders (Coggins & French, 1990). The authors concluded that girders facing oncoming traffic contained greater concentrations of chlorides since "oncoming traffic carries salts toward the bridge in a mist or spray form." The authors attributed the exterior beam to have lower chloride concentrations due to the salts being washed away from the exposed face by rain.

2.3   Reduced Capacity of Corroded Members

Several recent studies have investigated the capacity of decommissioned bridge beams with corrosion damage. Rogers et al. (2012) performed destructive tests on 19 decommissioned pretensioned concrete bridge beams from a 1969 bridge that had corroded pretensioned reinforcement. The researchers found that the 40-year old beams exhibited chloride-induced corrosion from sea spray. The results from the destructive tests indicated that "the most severely corroded beam sustained 69% of the load of an equivalent good-condition beam." ElBatanouny et al. (2014) found that pitting corrosion in prestressed strands caused a reduction in residual capacity in only 140 days - concluding that crack width was an important factor in "the formation and intensity of pitting in terms of pit depth." By load testing, ElBatanouny et al. found that the most

corroded member had a tested capacity of 86.7% when compared to the original control specimen.

Pape and Melchers (2013) found that as the degree of corrosion loss in the prestressing strands increased, then the maximum capacity of the girder decreased linearly. In determining the performance of three 45-year-old corroded prestressed concrete beams, the researchers concluded that using current design theory, estimated material properties, and neglecting cracking and corrosion damage, ultimately overestimates the actual capacity of the beams. In one beam, Pape and Melchers found that a 64% loss in prestressing cross-sectional area due to corrosion at the failure location contributed to a 49% reduction in original, theoretical design capacity.

Cai and Miao (2015) state that load capacity degradation is "due to the increasing age of the structural components and the aggressive environment bridge structures are exposed to." Abosrra et al. (2011) found that the first day of corrosion acceleration caused a slight increase in steel/concrete bond strength, but after 7 and 15 days of corrosion acceleration, there was significantly reduced steel/concrete bond strength.

2.4   Factors Influencing Shear Capacity

As stated in the introduction, for prestressed concrete girders, the end zones play an integral part of the overall function of the design. The end zone regions are where the prestress transfer from the steel to the concrete takes place. The prestress changes the stress state in the concrete, and as a result the prestress ultimately affects the shear capacity. The transfer length defines the extent of the bonding between the concrete and prestressing strands where less than the full prestress is applied to the beam. This transfer length, should it be reduced, could have adverse impacts on the shear capacity

11

by changing the state of stress from that which was used to calculate the shear capacity at a given section. Also in the end zone regions, it is typical to have transverse steel reinforcement stirrups that provide additional shear capacity. Ultimately, corrosion impacting the bonding of the prestressing strands in this region, or the deterioration of the transverse steel, can reduce the shear capacity of the girder.

2.5   Effect of Cracking at the End of Prestressed Members

During fabrication of prestressed concrete girders, there arises the possibility for cracking at the ends of the members when tensile stresses caused by the prestress force exceed the tensile strength of the concrete. A study performed for the Oklahoma Department of Transportation (ODOT) described "Y" cracking of the bottom flange to be the most serious form of end-region cracking. "Y" cracks are described as splitting cracks that "form at or near the bottom flange-web interface and are oriented vertically at the end face of the girder" (Merrill et al., 2005). Figure 4 is an example of "Y" cracks on the end face of a girder.
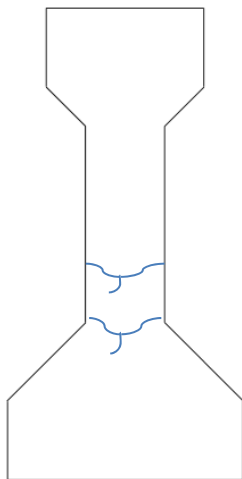
Figure 4. Example of "Y" cracks

The report states that "Y" cracks result from a "combination of lateral eccentricity of prestressing force and propagation of horizontal web-splitting cracks", which "create planes of weakness adjacent to columns of prestressing steel ends in the bottom flange." The report also states that "quantification of the increase in transfer length or corrosion of reinforcement due to end-region cracking has proven difficult, as have the in-place effects of such corrosion on structural capacity." The literature review for this study showed that "debonding up to 25 percent of strands has the most significant effect on reducing end-region stress concentration and "Y" cracking." The behavior of end zones is of interest, as other state DOTs are investigating cracking at prestressed girder ends (Transportation Research Board, 2016).

The ODOT study also found that end-region cracking that parallels the prestressed reinforcement "is more likely to affect structural capacity than cracking perpendicular to the reinforcement" (Merrill et al., 2015). The authors go on to state that loss of confining bond, leads to "longer transfer length or increased strand corrosion along the crack." Researchers found that corrosion of primary bottom prestressing strands was more likely to affect structural capacity than corrosion of draped strands or mild steel reinforcement. The greatest amount of moisture from deicing salts typically drips onto the girder end face.

2.6   Methods to Repair and Strengthen Prestressed Concrete Girders

It is particularly important for maintenance of aging infrastructure to determine rehabilitation methods for a structure when complete replacement may not be a feasible option. As stated by Cai and Miao (2015), bridges are the "backbones of the highway system [and] must be maintained and preserved to ensure safety to the traveling public."

Almusallam (2001) stated that the "degree of reinforcement corrosion and the resulting

decrease in the load-carrying capacity of both steel bars and the structural component

need to be evaluated to assess the residual strength of concrete and formulate repair

strategies." The NCHRP 654 report recommends that cracks less than 0.012 inches

width need not be repaired, with incremental repair strategies for cracks of widths

greater than 0.012 inches. Those repair strategies could include epoxy injection and

application of surface sealants. However, the NCHRP 654 report recommends

"different acceptable crack widths based on severity of the bridge's exposure

conditions, with a width limit of 0.007 inches in girders subject to deicing chemicals."

Ideally, before repair, one would want to know how to prevent an issue with their

infrastructure. In general, corrosion prevention methods can be divided into electrical

and non-electrical methods. Pritzl et al. (2014) consider non-electrical methods to

include "coatings, sealers, and corrosion inhibiting admixtures." The researchers stated

that cathodic protection is an electrical approach "that can be used to prevent corrosion

by shifting the reinforcing steel into a protected state." Pritzl et al. found that "surface

treatments (coatings) applied to the end zones of precast/prestressed concrete bridge

girders at the time of construction can successfully prevent beam end corrosion."

Darwin et al. (2002) found that methods to reduce corrosion of reinforcing steel were

divided into two categories: methods that slow the initiation of corrosion, and methods

that lengthen the corrosion period. Darwin et al. defines the corrosion period as "the

time between the initiation of corrosion and the end of service life." The primary

corrosion protection systems used for bridges have involved epoxy-coated

reinforcement, and increased cover over reinforcing bars since the mid-1970s (Darwin

et al., 2012). Mukherjee and Rai (2009) proposed that replacing metallic reinforcement

and strands with fiber reinforced polymer (FRP) materials may be a more positive

solution. The researchers state that FRP materials "significantly increases the bridge

life" and the increased costs of the non-metallic reinforcement may be justified.

One repair material that has proven successful for repair of structural damage is FRP.

Some of the major benefits of FRP include: "high strength to weight ratio, high fatigue

endurance, excellent corrosion resistance, low thermal expansion, and the ease of

fabrication, manufacturing, handling, and installation" (Cai and Miao, 2015). FRP is

available in many forms, the two most common are laminates and bars. Cai and Miao

found that structural systems strengthened with externally bonded FRP laminates

"combine the benefits of mechanical properties of FRP composites, the compressive

characteristics of concrete, and the ductility and deformation capacity of steel" –

thereby improving the load capacity of the structure. A technical bulletin by the

International Federation for Structural Concrete discussed design advantages of using

externally bonded FRP reinforcement in reinforced concrete structures. Those

advantages included: delaying crack formation in the shear span, improving

serviceability and durability due to reduced cracking, improving the shear resistance of

members, and achieving "greater structural efficiency as the neutral axis remains at a

lower level in the prestressed case" (International Federation for Structural Concrete,

2001).

ElSafty (2013) explored the potential of carbon fiber reinforced polymer (CFRP)

systems for impact-damaged girders. While ElSafty was concerned with flexural

capacity of impact-damaged girders, there is potential for the CFRP retrofit to improve

shear capacity of girders exhibiting induced deterioration as well. ElSafty concluded that CFRP systems "can be designed to restore lost flexural capacity, possibly enhance the original capacity and maintain the desired failure mode." He concluded that the outcome of the project would contribute to "savings of millions of dollars in repairing damaged prestressed concrete girders."

Higgins et al. (2012) focused on the use of CFRP systems for increasing shear strength of reinforced concrete girders. They found that repair systems for shear using discrete CFRP strips "provided a significant increase in ultimate strength capacity compared to unrepaired members." They also caution that repairing for shear using CFRP "must recognize the impact of the increased shear capacity on the flexural demands to prevent anchorage failures at poorly detailed flexural bar cutoff and anchorage locations." Higgins et al. concluded that it was possible to increase a member's shear strength using a "targeted repair approach applying CFRP material only to a critical section rather than over the entire member." It was also concluded that the addition of longitudinal CFRP strips "did not increase shear capacity due to debonding and bending of fibers at the poorly constrained diagonal cracks."

CFRP U-wraps are another potential application of CFRP material for repair. CFRP U-wraps are when the FRP is applied continuously around the sides and bottom face of the beam in a "U shape." Ray et al. (2011) suggest that CFRP U-wrapped anchors should be placed close to the initiation point of debonding so that its resistance can be activated before significant debonding has occurred. The researchers include that debonding initiates from a flexural or flexural-shear crack that forms near the load application

point; the crack propagates downward at a 30 degree angle, where the U-anchor should

be placed to maximize the total load-carrying capacity.

3   Experimental Design

The literature review yielded the following conclusions: there are many factors that cause steel to be susceptible to corrosion – including cracking at the end of prestressed members during fabrication. Corrosion impacting embedded steel within concrete can affect the prestressed member's live load capacity through deteriorated reinforcement steel, and can affect shear capacity through reduced bonding of prestressed strands and the concrete; however, there are methods to repair and strengthen prestressed concrete girders including those still in-service.

This research effort intends to build on the existing body of literature by investigating the effect of varying levels of corrosion on shear capacity. The literature review also yielded that much of the focus on repair materials for prestressed concrete girders have been for maintaining flexural capacity, or for repairing damage to the girders from impacts.

3.1   Objectives

The goal of this research is to expand on the current body of knowledge surrounding corrosion of prestressed concrete girders due to extreme environments, with particular focus on how end zone deterioration ultimately affects the girder's shear capacity.

After examining the current literature available, four objectives were defined. A typical corrosion condition for a prestressed concrete bridge girder includes exposed and potentially visible delamination of reinforcement, and spalling concrete. One particular area of interest is how specific levels of corrosion in pretensioned girders affect different attributes of the structure (e.g. initial corrosion may affect the bonding of steel and concrete, while more advanced corrosion may impact the capacity of the

reinforcement steel itself). Based on this work it is believed that for aged infrastructure, repair and strengthening of members for shear capacity may be achieved with externally bonded fiber-reinforced polymer sheets.

The objectives of the research were to:

1. Conduct quantitative and qualitative analyses on the effect of end zone deterioration (i.e., corrosion-induced) on the prestress force and shear capacity.

2. Conduct quantitative and qualitative analyses on the effect of end zone deterioration on bonding of the concrete and embedded materials.

3. Develop a procedure for visual inspection of end regions of AASHTO girders, with recommendations on relating end region deterioration to reduced strength.

4. Conduct quantitative and qualitative analyses on the effects of repair material on heavily corroded sections of members. Ideally, relating the necessary material for repair to the level of deterioration.

3.2   Methodology

This research project is divided into two sections: lab experiments and field inspections. Lab experiments to accelerate corrosion in girder end regions of prestressed concrete girders took place over the course of the research project. The prestressed girders used were approximately half-scale AASHTO Type II girders that replicate girders from a bridge taken out of service in 2013 (I-244 bridge over the Arkansas River in Tulsa County) and tested by other graduate students in the research group. This bridge was representative of a large number of aging bridges in the state of Oklahoma. Two different girder designs, corresponding to the different prestressing strand configurations used in the bridge were examined. Nine girders were constructed with an

emphasis on consistency with the original design and engineering properties. One end

region of each girder was exposed to an accelerated corrosion process. There were three

different levels of corrosion exposure applied to all nine girders to illustrate varying

environmental conditions (e.g., 2 months of exposure to two girders to be tested in the

deteriorated state and one to be retrofitted in a later effort). Six of the girders were shear

tested with end zone deterioration, and a retrofit of fiber-reinforced polymer sheets was

designed for the remaining three girders. For the six girders, the shear testing helps

provide an understanding of the effects of end region deterioration on strand anchorage

and shear capacity. Concurrently with the lab experiments, efforts were placed on

visiting and inspecting similar bridges to those used in the research project (prestressed

concrete bridges with AASHTO Type II girders constructed in the 1960s and 1970s) to

identify varying levels of visible deterioration due to corrosion. Together, the

observations from the field inspections and the lab experiments were used to analyze

the effects of corrosion on ends of prestressed, precast concrete girders to inform

recommendations for in-situ rehabilitation based on the varying levels of deterioration.

3.2.1   Laboratory Experiments

For the laboratory experiments, the following occurred: construction of the prestressed

concrete girders, end zone deterioration of those girders through the use of an

accelerated corrosion setup, shear testing of the girders, and finally a discussion of a

potential retrofit design option.

3.2.1.1   Prestressed Concrete Girder Specimens

The prestressed concrete girders were designed to be half-scale AASHTO Type II

girders while maintaining similar properties (concrete compressive strength, stress state,

etc.) as the full-scale decommissioned I-244 bridge from Tulsa, Oklahoma. Since shear

capacity in prestressed concrete beams is affected by the effective prestress, the beam

designs were developed by determining the stress states for the full-scale

decommissioned girders and adjusting the prestress configuration for the half-scale

girders to obtain service level stress states equivalent to the full-scale girders within an

acceptable range. Using a design spreadsheet based on the ACI and AASHTO methods,

developed by another graduate student, the girders were designed through multiple

iterations (Cranor, 2015). The girders were designed to replicate two girder designs,

Beam "A" and Beam "C", from the original design drawings of the decommissioned

bridge. The design spreadsheet considered the concrete stress at release and in service.

Reinforcing steel was also designed to follow the reinforcement configuration of the

original Beam "A" and Beam "C" girders from the drawing set provided by the

Oklahoma Department of Transportation (see appendix for rendering of Beam "A" and

Beam "C", as well as screenshots of the design for the girders constructed for this

thesis).

After many iterations, the half-scale girder design yielded the closest stress values when

harped prestressing strands were used. However, the prestressing bed at Fears Lab

placed limitations on construction that would prevent the ability to use harped

prestressing strands. The girder designs were updated to account for different

prestressing strands locations with emphasis on non-draped designs, transformed

section calculations, and stress equivalence in the stress in service category.

The final design included two ½ in. special strands located at 4 in. from the bottom of

the section with a 186 ksi prestress for the "Girder A" design and two 0.6 in. strands at

4 in. with a 202.5 ksi prestress for the "Girder C" design, both using No. 3 shear stirrup bars. The design called for at least 2 in. of center-to-center spacing between the two prestressing strands. The design also considered pretensioned anchorage zones and consistent concrete-to-steel shear strength contribution ratios. For the full-scale Beam "A", it was approximated to be 30% concrete to 70% steel, similarly, for the full-scale Beam "C" it was approximated to be 29% concrete to 71% steel. Using the design spreadsheet, the concrete-to-steel ratios were determined through determination of the transverse steel spacing and bar sizes. The concrete-to-steel strength contribution ratios at ¼ of the span from the support and h/2 from the support, the critical sections in the various design codes, are presented in Table 1 and Table 2.

Table 1. Concrete-to-steel strength contribution ratios for Girder A design

	Beam "A" (full scale ODOT)		Girder A (half-scale test specimen)	
	L/4	h/2	L/4	h/2
Concrete Contribution	31%	28%	26%	26%
Steel Contribution	69%	72%	74%	74%

Table 2. Concrete-to-steel strength contribution ratios for Girder C design

	Beam "C" (full scale ODOT)		Girder C (half-scale test specimen)	
	L/4	h/2	L/4	h/2
Concrete Contribution	29%	29%	19%	18%
Steel Contribution	71%	71%	81%	82%

Also using the design spreadsheet, the girders were designed to have a stress state similar to the stress state of the original Beams "A" and "C" with a specific focus on the in-service compressive stress, which has the largest impact on shear capacity. The in-service stresses were based only of the effects of prestress and dead load. Table 3 and Table 4 present the concrete stress values at release and in service. When the formwork for the girders was constructed, the depth of the girder was 4.5 in. greater than anticipated, which increased the stresses in the actual specimens.

Table 3. Concrete stress values for Girder A design

	Beam "A" (full scale ODOT)	Girder A (half-scale test specimen)	Difference (%)
	Concrete Stress at Release		
f_1 (ksi)	-0.239	-0.056	76.5
f_2 (ksi)	-1.151	-1.101	4.3
	Concrete Stress in Service		
f_1 (ksi)	-0.450	-0.211	53.1
f_2 (ksi)	-0.903	-0.896	0.8

Note: f_1 indicates the maximum stress at the section top, f_2 indicates the maximum stress at the section bottom; (+) indicates compression, (-) indicates tension.

Table 4. Concrete stress values for Girder C design

	Beam "C" (full scale ODOT)	Girder C (half-scale test specimen)	Difference (%)
	Concrete Stress at Release		
f_1 (ksi)	-0.268	-0.018	93.3
f_2 (ksi)	-1.871	-1.604	14.3
	Concrete Stress in Service		
f_1 (ksi)	-0.768	-0.176	77.1
f_2 (ksi)	-1.31	-1.35	3.1

Note: f_1 indicates the maximum stress at the section top, f_2 indicates the maximum stress at the section bottom; (+) indicates compression, (-) indicates tension.

Concurrently with the design of the prestressed concrete girders, the design and construction of the approximately 58 ft.-long prestressing bed at Fears Structural Laboratory occurred. Steel formwork was designed and fabricated for construction of the girders (see appendix for design and drawing of final girder section). The prestressing bed consists of two steel abutments bolted to the Fears Lab strong floor and a wooden platform for supporting the formwork. It was designed to cast up to 48 ft of beam at one time. The prestressing bed has a "dead end" for strand anchorage at the south which has no moveable parts, and a "live end" at the north where the prestress is applied. The live end prestressing abutment and the overall prestressing bed are shown in Figure 5.
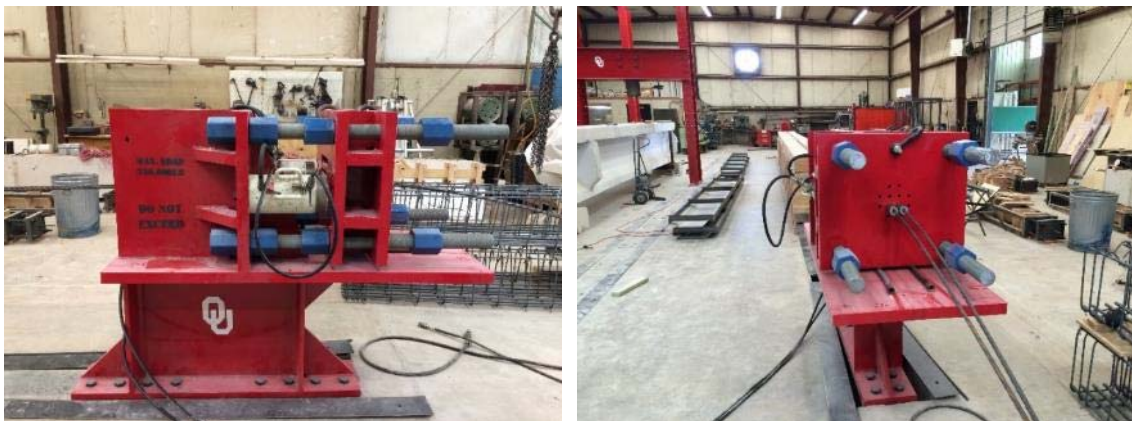
Figure 5. Prestressing Bed at Fears Lab

The concrete mix utilized was identified from mixes considered technically comparable to the original concrete design used for the original girders based on compressive strength. The final mix design had a water/cement ratio of 0.37, no entrained air, and a theoretical unit weight of 150.9 lb/ft^3.

Table 5 presents the final proportions used for the concrete mix design.

Table 5. Mix proportions of the concrete at Saturated Surface-dry (SSD) condition

Material	Weight (lb/yd^3)
Cement	851
Sand	1459
Rock	1372
Water	315
Total	**3997**

Concrete cylinder compression tests were performed for quality control purposes and to ensure the required compressive strength for the girders was achieved. The girders were cast using the prestressing bed over a period of five weeks. In total, ten, 18-ft long girders were cast: four using the Girder A design (only three were used however as there was a problem with consolidation of the first one cast), and six using the Girder C design. Three of the Girder C specimens were reserved for future retrofitting. The girders were cured for at least 28 days inside of Fears Lab and then taken outside in preparation for the accelerated corrosion setup, shown in Figure 6.

Figure 6. Newly cast half-scale prestressed concrete girders

3.2.1.2 Corrosion Accelerant Setup

After the girders were designed and cast, the next step was to begin the corrosion induced end-zone deterioration. As part of this effort, the corrosion accelerant process needed to be developed. Initially, a literature review was performed to understand chloride solutions successfully used in previous research, as well as the optimum duration for wet/dry cycles of chloride saturated water (e.g., 12 hrs. on/off vs. 2 hrs. on/off). Ultimately, a 5 percent by weight chloride solution was chosen and sodium chloride was used for the solution. A large plastic tub was selected to serve as a reservoir, from which a submersible pump was installed to pour the chloride solution over the end of the beams. Perforated plastic tubes were bonded to the beam ends approximately 6 in. from the beam ends. Four holes (3/32 in.) were drilled in the plastic tubes for each beam for the chloride solution to disperse over the beam ends. A valve was used to control the flow of the chloride solution through the perforated tubing. The final arrangement is shown in Figure 7. A cycle time of two hours on and two hours off was chosen based on the literature review, limitations of available timers, and to ensure drying between cycles.

After 28 days of curing for all beams, the beams were subjected to the wet/dry accelerated corrosion process. The exposure process adhered to the following:

a. Three girders, one from the Girder A and two from the Girder C reinforcement configuration, were subjected to the corrosion accelerant for two months.

b. Two girders, one from the Girder A and one from the Girder C reinforcement configuration, were subjected to the corrosion accelerant for four months.

c. Three girders, one from the Girder A and two from the Girder C reinforcement configuration, were subjected to the corrosion accelerant for six months.

d. One girder, from the Girder C reinforcement configuration, was subjected to the corrosion accelerant past six months, for a longer term exposure.

Figure 7. Corrosion Accelerant setup (red arrows indicate the direction of flow from the perforated tubes)

The corrosion exposure setup was monitored throughout testing to ensure a consistent concentration of chloride. The progress of the corrosion was monitored to determine whether other measures should be taken, such as, inducing cracking into the end zones of the members to facilitate more moisture movement or applying an electrical current. Ultimately, there were no deviations from the originally designed corrosion accelerant setup. Cracks occurred during fabrication of some of the girders (e.g., during the

prestress release). Before starting the acceleration corrosion process on the girders, pre-existing cracks were recorded.

3.2.1.3 Shear Testing of Corroded Specimens

Following the accelerate corrosion period, each end of the exposed specimens was tested in shear. A three point bending setup using a hydraulic actuator to apply load to the girders was used to simulate the maximum shear stress at the critical section used for shear design, and the load point location was chosen to induce a bond-shear type failure. The opposite end of the beam from that being tested overhung the support to prevent damage during the first test. The critical section for shear was determined by using an "a/d" ratio of 2. The critical section is important in that it is the location where a shear failure is more likely to be created as opposed to a moment induced failure. The support was located 4 in. from the end of the beam and the center-to-center distance between the supports was 9 ft; leaving 8 ft-8 in. of overhang. A single point load was applied through a 6 in. wide plate, centered 41 in. from the end of the beam, using a hydraulic actuator. Sand was placed between the load plate and the beam to ensure uniform load distribution. The girders were loaded in 5000 lb increments before initial cracking, and 2000 lb increments after initial cracking to failure.

Deflection at the load point was measured using wire potentiometers (wire pots) on each side of the beam, strand end slip was measured using linear voltage differential transformers (LVDTs) attached to the prestressing strands on the non-corroded end and placed touching the strand ends on the corroded end. Manual deflection measurements were also taken after each load increment using a steel ruler. Visual mapping of cracking was conducted during the testing by marking cracks with a permanent marker

and noting the load increments. Data was collected from all instruments during testing using a single data acquisition system. The data were used to compare the findings to the nominal design/theoretical values calculated using the ACI and AASHTO LRFD codes and to identify the failure mechanism. The results of tests of the undamaged ends of the girders were compared to tests of the corroded girder ends to identify differences in performance. Figures 8 – 14 illustrate the shear test setup.
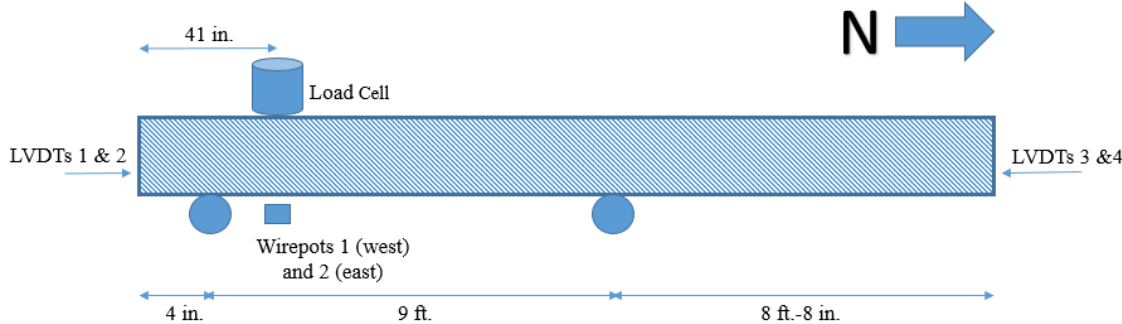
Figure 8. Shear Test Schematic (not to scale)
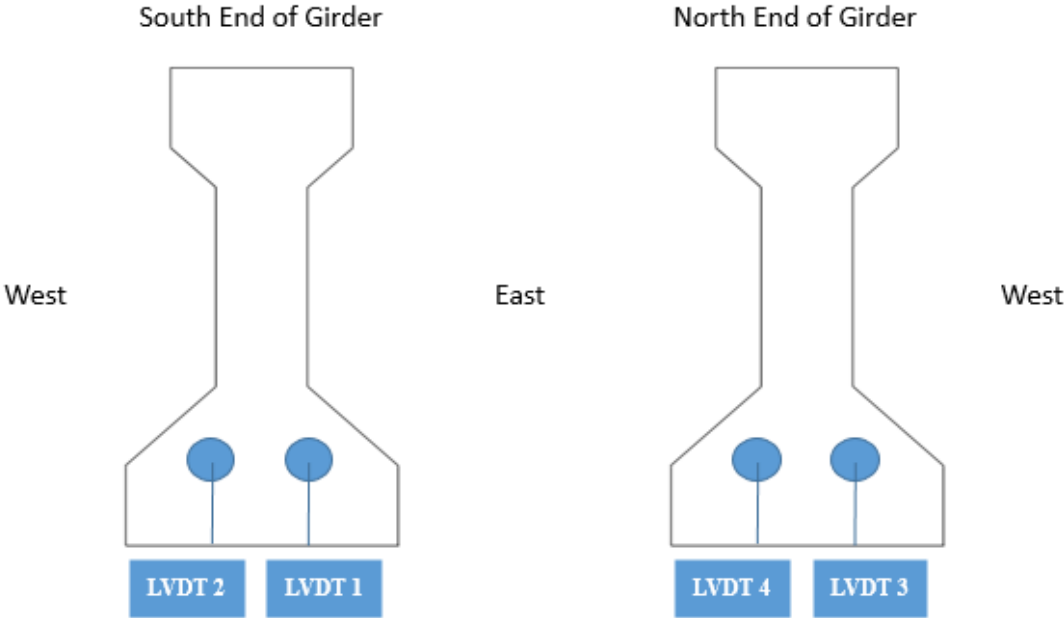
Figure 9. Location of LVDTs on girders during shear testing
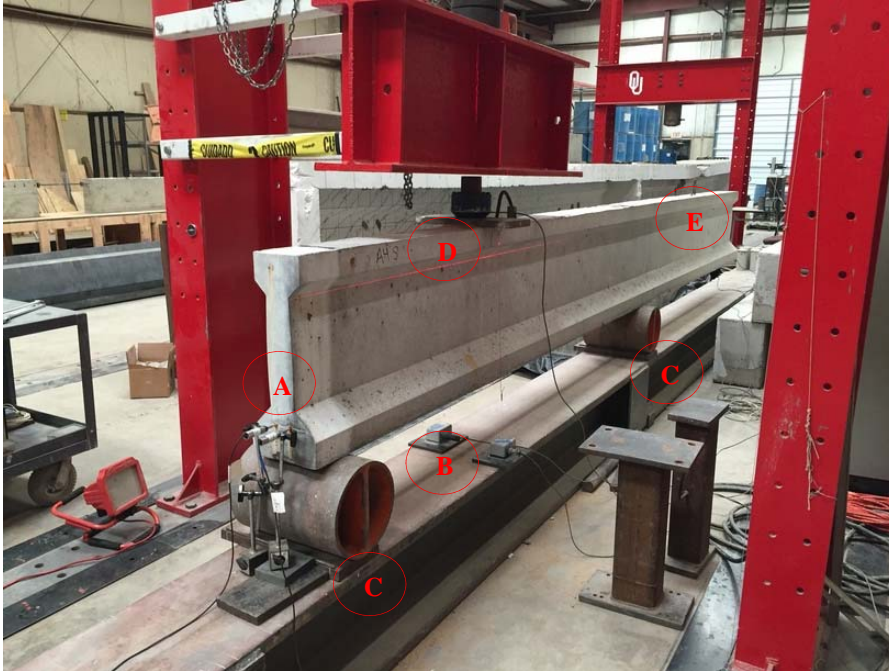
Figure 10. Shear Test Setup - LVDT 1 & 2 (A), Wirepots 1 & 2 (B), Supports at 9 ft. center-to-center (C), Single Load Point at 41 in. from end of beam (D), and 8 ft.-8 in. overhang of the beam (E) – looking towards the north

Figure 11. Shear Test Setup - LVDT 1 (right) and LVDT 2 (left) – looking towards the north

Figure 12. Shear Test Setup - LVDT 3 & 4 (F) (foreground), load point, and supports (background) - looking towards the south

Figure 13. Shear Test Setup - LVDT 3 (right) and LVDT 4 (left) - looking towards the south

Figure 14. Shear Test Setup - Wirepot 1 (left/west) and Wirepot 2 (right/east) - looking towards the north

3.2.1.4 Retrofit of Remaining Corroded Specimens

While outside the scope of this thesis, a retrofit will be designed for the three remaining corroded girders using fiber reinforced polymer sheets and the information collected during shear testing of the first six corroded girders as part of the larger research project. A literature review was performed on the products related to this topic and to determine the general types that are applicable to this research effort. After consideration, it is recommended that a Carbon Fiber Reinforced Polymer (CFRP) strip be applied to the ends of the girders – the location most critical to the shear strength.

3.2.2 Field Data Collection

The Oklahoma bridge inventory was surveyed using the National Bridge Inventory (NBI)[1] and other available online resources to assess the current state of deterioration in concrete bridges and identify those that fit desired specifications for field visits. The construction period of the bridges to be investigated were 1960 through 1979 in order to match the full-scale decommissioned girders. Site visits to a representative sample of these bridges were conducted to verify and document the levels of end region deterioration in Oklahoma. Documentation and data were analyzed to identify common patterns, determine frequency of identified concerns, and ultimately, relate those identified concerns if possible to potential causes.

3.2.2.1 Bridge Selections

All 22,912 bridges in Oklahoma, as represented by the data provided from the Federal Highway Administration's (FHWA) National Bridge Inventory (NBI), were filtered through to select bridges to inspect for this research effort. Using the FHWA's Recording and Coding Guide for the Structure Inventory and Appraisal of the Nation's Bridges (e.g. (Features Intersected (6A)), bridges were selected using the following criteria:

- Features Intersected (6A): Did not include bridges with "river" and "creek"
- Construction Year (27): 1960-1979
- Design Load (31): M13.5/H15, M18/H20 and MS18/HS20 (same loading as the decommissioned bridge)

---

[1] http://www.fhwa.dot.gov/bridge/nbi.cfm

- Navigation Control (38): "N - Not Applicable, No waterway"

- Structure Open, Posted, or Closed to Traffic (41): "A - Open, no restriction"

- Type of Service under bridge: Highway, Railroad, Highway-Railroad

- Structure Kind (43A): 5 - Prestressed Concrete

- Structure Type (43B): 2 – Stringer/Multi-beam or Girder

This criteria was used to remove bridges that were: not constructed of prestressed concrete, spanned over rivers and creeks, and thus were difficult to inspect, or were outside of the construction age this research intended to consider. The aforementioned criteria helped to narrow down the possible bridges to a more manageable 215 bridges. When considering the same design load as used for the decommissioned I-244 bridge in Tulsa County, the 116 listed in Table 6 remained, which is organized by Oklahoma Department of Transportation (ODOT) Field Division (see Figure 15).

Table 6. Bridges considered for a site visit by ODOT Field Division

ODOT Field Divisions	Number of Bridges (Total – 116)
1	19
2	29
3	1
4	23
5	1
6	0
7	8
8	35
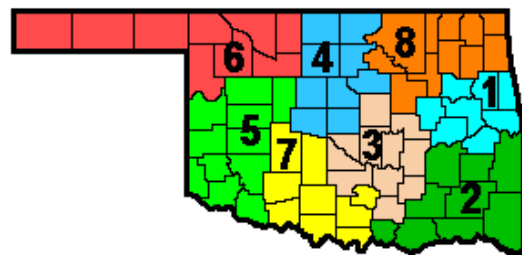
Figure 15. Geographical location of ODOT Field Divisions

In the field, preference was placed on visiting bridges with significant ratings (i.e. a lower) on the superstructure, or main load carrying system, of the bridge. The goal being to select, and inspect bridges with a variety of superstructure ratings. Per the

FHWA's Recording and Coding Guide, the superstructure rating is intended to describe the physical condition of all structural members. The Guide states the structural members should be inspected for "signs of distress which may include cracking, deterioration, section loss, and malfunction and misalignment of bearings." Also, bridges were pre-screened with available online resources (e.g., Google Maps) to determine potential traffic levels, and access issues.

3.2.2.2 Picture Reference System

Photos were taken of the overall bridge, each girder end, and any other pertinent locations for each bridge visited. These provided a visual record of the bridge condition at the time of the field visit. At each bridge, photos were taken of each girder end at the abutments along with any visual deficiencies such as cracking, spalling, and corroded bearing plates. For certain deficiencies to be more noticeable, a water bottle was used to spray the surface and highlight the area of concern. In order to have a uniform approach for referencing bridge locations, the following system was followed:

- The first set of numbers (e.g. 16606) are always the NBI Structure #.
- The girders are numbered in sequential order with the northernmost girder (for east-west bridges) or westernmost girder (for north-south bridges) as first. Since the spans are (almost) always the end spans of the bridge they are not numbered but rather signified by their direction. Photos were taken of each side of each girder end resulting in north/south or west/east side photos of each girder.
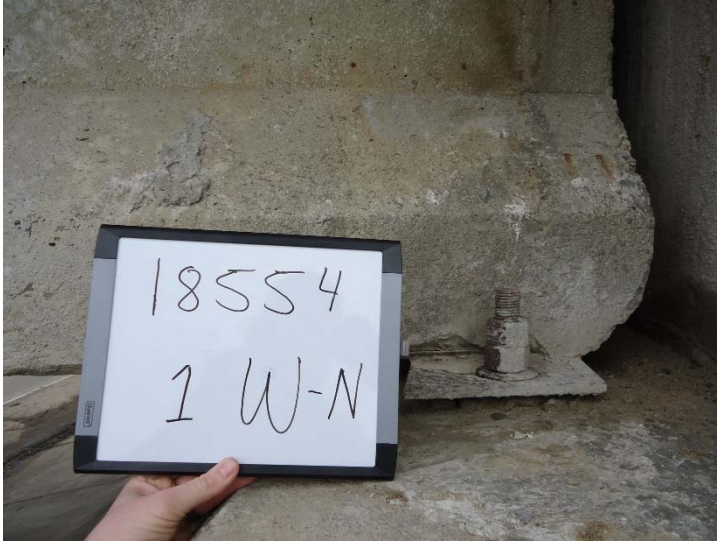
Figure 16. Bridge #18554, photo taken from northern side of the northernmost, west exterior girder

In the example shown in Figure 16, "18554" is the NBI Structure #, "1W-N" means the picture is taken from the northern side ("N") of the northernmost ("1") girder on the western end ("W") of the bridge. Figure 17 and Figure 18 illustrate the picture reference system in a plan view layout of typical multi-span, multi-beam bridges.
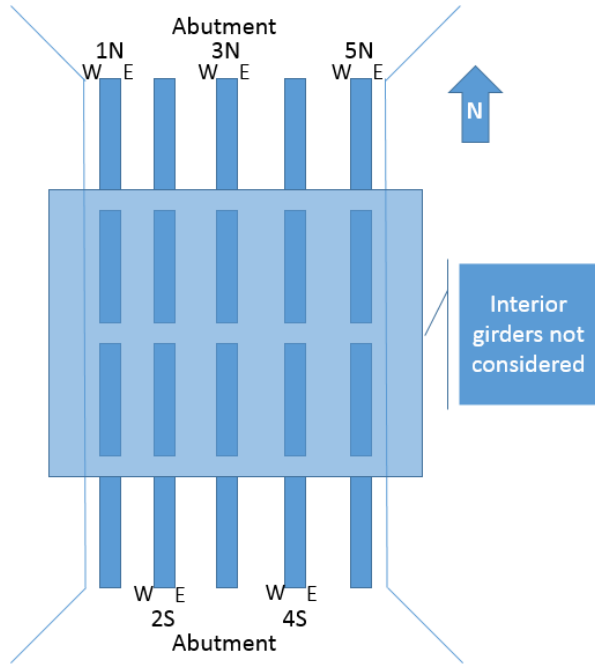
Figure 17. Plan view of an example north-south bridge using the picture reference system
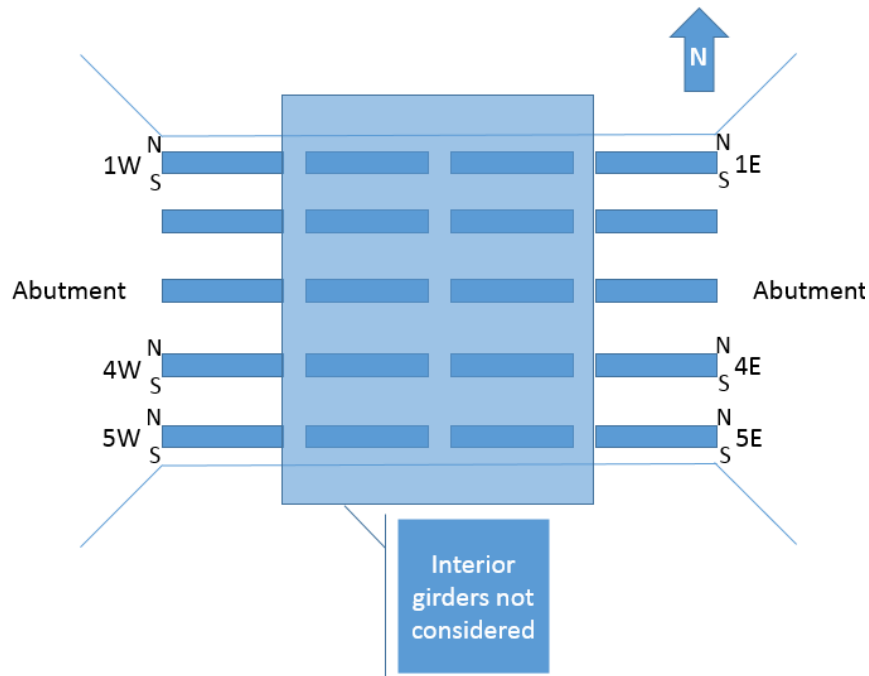
Figure 18. Plan view of an example east-west bridge using the picture reference system

4 Results and Analysis

The following section presents the results from the testing and field studies performed as discussed in the Experimental Design section, and discuss the interpretation of those results. Shear testing of the girders is discussed first. The results vary by both girder design, and time exposed to the corrosion accelerant setup. Followed by a discussion of the results of the site visits associated with the field experiment/field data collection aspect of this project. Finally, there is a brief discussion regarding the visual deterioration seen in the lab experiments in comparison to the bridges seen in the field.

4.1 Experimental

4.1.1 Compressive Strength of Beams

During the casting of the girders, cylinders were taken to perform compression tests at the following intervals: 1 day, 7 days, and 28 days. For each interval, three cylinders were tested, and the compressive strength was calculated as an average of the results from each cylinder test. Table 7 shows the average compressive strengths for each time interval for all nine girders.

Table 7. Compressive Strength of Girders

Girder	Compressive Strength (psi)		
	1 day	7 day	28 day
A2	4,080	6,600	6,490
A3	5,400	6,820	7,000
A4	4,590	5,720	5,780
C1	5,650	6,890	7,600
C2	6,220	7,150	8,250
C3	5,030	6,740	7,050
C4	5,030	6,940	7,160
C5	4,320	5,630	6,140
C6	4,530	6,180	6,630

All of the measured compressive strengths were larger than the targeted compressive strength of 4,000 psi at prestress release (1-day). However, there is a large variation in the measured strengths, with the maximum value being more than 50% larger than the target. The compressive strength of Girder A4 was 4% less than the design compressive strength of 6,000 psi at 28-days. The remaining girders exceeded the design compressive strength but there was a large variation. The maximum value was 37% greater than the design compressive strength. The variation in compressive strength could affect the prestress transfer and development length, as well as the girder's shear capacity. Larger compressive strengths would lead to shorter transfer and development lengths, and higher shear capacity.

4.1.2   Shear Test

The cracking load, and failure load were determined via the notes taken that day when testing, along with the load-deflection data provided from the data acquisition system. The locations of the LVDTs and wire pots are referenced in the Experimental Design section as Figure 8 and Figure 9 . Whenever the north side of the girders were tested LVDT 1 and 2 were not in use as the overhang did not allow for measuring the slip on that overhung end.

For the discussion to follow, the location of the shear test is abbreviated as follows: first the girder (i.e., A4), then the end of the girder (i.e., north or south), and lastly if it is the "corroded end" then a "C" follows. The label for the end of the girder identifies the location in the prestressing bed which may affect transfer length. The label is also significant in that the accelerated corrosion process was not consistently applied on one directional end (i.e., not all of the girders were corroded on the north end of the girders).

As an example, in describing the south end corroded of Girder A4, the abbreviation is A4SC. A summary of the results of all shear tests is given in Table 8. The results of each test is presented in greater detail in the following sections.

Table 8. Failure mechanisms of girders during shear test

		Corrosion Accelerated End	Control End
2-Month Tests	Girder A4	Bond-shear failure; slip before flexural cracking	Bond-shear failure; flexural-shear cracking before slip
	Girder C1	Bond-shear failure; slip before web-shear cracking	Bond-shear/flexure failure; flexural-shear cracking before slip; flange deterioration
4-Month Tests	Girder A3	Bond-shear failure; slip before flexural cracking	Bond-shear failure; maybe flexural failure first; flexural-shear cracking before slip
	Girder C2	Bond-shear failure; slip before web-shear cracking	Bond-shear failure; cracking before slip
6-Month Tests	Girder A2	Web-shear failure; flexural cracking initially	Bond-shear failure; web-shear cracking before slip
	Girder C3	Bond-shear/flexure failure; web-shear cracking before slip; concrete crushed at load point	Bond-shear failure; web-shear cracking before slip

4.1.3 Two-month Shear Testing

For the two-month shear testing of Girders A4 and C1, the corroded end of the girders had a higher failure load than the control ends. The control end of Girder A4 had a failure load of roughly 77% of the corroded end. For Girder C1, the control end failure load was roughly 83% of the corroded end failure load.

Initial photos were taken of the girder before the testing began (Figure 19). The shear

loading increased in approximately 5 kips intervals, until flexural cracking occurred at

approximately 41 kips. The girder was then loaded in 2 kips intervals until the girder's

failure at approximately 56 kips. A web shear crack appeared at the girder's failure, and

more cracks formed under continued load. The load vs. deflection graph (Figure 20) for

this test illustrates that: the load-deflection relationship was mostly linear until the

cracking load where the girder began to behave non-linearly; at the cracking load

deflection was roughly 0.15 in.; at the failure load the deflection of the girder was

approximately 0.36 in.; the girder had a maximum deflection of almost 0.6 in.

Figure 19. Before shear testing of A4SC
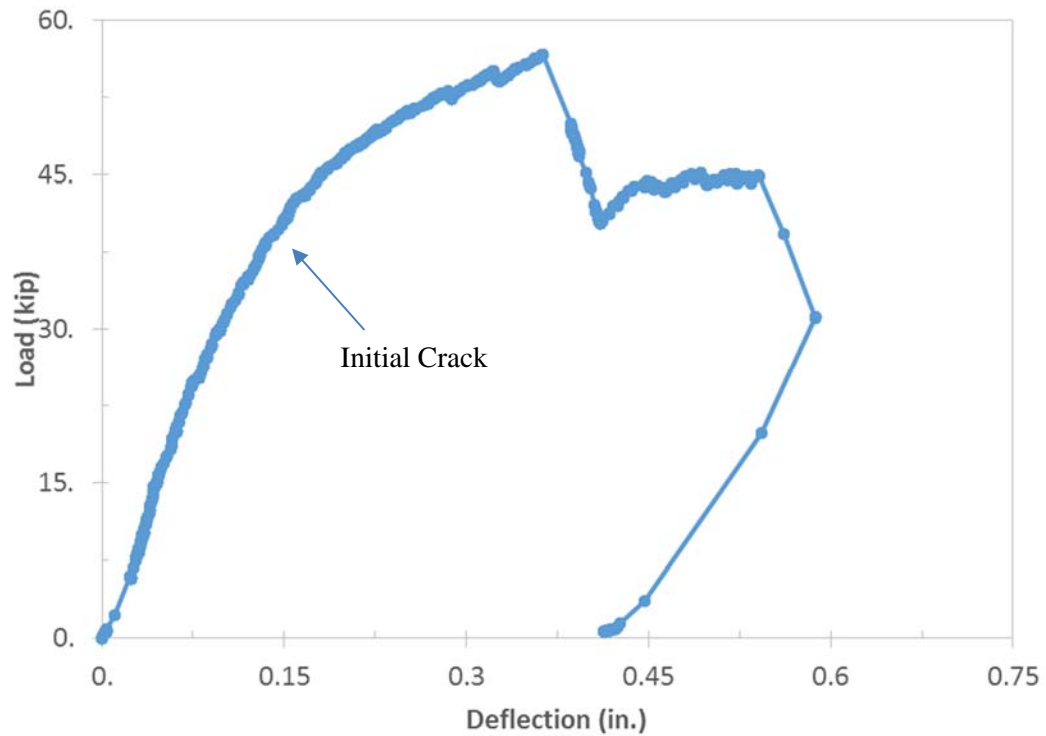
Figure 20. Load vs. Deflection of A4SC

The load vs. slip graph (Figure 21) shows that slip began simultaneously with the applied load. Results from LVDT 3 and 4 were removed from the graph because the slip was approximately zero for these strands. LVDT 2 had more slip than LVDT 1 as shown in Figure 22. As the graph illustrates more than approximately 0.08 in. of slip occurred before visible cracking of the girder began. The shear failure caused the slip to occur before the first flexural crack was visible.

Figure 23 is a photo of the visual map of cracking that occurred during the shear testing of A4SC.
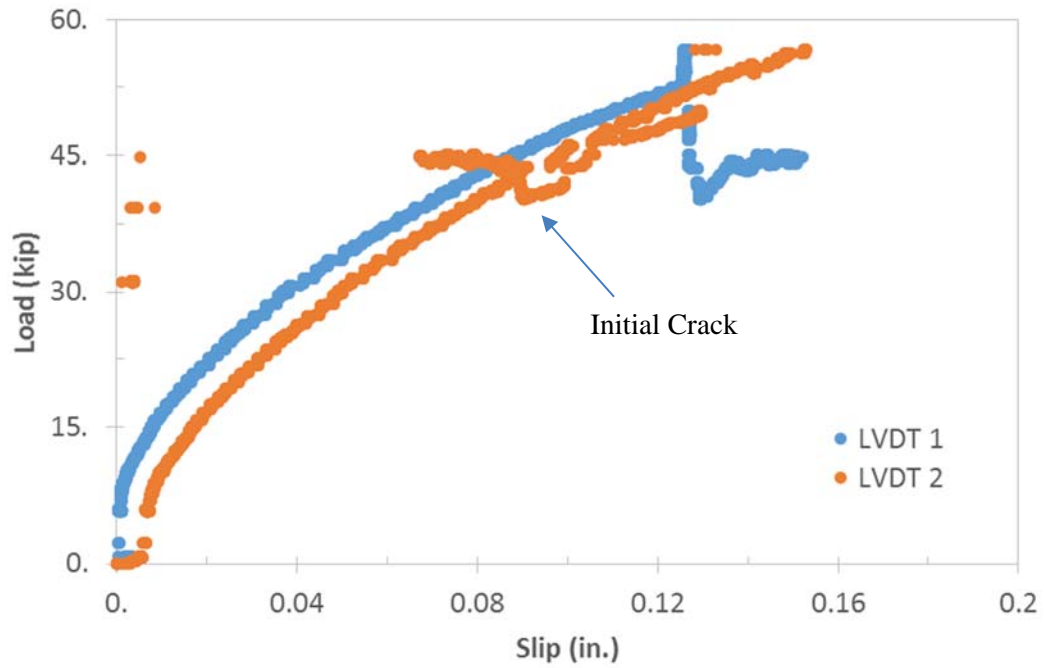
Figure 21. Load vs. Slip of A4SC

Figure 22. Slip during (left) and after (right) shear test on A4SC (LVDT 2 (left) and LVDT 1 (right))

Figure 23. Visual Map of Cracking for Shear Test on A4SC

4.1.3.2 A4N

The north end of the girder, the control end, was tested second. Initial photos were taken

of the girder before the testing began (Figure 24). The cracking load, determined

visually, occurred at approximately 41 kips. The girder was then loaded in a 2 kip

interval when further cracking occurred at 43 kips, after which the beam could take no

further load. The beam was continuously re-loaded up to 43 kips until it became

apparent that the beam had failed. A flexural-shear crack was the first crack that

occurred, then by 43 kips, multiple web shear cracks appeared along the beam. The load

vs. deflection graph (Figure 25) for this test illustrates that: the load-deflection

relationship was mostly linear until the cracking load where the load had quick decline;

44

the beam did not take much loading past 41 kips; at the cracking load the deflection was approximately 0.07 in.; the maximum deflection was roughly 0.58 in.

The load vs. slip graph (Figure 26) shows that slip appears to have occurred after cracking, and thus did not contribute to the shear failure. Figure 27 illustrates the cracking along the girder.
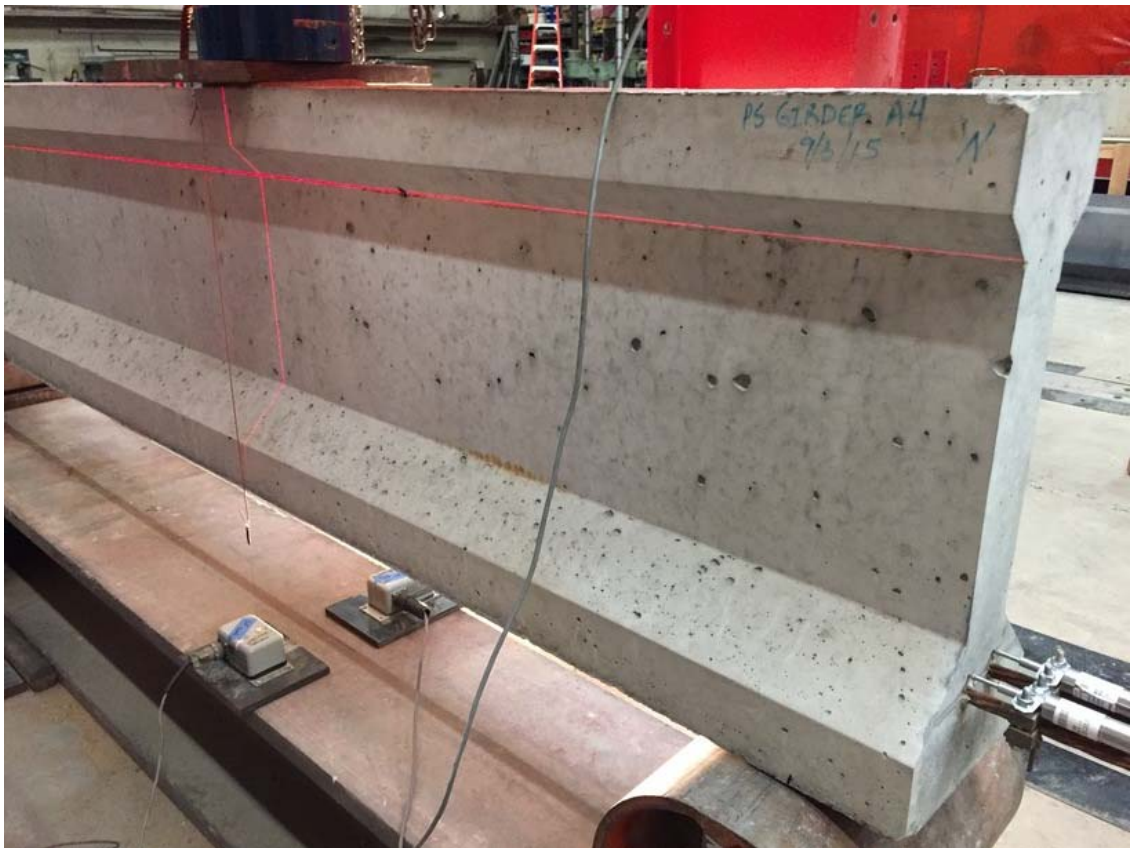
Figure 24. Before shear testing of A4N
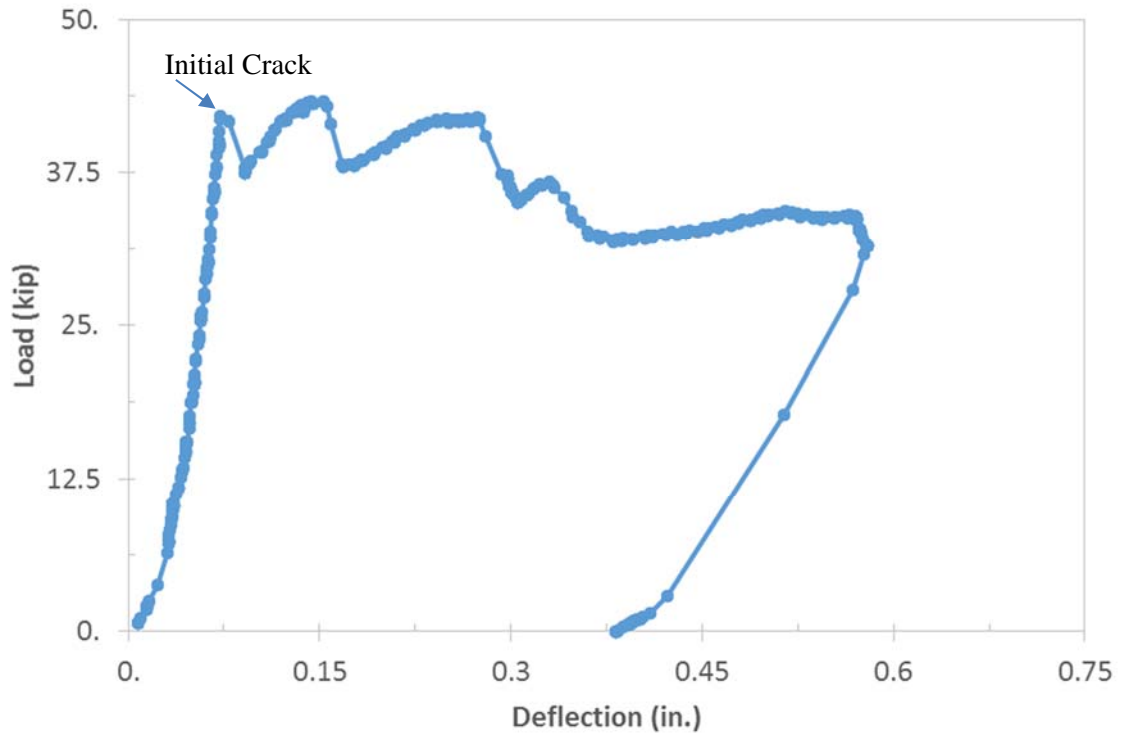
Figure 25. Load vs. Deflection of A4N
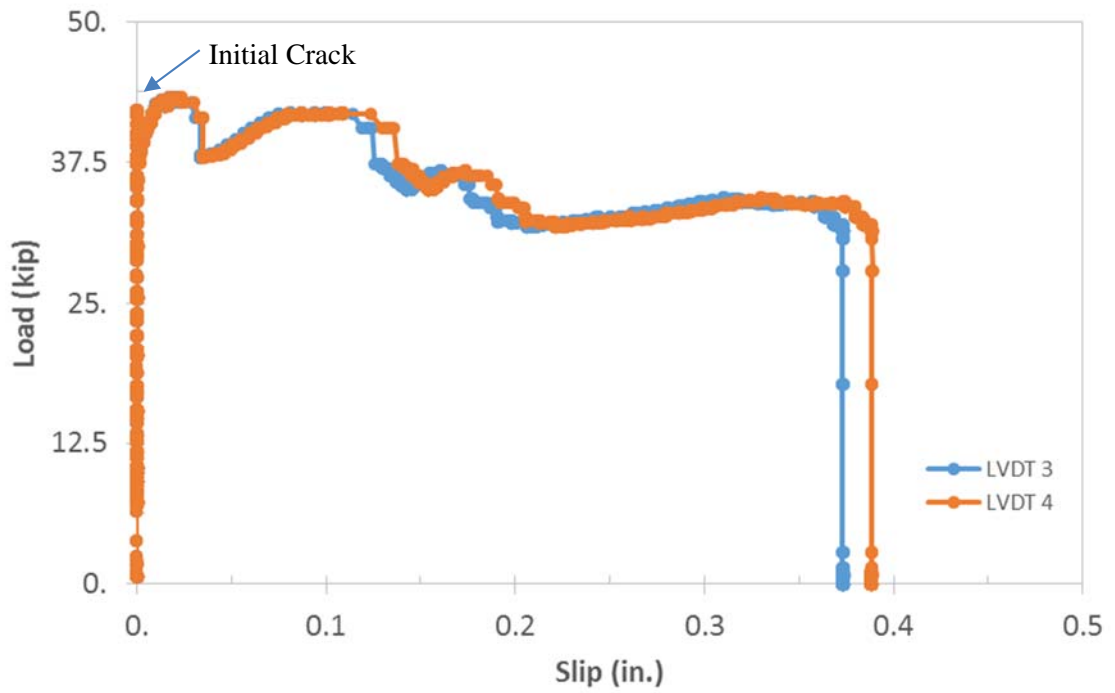
Figure 26. Load vs. Slip of A4N
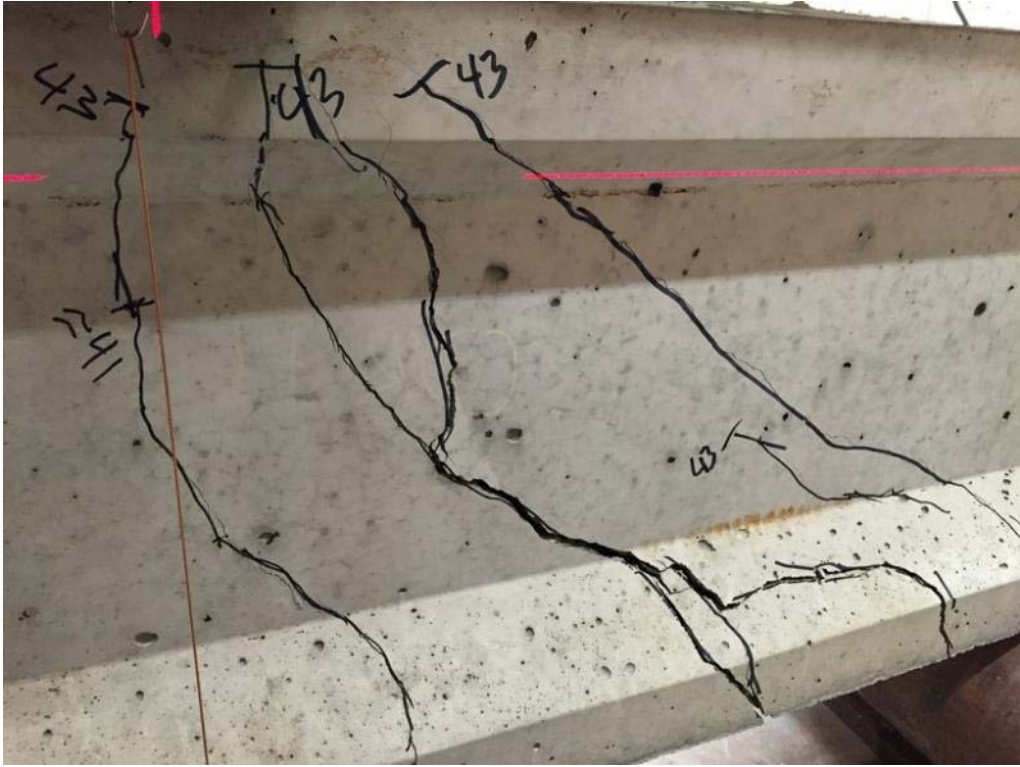
Figure 27. Visual Map of Cracking for Shear Test on A4N

For Girder C1, the north end of the girder was tested first. The north end of the girder, was also the end exposed to the accelerated corrosion setup. Initial photos were taken of the girder before the testing began (Figure 28). Web-shear cracking occurred at approximately 45 kips from the bottom of the flange up towards the load point, and the beam failed at approximately 52 kips. The girder exhibited both horizontal and shear cracks, typically indicative of a bond failure. The load vs. deflection graph (Figure 29) for this test illustrates that: the load-deflection relationship was mostly linear until the cracking load where the beam began to behave non-linearly; at the cracking load the deflection was roughly 0.05 in.; the maximum deflection was approximately 0.64 in.

The load vs. slip graph (Figure 30) shows the slip occurred at the same time the loading began. LVDT 3 and 4 were removed from the graph because the slip was approximately zero for these strands; LVDT 1 seemed to be out of range, and also did not measure any slip. Approximately 0.08 in. of slip occurred before visible cracking of the beam began.

Figure 31 shows a visual map of the cracking that took place during the shear testing; again, there was both horizontal and shear cracks. The web-shear cracks had a width between roughly 0.25 in. wide and 0.35 in. wide. Figure 32 illustrates the visible slip of the strand measured by LVDT 2.

Figure 28. Before shear testing of C1NC
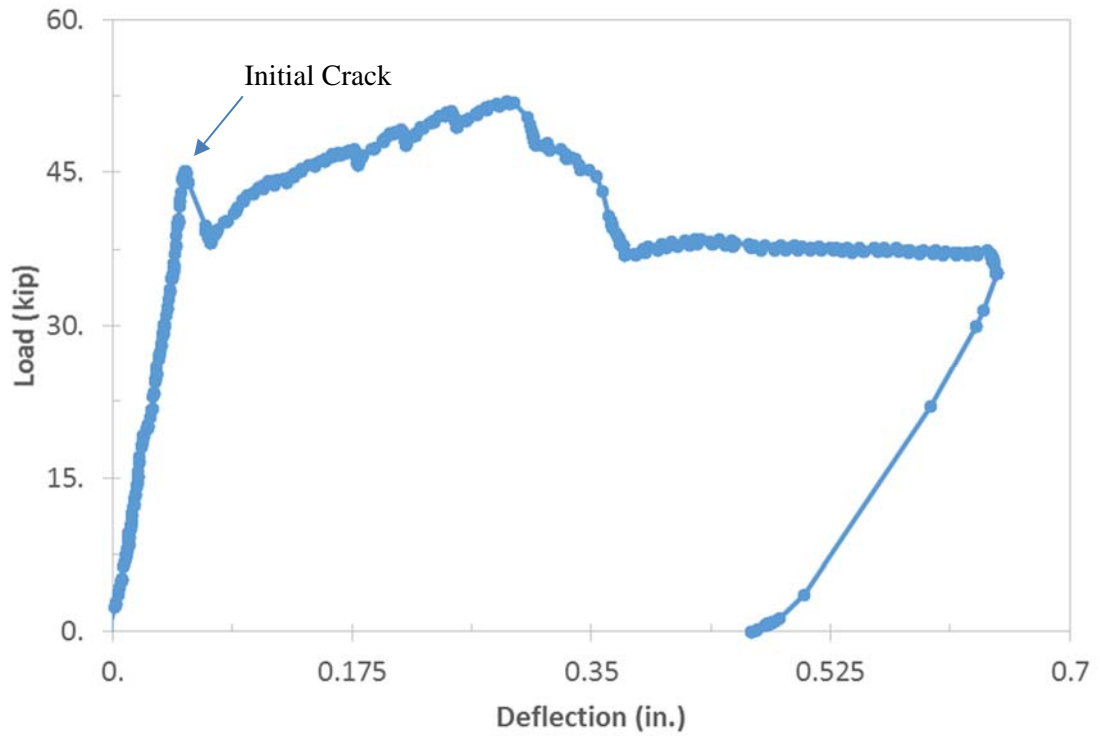
Figure 29. Load vs. Deflection of C1NC
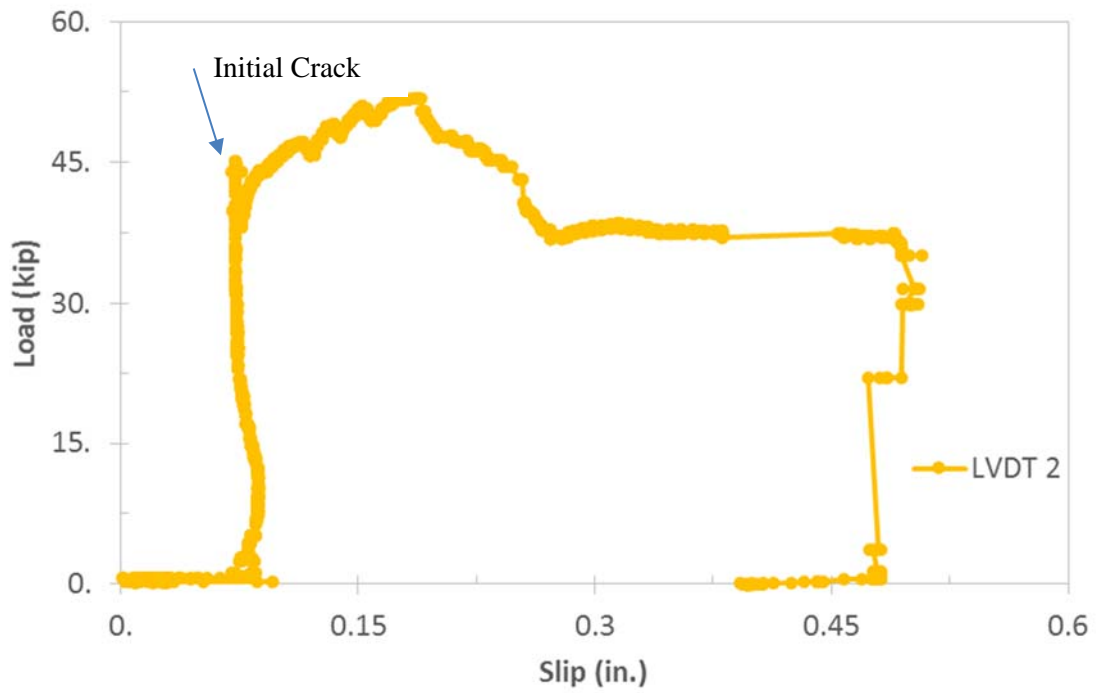
Figure 30. Load vs. Slip of C1NC

50

Figure 31. Visual Map of Cracking for Shear Test on C1NC

Figure 32. Visible Slip (LVDT 2 - left) after Shear Test on C1NC

The south end of Girder C1, the control end, was tested after the corroded end. Initial

photos were taken of the girder before the testing began (Figure 33). Cracking occurred

at approximately 28 kips, the girder was then loaded in 2 kip intervals when the beam

failed at approximately 43 kips. A flexural-shear crack was the first crack that occurred,

then by 43 kips, multiple web shear cracks, as well as a horizontal crack near the strands

appeared along the beam. At the widest, the main flexural-shear crack was

approximately 0.3 in. wide. The load vs. deflection graph (Figure 34) for this test

illustrates that: the load-deflection relationship was mostly linear until the cracking

load, and then the relationship became non-linear; the maximum deflection was

approximately 0.7 in.

The load vs. slip graph (Figure 35) shows that slip occurred after cracking, and thus did

not contribute to the shear failure. The flange did separate at the stop as evident by

Figure 36, so this could be a bond-shear/flexure failure. Figure 37 and Figure 38

illustrate the visual map of cracking of the girder.

Figure 33. Before shear testing of C1S

Initial Crack
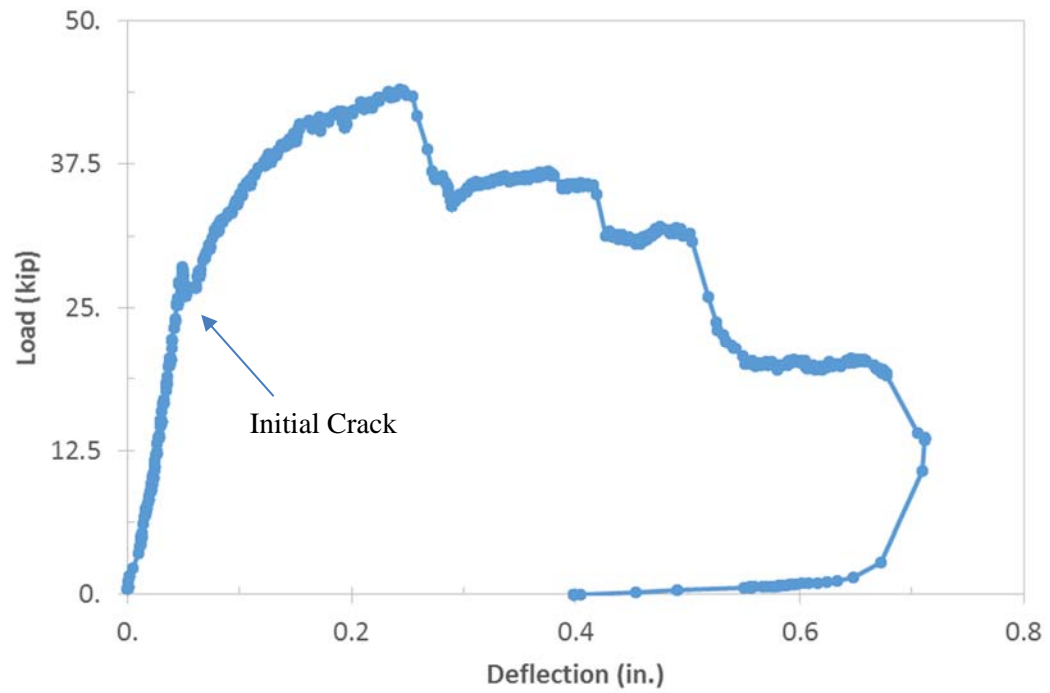
Figure 34. Load vs. Deflection of C1S
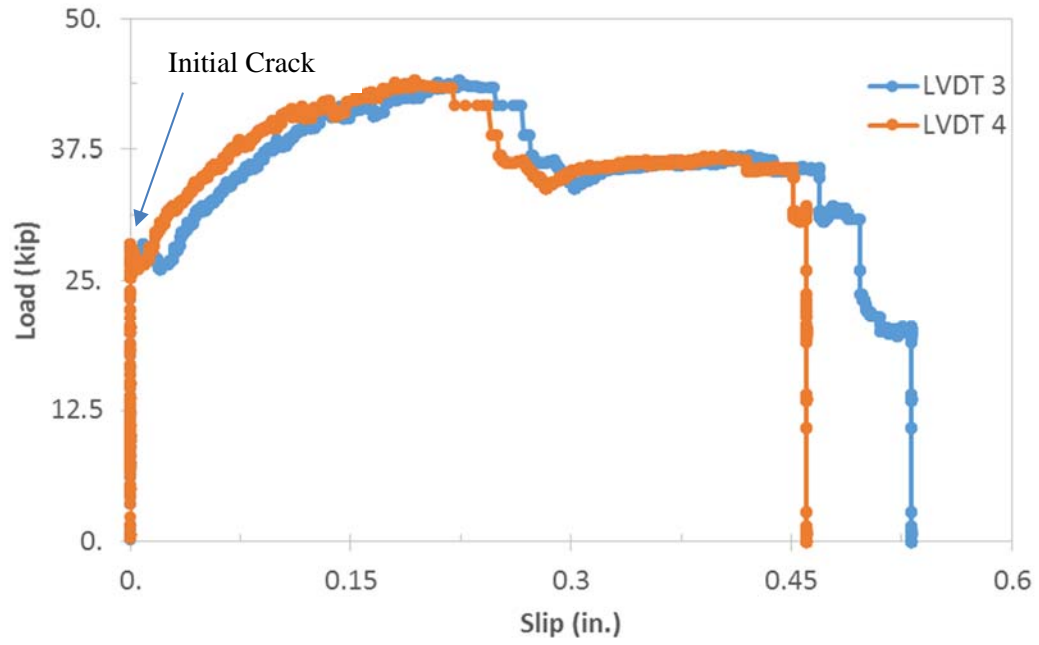
Figure 35. Load vs. Slip of C1S

Figure 36. C1S upon completion of shear test

Figure 37. Visual Map of Cracking for shear test on C1S

Figure 38. Visual Map of Cracking for shear test on C1S

4.1.4   Four-month Shear Testing

For the four-month shear testing of Girder A3, the corroded end of the girder had a

higher failure load than the control, or non-corroded end. However, for Girder C2, the

opposite was true – the corroded end had a lower failure load than the control end. The

control end however was tested first this time, as opposed to the previous tests. The

control end of Girder A3 had a failure load of roughly 87% of the corroded end. For

Girder C2, the non-corroded end failure load was roughly 122% of the corroded end

failure load.

4.1.4.1   A3SC

For Girder A3, the south end of the girder was tested first. The south end of the girder

was also the end exposed to the accelerated corrosion setup. Flexural cracking occurred

at approximately 45 kips. The girder was then loaded in 2 kip intervals until the beam's

failure at approximately 57 kips when a large web-shear crack appeared. The load vs. deflection graph (Figure 39) for this test illustrates that: the load-deflection relationship was mostly linear until the cracking load where the beam began to behave non-linearly; the deflection at the cracking load was approximately 0.07 in.; the maximum deflection was slightly more than 0.2 in. Figure 40, Figure 41, and Figure 42 illustrate the cracking of the girder during and after the shear test.

The measured slip data was not conclusive, and therefore is not presented.
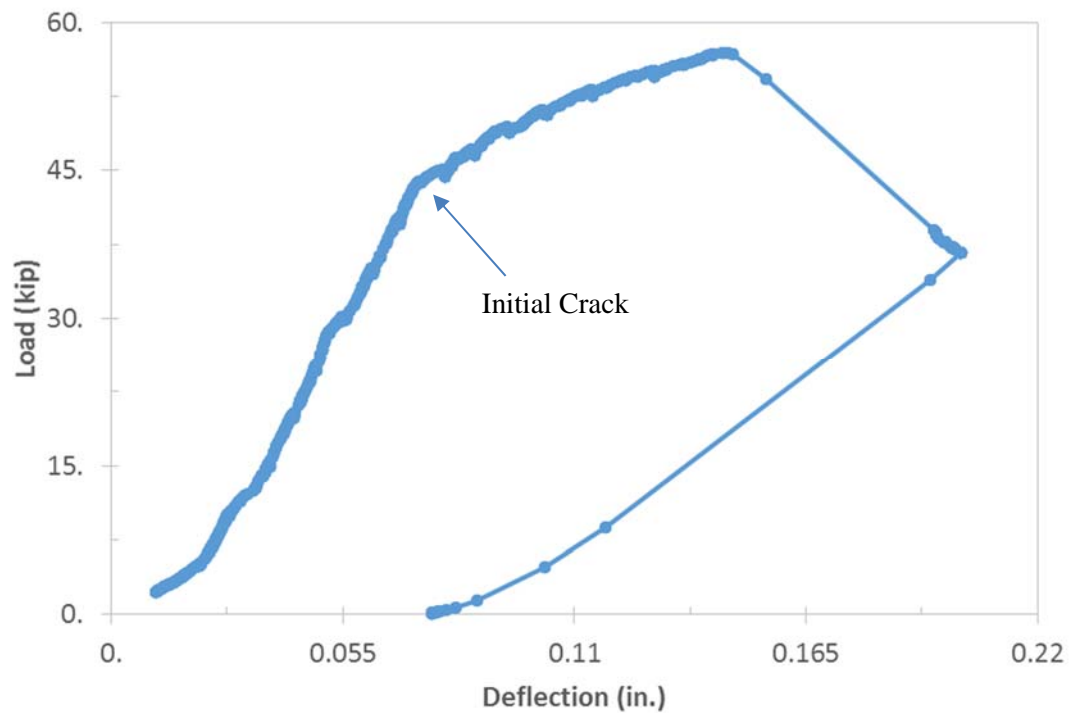
Figure 39. Load vs. Deflection of A3SC

Figure 40. Web-shear crack on A3SC
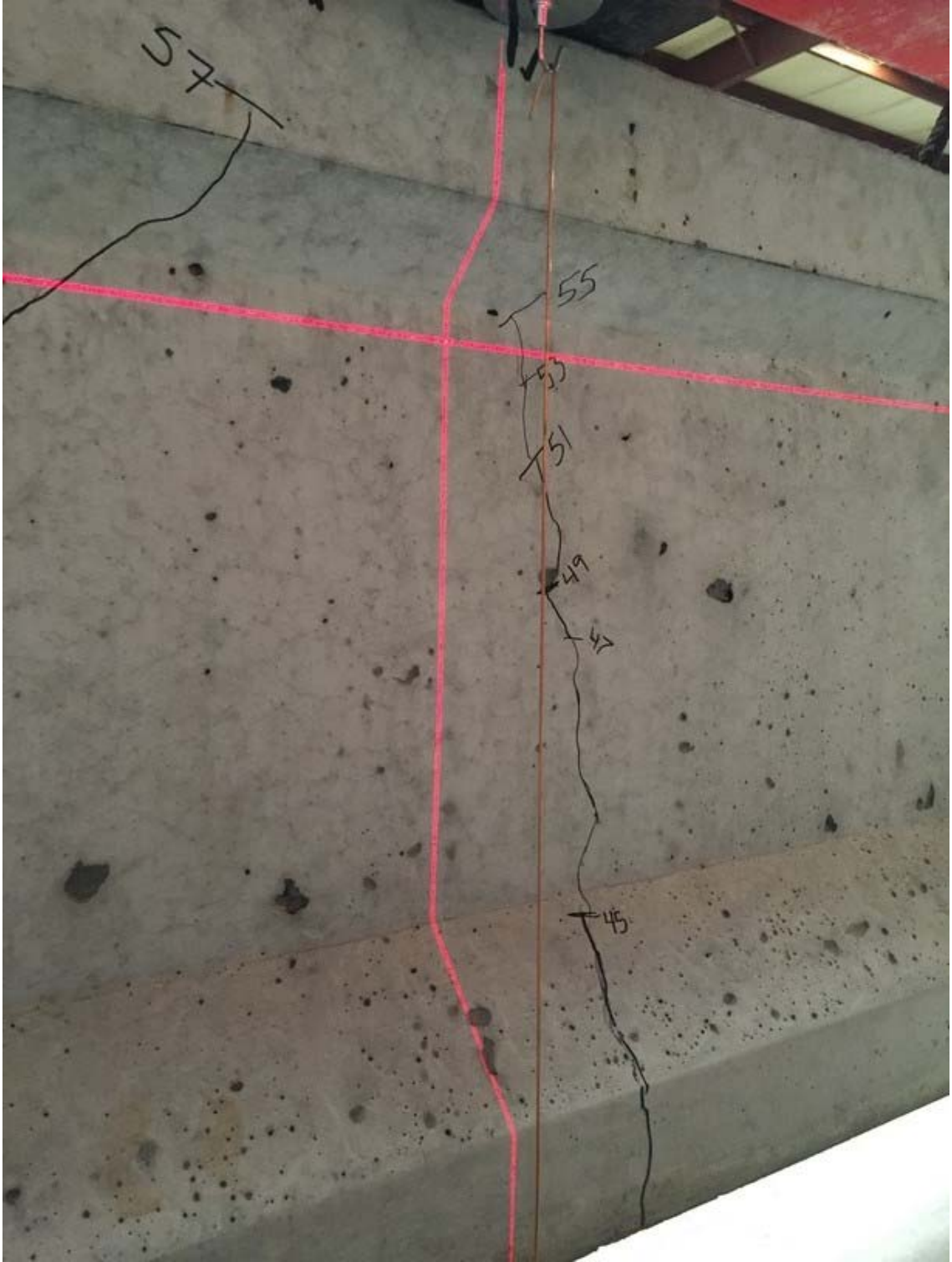
Figure 41. Flexural crack on A3SC

Figure 42. Web shear and flexural cracks of Girder A3SC

4.1.4.2   A3N

For Girder A3, the north end of the girder, the control end, was tested after the corroded

end. Cracking occurred at approximately 46 kips. The girder was then loaded in 2 kip

intervals until further cracking occurred at 50 kips; much load was lost and the beam

was reloaded when it failed completely at 41 kips. The load vs. deflection graph (Figure

43) for this test illustrates that: the load-deflection relationship was mostly linear until

the cracking load where the beam had a small deformation; the beam was reloaded until

about 50 kips when more cracking occurred, as well as a larger deflection, and then the

beam was loaded until it failed completely and was left with a maximum deflection of

approximately 0.74 in.

The load vs. slip graph (Figure 44) shows that slip was not measured until after cracking, and thus did not contribute to the shear failure. A bond failure occurred as the strand slip was slightly greater than 0.4 in. Figure 45 shows the visual map of cracking of A3N.
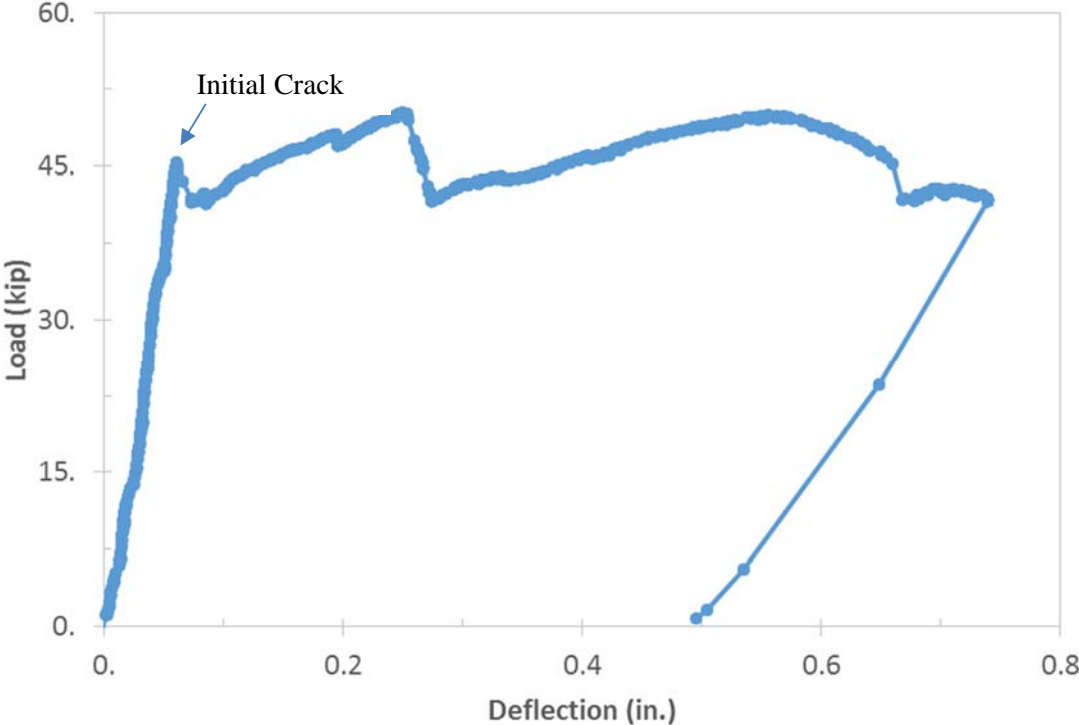
Figure 43. Load vs. Deflection of A3N
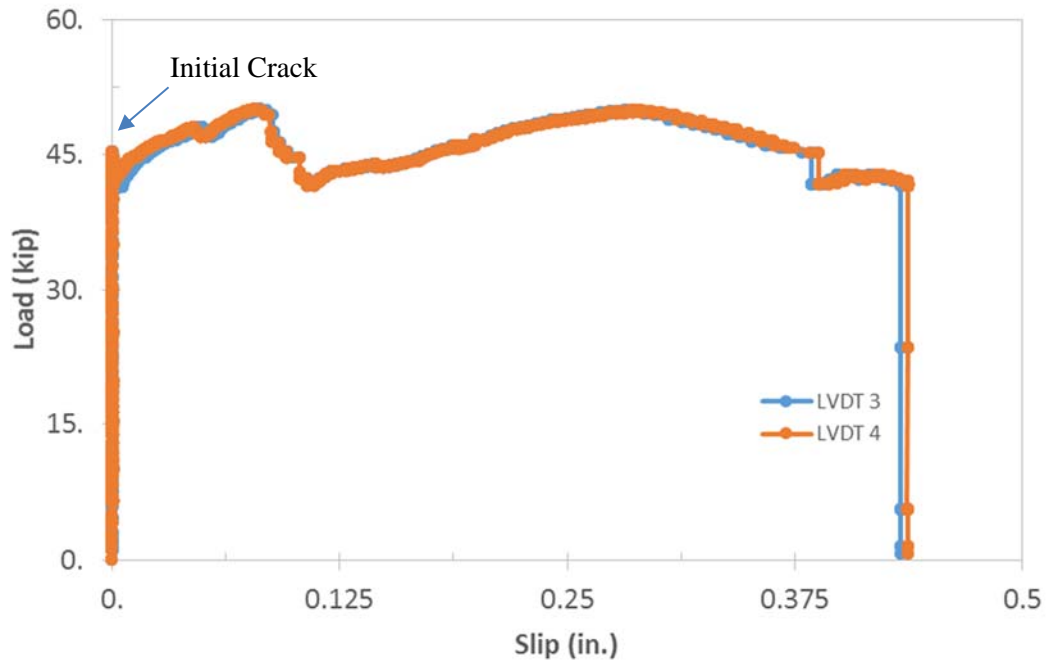
Figure 44. Load vs. Slip of A3N

Figure 45. Visual Map of Cracking along A3N

For Girder C2, the north end of the girder was tested second. The north end of the girder was also the end exposed to the accelerated corrosion setup. Initial photos were taken of the girder before the testing began; a horizontal crack below the web/flange interface of the girder (Figure 46 and Figure 47) was observed. Failure occurred at approximately 40 kips. A large web-shear crack appeared when the beam began to crack/fail, and widened and extended as additional load was applied. The load vs. deflection graph (Figure 48) for this test illustrates that: the load-deflection relationship was mostly linear until the cracking/failure load; there then was a long residual load curve; followed by a strange unloading curve. The maximum measured deflection for the girder was approximately 0.65 in.

The data from LVDT 2 was unreliable, so the data is not presented (Figure 49). Strand slip could have contributed to the shear failure, as more than 0.05 in. of slip occurred before visible cracking of the beam began. Figure 50, Figure 51, and Figure 52 illustrate the visual map of cracking of the girder.

Figure 46. Initial photos of C2NC

Figure 47. Horizontal crack below the web/flange interface of C2NC
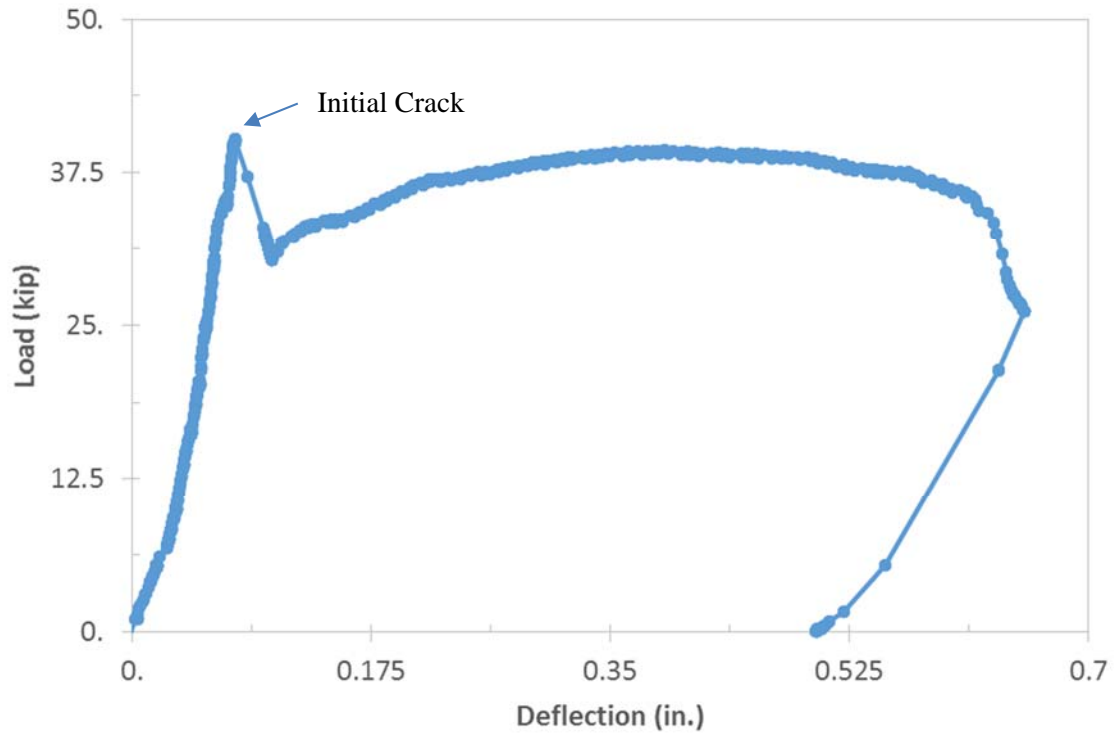
Figure 48. Load vs. Deflection of C2NC
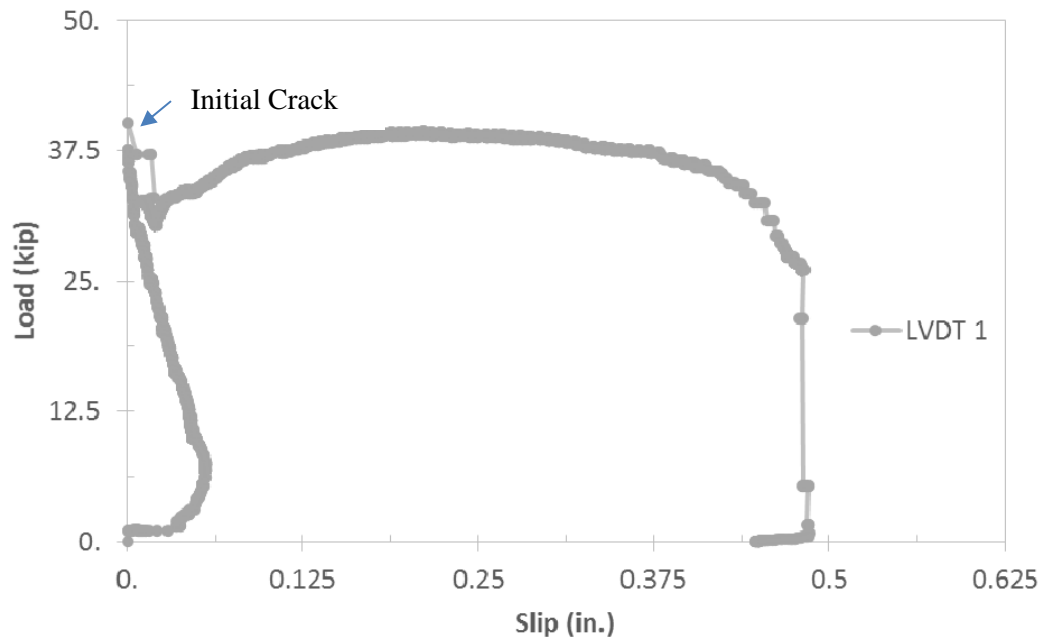
Figure 49. Load vs. Slip of C2NC

Figure 50. Visual Map of cracking of C2NC

Figure 51. Visual Map of cracking of C2NC

Figure 52. Visual Map of cracking of C2NC

4.1.4.4 C2S

For Girder C2, the south end of the girder, the control end, was tested before the

corroded end. Cracking occurred at approximately 45 kips, and then the girder was

loaded until failure at approximately 49 kips. The load vs. deflection graph (Figure 53)

for this test illustrates that: the load-deflection relationship was mostly linear until the

failure load; the beam was reloaded slightly until it was apparent that the beam had

failed; there was a large residual capacity, with a maximum deflection of approximately

0.7 in.

The load vs. slip graph (Figure 54) shows the non-linear relationship between the load

and measured slip. A bond failure occurred as the strand slip was slightly greater than

0.43 in. Slip appears to have occurred after cracking, and thus did not contribute to the shear failure. Figure 55 and Figure 56 show the visual map of cracking of C2S.
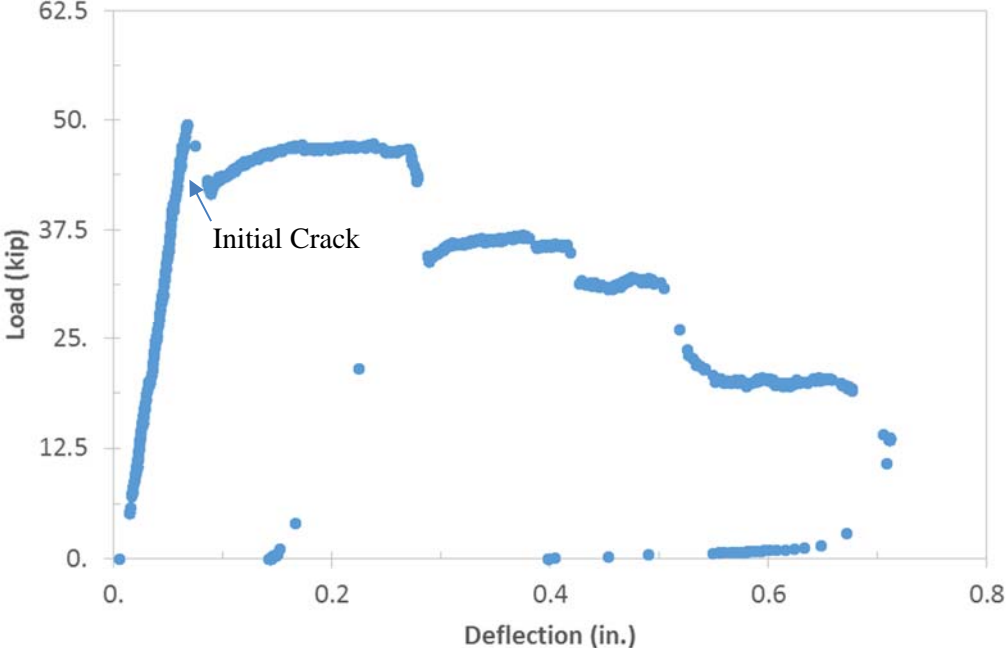
Figure 53. Load vs. Deflection of C2S
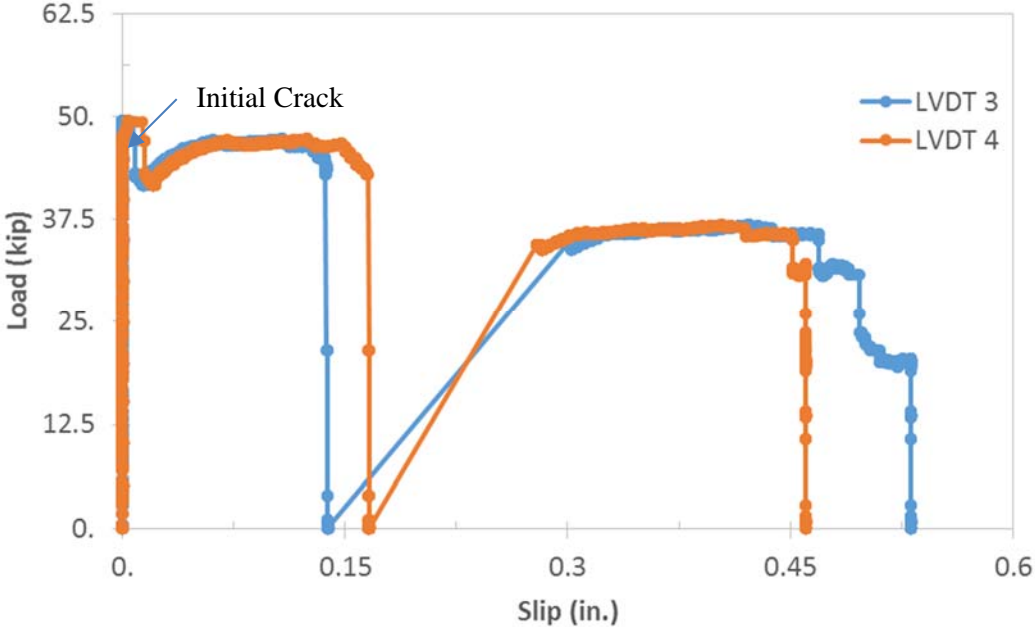
Figure 54. Load vs. Slip of C2S

Figure 55. Cracking of C2S

Figure 56. Cracking of C2S

4.1.5   Six-month Shear Testing

For the six-month shear testing of Girders A2 and C3, the corroded end of the girders had a higher failure load than the control ends. The control end of Girder A2 had a failure load of roughly 51% of the corroded end. For Girder C3, the control end failure load was roughly 51% of the corroded end failure load.

4.1.5.1   C3NC

For Girder C3, the north end of the girder was tested first. The north end of the girder was also the end exposed to the accelerated corrosion setup. Before shear testing, photos were taken to document the condition (Figure 57). Cracking occurred at approximately 45 kips, and the beam failed at approximately 53 kips. The load vs. deflection graph (Figure 58) for this test illustrates that: the load-deflection relationship was mostly linear until the cracking load; the cracking load caused a quick deflection of the beam; additional load caused a non-linear relationship between the load and deflection; the maximum deflection was recorded at slightly more than 0.5 in.

The load vs. slip graph (Figure 59) shows slip occurring after cracking of the girder had initiated. LVDTs 3 and 4 were removed because the slip was approximately zero for these strands. The girder had multiple web-shear cracks at the time of failure (Figure 60, and Figure 61). The top flange of the girder also started to fail (Figure 62 and Figure 63).

Figure 57. C3NC before testing
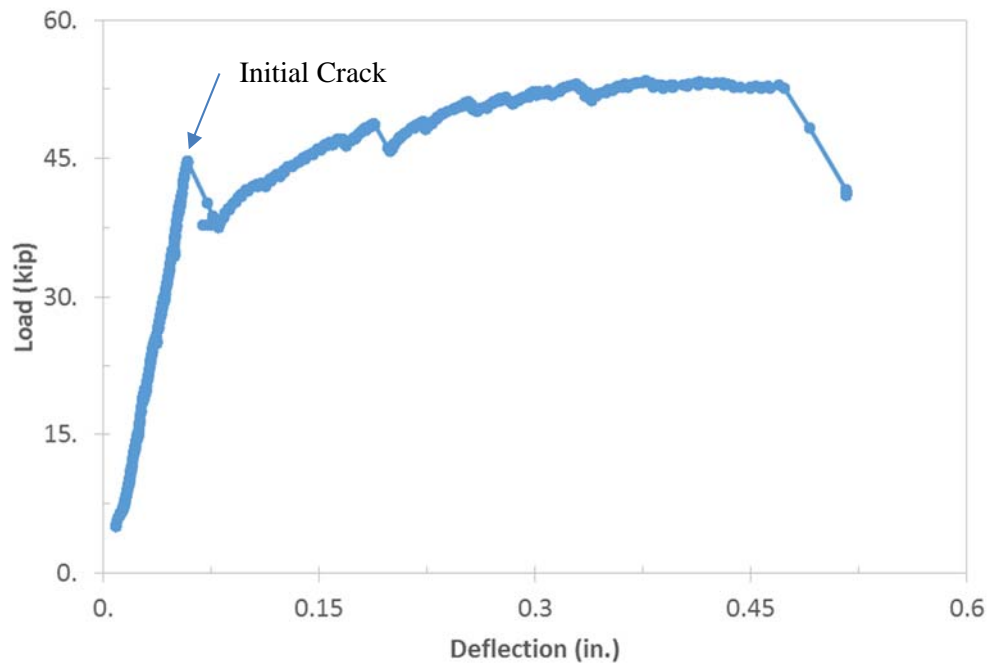
Figure 58. Load vs. Deflection of C3NC
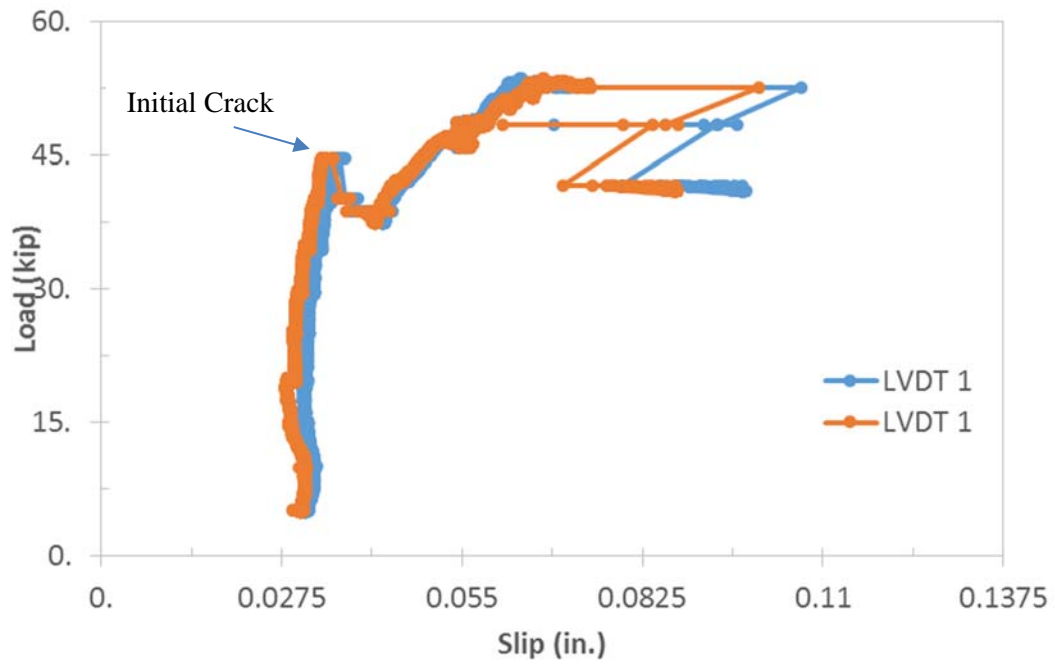
Figure 59. Load vs. Slip of C3NC
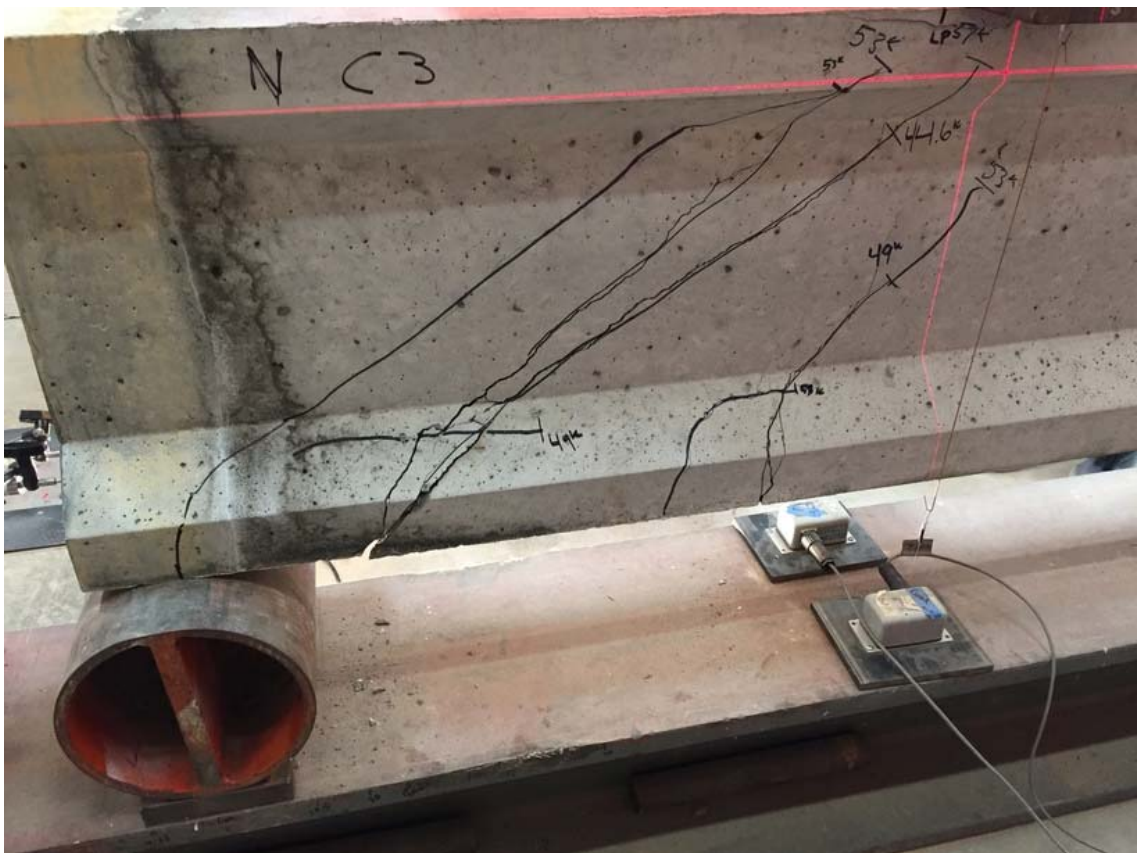
Figure 60. Shear cracking of C3NC after shear test

Figure 61. Shear cracking of C3NC after shear test

Figure 62. Concrete failure at top of top flange, C3NC

Figure 63. Concrete failure at top of top flange, C3NC

4.1.5.2   C3S

For Girder C3, the south end of the girder, the control end, was tested second. Web-shear cracking occurred at approximately 27 kips. The load vs. deflection graph (Figure 64) for this test illustrates that: the load-deflection relationship was mostly linear until the cracking/failure load; the residual load capacity was fairly stable around 26 kips; the maximum deflection was roughly 0.36 in.

The load vs. slip graph (Figure 65) shows the non-linear relationship between the load and measured slip. A bond failure occurred as the strand slip was greater than 0.3 in. Slip appears to have occurred after cracking, and thus did not contribute to the shear failure. Cracking occurred along the side and under the beam (Figure 66 and Figure 67).
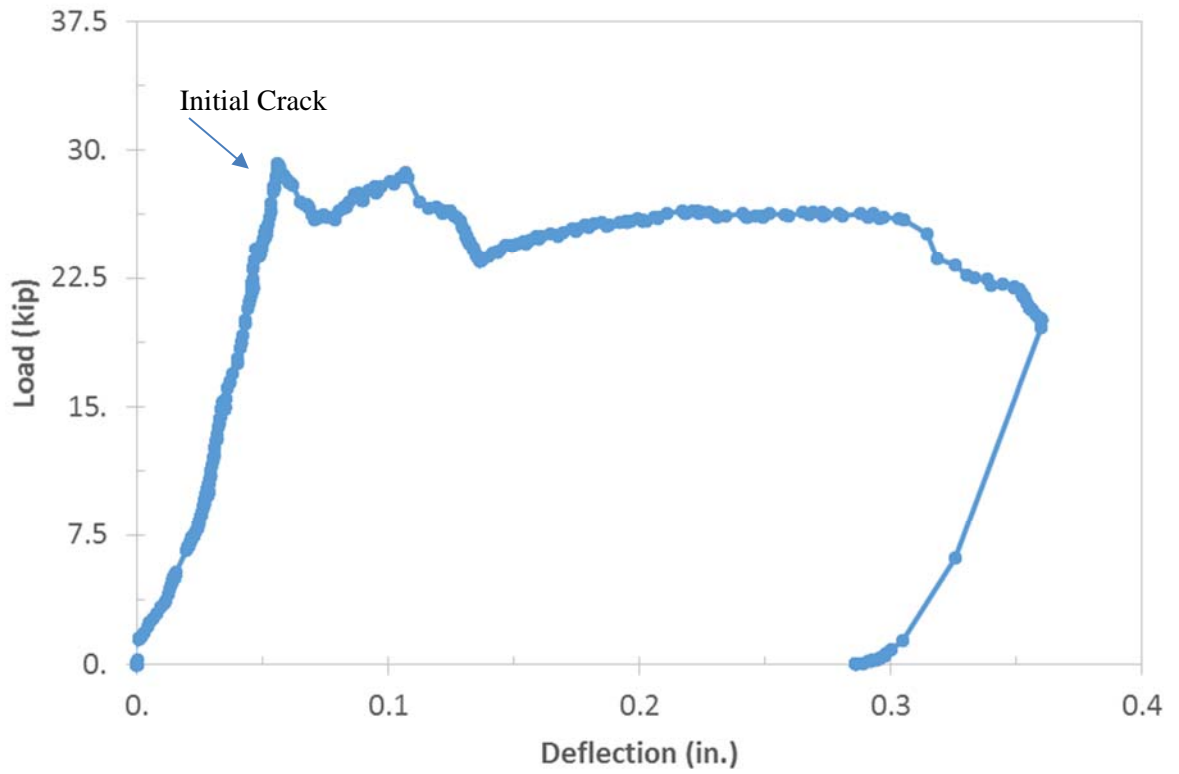
Figure 64. Load vs. Deflection of C3S
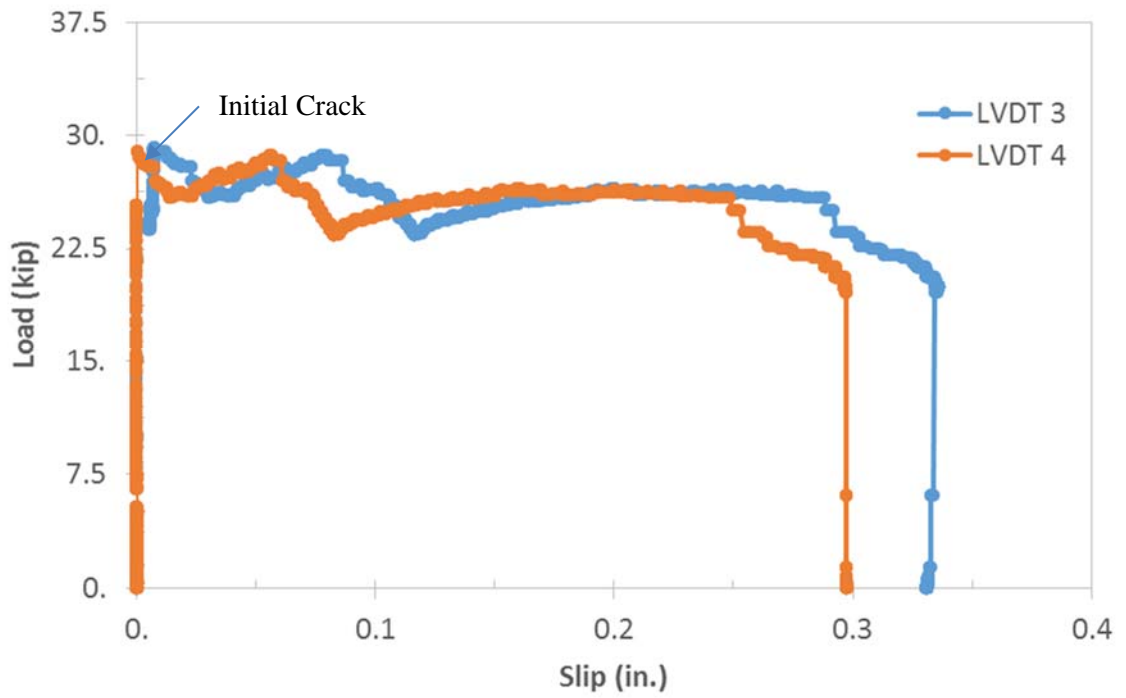
Figure 65. Load vs. Slip of C3S

Figure 66. Visual map of cracking of C3S

Figure 67. Visual map of cracking of C3S

4.1.5.3 A2SC

For Girder A2, the south end of the girder was tested first. The south end of the girder was also the end exposed to the accelerated corrosion setup. Prior to testing, photos were taken of the girder (Figure 68). Flexural cracking occurred at approximately 47 kips, and the beam failed at approximately 57 kips. The load vs. deflection graph (Figure 69) for this test illustrates that: the load-deflection relationship was mostly linear until the cracking load; after the cracking load, the curve changed its trajectory but was still relatively linear; the failure caused a large deflection of the beam. The maximum deflection was roughly 0.25 in. The girder had multiple web-shear cracks and one large flexural crack at the time of failure (Figure 70 and Figure 71). While slip was

measured during this test (Figure 72), the data did not prove reliable upon investigation after completing the shear test, and therefore is not presented.

Figure 68. Prior to testing of A2SC
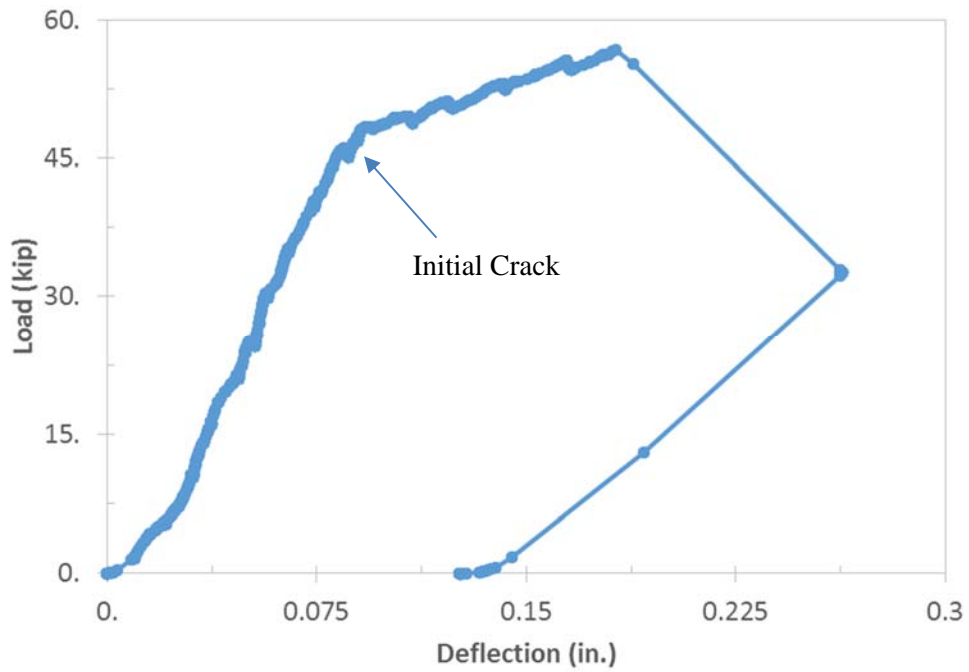
Figure 69. Load vs. Deflection of A2SC

Figure 70. Visual map of cracking of A2SC

Figure 71. Visual map of cracking of A2SC

Figure 72. Visible Slip of A2SC

For Girder A2, the north end of the girder, the control end, was tested after the corroded end. Prior to testing, photos were taken of the girder (Figure 73). Cracking occurred at approximately 25 kips. The load vs. deflection graph (Figure 74) for this test illustrates that: the load-deflection relationship was mostly linear until the cracking load; after the cracking load, the deflection increased slightly as it lost the load applied to it; the beam was reloaded several times up to the 27-29 kips range until its apparent failure; the maximum deflection was approximately 0.38 in.

The load vs. slip graph (Figure 75) shows the non-linear relationship between the load and measured slip. A bond failure occurred as the strand slip was a little greater than 0.38 in. Slip appears to have occurred after cracking, and thus did not contribute to the shear failure. Cracking along the beam went under the bottom of the beam near one of the strands (Figure 76, Figure 77, and Figure 78).

Figure 73. Prior to testing A2N
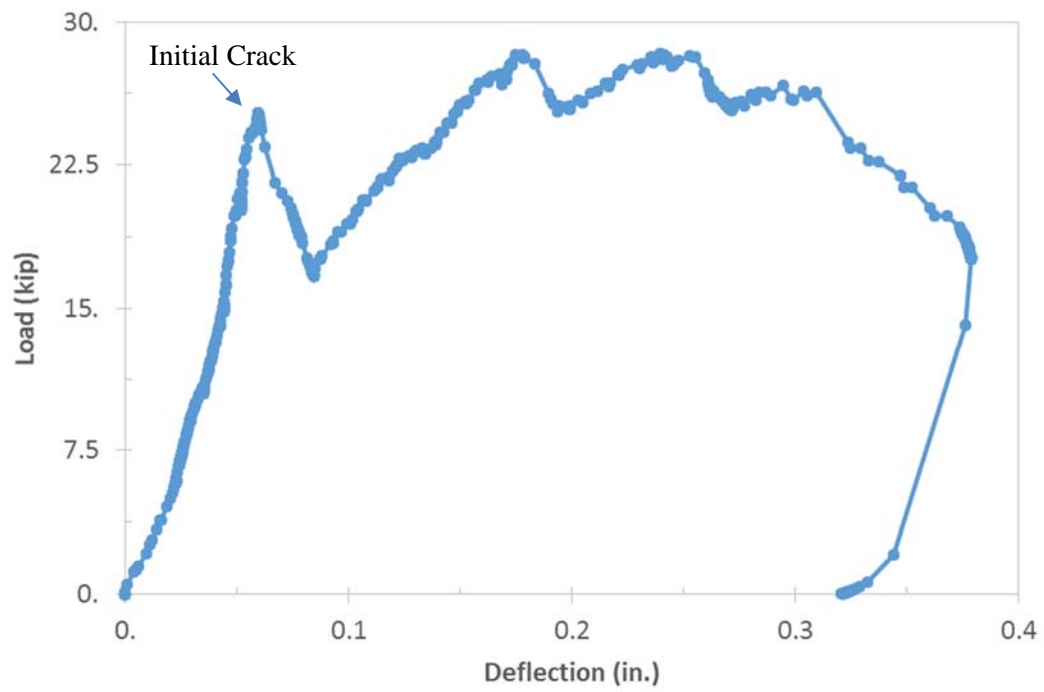
Figure 74. Load vs. Deflection of A2N
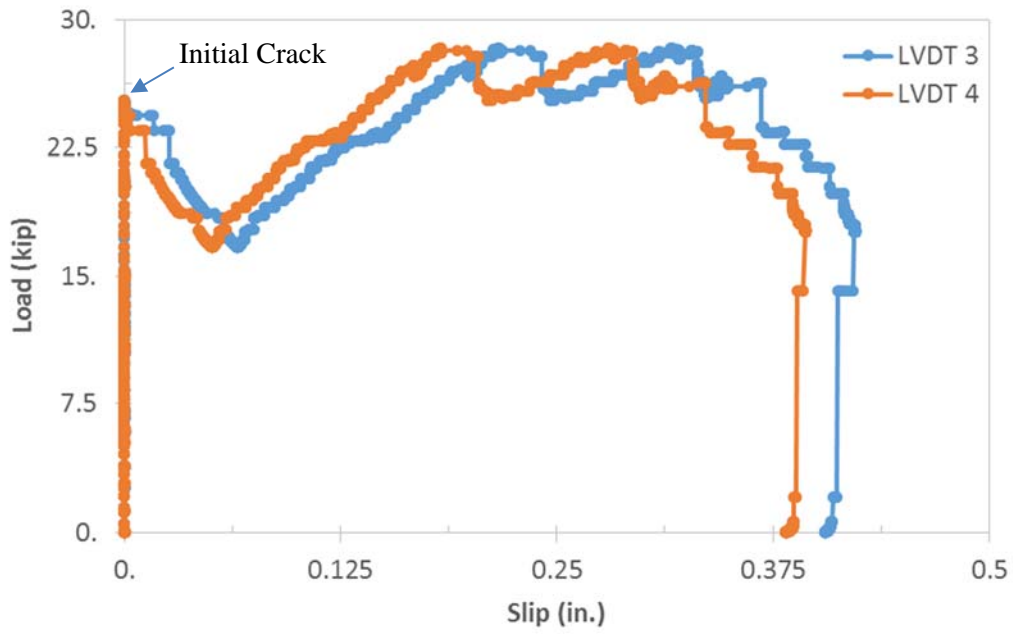
Figure 75. Load vs. Slip of A2N

Figure 76. Cracking along the flange and web of A2N

Figure 77. Cracking from bottom flange to top flange of A2N

Figure 78. Cracking near prestressing strands

4.2 Experimental Results Summary

Table 9 compares the design values to the measured values for each shear test. For example, for A4SC, the failure load of 56 kips, corresponds to a M_{max} of 113 k-ft., and a V_{max} of 36.5 kips. The design value for the shear capacity, using the LRFD 2007 method, is 45.5 kips.

Table 9. Design vs. Measured values for each shear test

	Measured			Design			
Test	Failure Load, kips	M_{max}, kip-ft	V_{max}, kips	M_n, kip-ft	V_n LRFD 2007, kips	V_n LRFD 2012, kips	V_n ACI, kips
A4SC	56	113.0	36.5	126.2	45.5	27.2	53.4
A4N	43	86.6	27.9				
C1NC	52	104.9	33.8	165.7	46.6	27.7	59.1
C1S	43	86.6	27.9				
A3SC	57	115.0	37.1	127.3	46.5	27.8	55.1
A3N	50	100.8	32.5				
C2NC	40	80.6	26.0	166.4	47.1	27.9	60.0
C2S	49	98.8	31.9				
C3NC	53	106.9	34.5	165.0	46.2	27.4	58.3
C3S	27	54.2	17.4				
A2SC	57	115.0	37.1	126.9	46.0	27.5	54.1
A2N	29	58.3	18.7				

Figure 79 illustrates for comparison the design and measured shear values for each girder. Overall, the measured shear values were less than the design shear capacity (ACI and AASHTO LRFD 2007 methods) for each girder. The measured compressive strengths were used to calculate shear capacities, which should account for the variation in compressive strength related to concrete shear strength. The a/d ratio used was 2 which is near the limiting value for the methods given by the codes which may have reduced the applicability of the code equations. Due to variation in compressive

strengths, transfer lengths may have been greater than estimated during calculation of
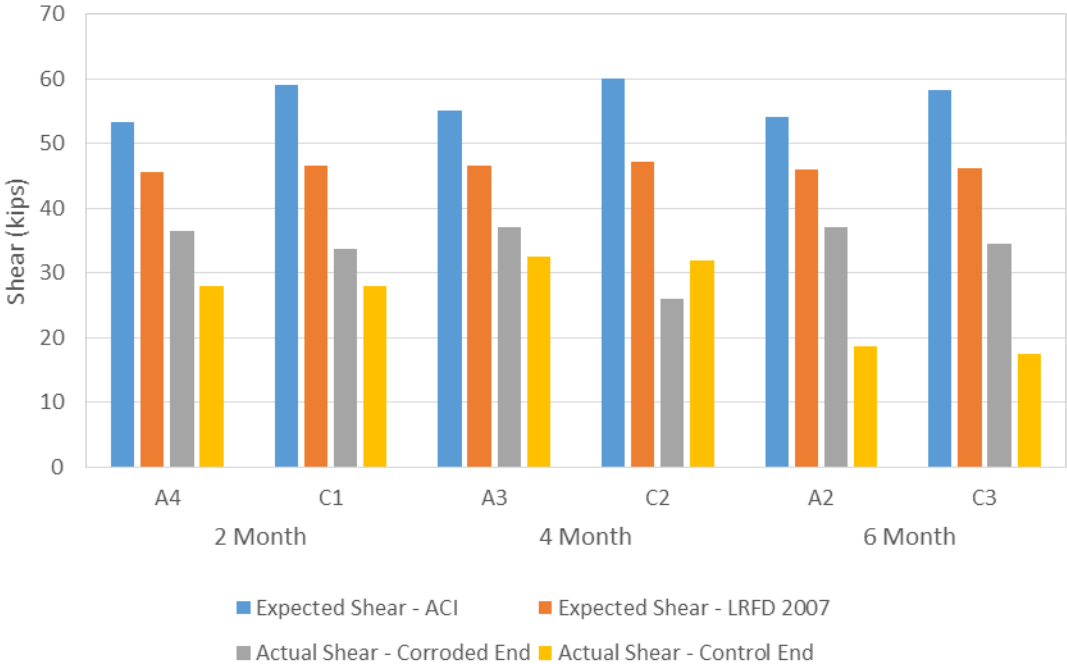
shear capacity.

Figure 79. Design Shear Capacity vs. Measured Shear at Failure

All of the corroded ends had a larger measured shear than the control end, except for

Girder C2. Similar results were shown by Abosrra et al. (2011) for minor corrosion.

With the exception of Girder C2, the corroded end of the girders were tested first. The

order of testing could have potentially impacted the condition of the beam and had an

impact on the remaining end – resulting in less resistance available. The corroded ends

of the girders may have had a larger measured shear, due to increased moisture from the

corrosion accelerant process which was applied shortly after the theoretical curing

process. For many of the girders, the prestressing strands slipped prior to cracking of the

beam, this slip is believed to have caused the beams to failure sooner than they

otherwise may have. The six-month, control ends of girders A2 and C3 had a

significantly lower actual shear than the other tested control ends. It is not immediately clear as to why this occurred.

Figure 80 and Figure 81 illustrate the varying failure loads by girder design. Overall, the corroded ends of the girders with the Girder A design, sustained a larger failure load than those corroded ends of the girders with the Girder C design. The larger diameter of the 0.6 in. strands used in the Girder C design may have contributed to earlier slip and reduced capacity. Further research could explain if the larger strands in the Girder C design contributed to being more likely to slip, and in turn fail sooner.
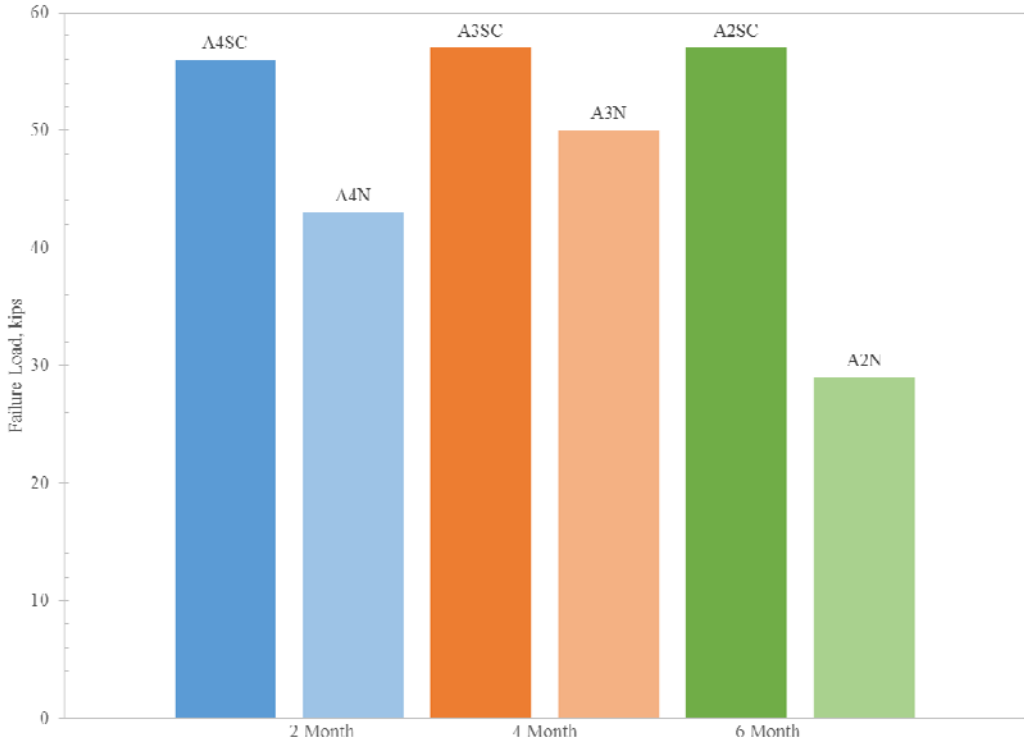
Figure 80. Failure Loads for Girder A Design
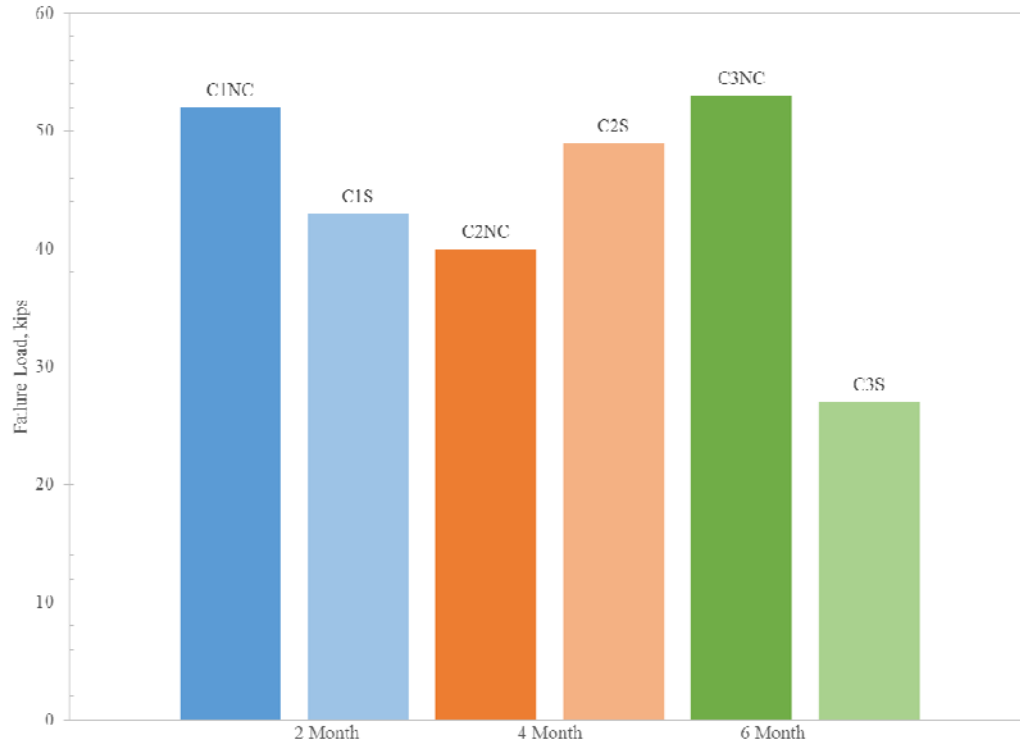
Figure 81. Failure Loads for Girder C Design

Figure 82 illustrates the comparison of the applied load at 0.01 in slip and at the

initiation of cracking of the girder for the end tested. During the testing of one end, the

other end of the girder had zero slip for the six tests where slip was measured on both

ends. Also, there were three tests that had unreliable data due to the LVDTs being

clamped to the support instead of the web of the beam and/or insufficient contact with

the strands due to the irregular surface of the corroded ends. Of note, C3S and A2N

both decreased in loading after cracking and then slip occurred at the decreased loading

(i.e., cracking occurred before slip). The girders that had unreliable slip data are not

presented in Figure 82.
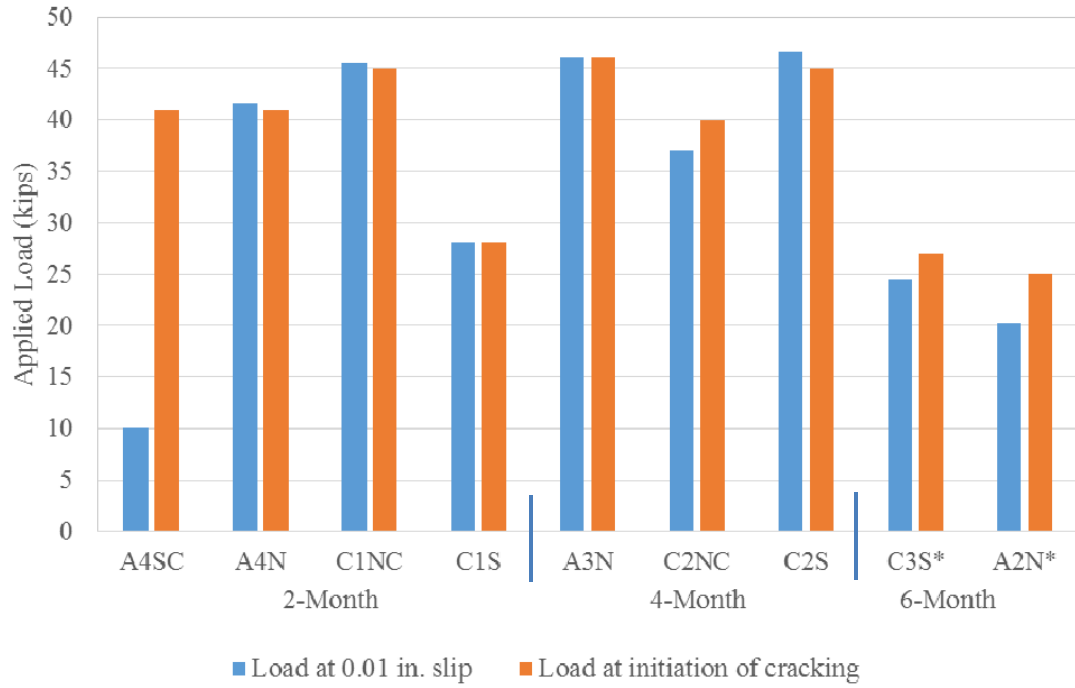
Figure 82. Comparison of load at 0.01 in. slip and initiation of cracking (*Note: C3S and A2N decreased in loading after cracking and then slip occurred at that decreased load)

4.3   Field Visits

4.3.1   Data Analysis

4.3.1.1   Structural Evaluation

The FHWA uses appraisal ratings to "evaluate a bridge in relation to the level of service which it provides on the highway system of which it is a part" (Federal Highway Administration, 1995). The structural evaluation rating compares the existing bridge to a bridge that would be built to current standards. Table 10 discusses the description for each rating used, and Figure 83 illustrates the structural evaluation ratings of bridges under the criteria used for inspection and all of the prestressed concrete girder bridges in Oklahoma built between 1960 and 1979.

Table 10. Structural Evaluation Criteria (Federal Highway Administration, 1995)

Code	Description
9	Superior to present desirable criteria
8	Equal to present desirable criteria
7	Better than present minimum criteria
6	Equal to present minimum criteria
5	Somewhat better than minimum adequacy to tolerate being left in place as is
4	Meets minimum tolerable limits to be left in place as is
3	Basically intolerable requiring high priority of corrective action
2	Basically intolerable requiring high priority of replacement
1	This value of rating code not used
0	Bridge closed
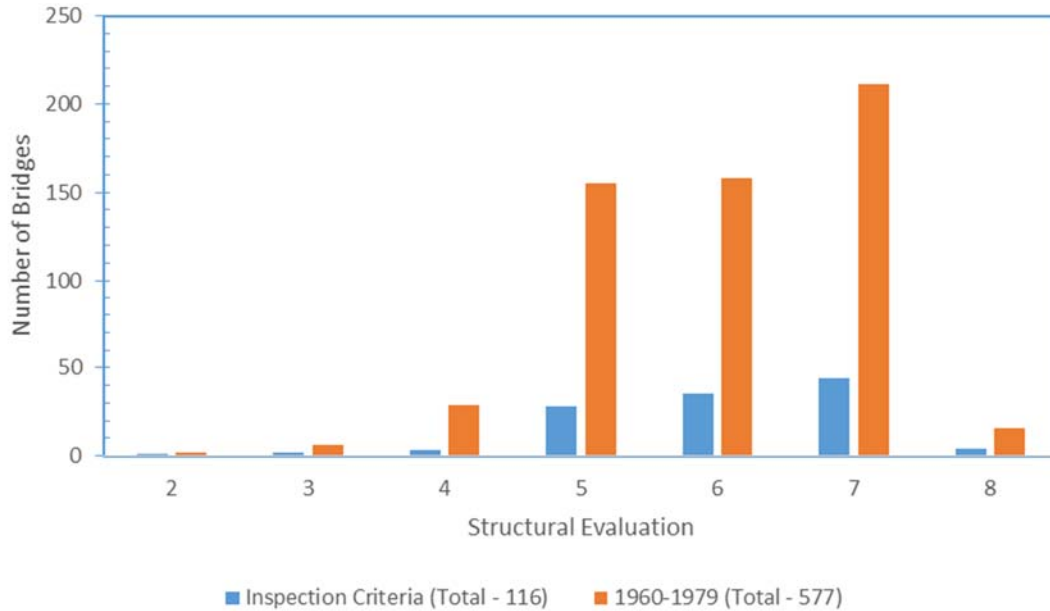
Figure 83. Oklahoma Prestressed Concrete Girder Bridges by Structural Evaluation

Of the 577 bridges built between 1960 and 1979, 94% of the bridges are better than the

minimum criteria, with some equal to the present desirable criteria. Of the remaining,

there were 29 bridges that met the minimum tolerable limits, and 8 bridges that were

considered intolerable: six requiring corrective action, and two requiring replacement.

4.3.1.2 Superstructure Condition

According to FHWA's Recording and Coding Guide for the Structure Inventory and

Appraisal of the Nation's Bridges, condition ratings are used to describe existing

bridges in relation to the original, as-built condition (Federal Highway Administration,

1995). The guide states the following in respect to condition ratings:

> *"Condition codes are <u>properly used</u> when they provide an overall*
> *<u>characterization</u> of the general condition of the <u>entire component</u>*
> *being rated. Conversely, they are <u>improperly used</u> if they attempt to*
> *describe <u>localized</u> or nominally occurring instances of deterioration*
> *or disrepair. Correct assignment of a condition code must, therefore,*
> *consider both the severity of the deterioration or disrepair and the*

91

> *extent to which it is widespread throughout the component being*
> *rated."*

The following is stated regarding superstructure condition ratings:

> *"This item describes the physical condition of all structural*
> *members… The structural members should be inspected for signs of*
> *distress which may include cracking, deterioration, section loss, and*
> *malfunction and misalignment of bearings. The condition of bearings,*
> *joints, paint system, etc. shall not be included in this rating, except in*
> *extreme situations, but should be noted on the inspection form."*

Table 11 discusses the description for each rating used, and Figure 84 illustrates the

superstructure condition ratings of bridges under the criteria used for inspection, and all

of the prestressed concrete girder bridges built between 1960 and 1979. Additional

information on the superstructure condition ratings are included in the appendix.

Table 11. Superstructure Condition Ratings (Federal Highway Administration, 1995)

Code	Description
9	Excellent Condition
8	Very Good Condition
7	Good Condition
6	Satisfactory Condition
5	Fair Condition
4	Poor Condition
3	Serious Condition
2	Critical Condition
1	"Imminent" Failure Condition
0	Failed Condition
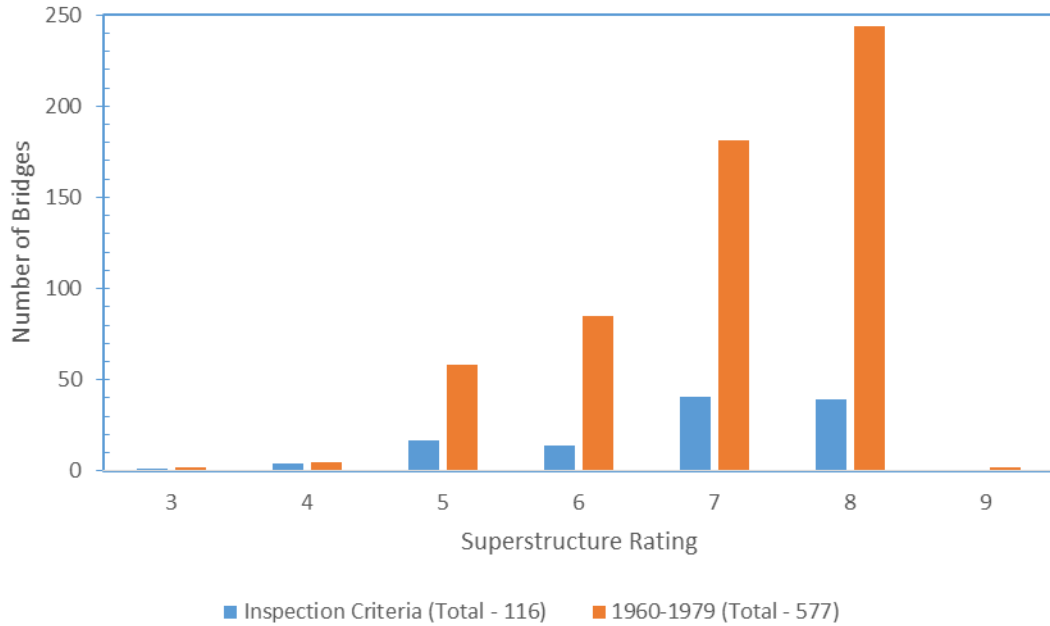
Figure 84. Oklahoma Prestressed Concrete Girder Bridges by Superstructure Rating

Of the 577 bridges built between 1960 and 1979, almost 99% of the bridges have superstructure ratings equal to or better than fair condition. There were five bridges rated in poor condition, and two bridges in serious condition.

4.3.1.2.1 Ownership and Superstructure Ratings

The vast majority of the prestressed concrete girder bridges, constructed in 1960-1979, are under the ownership and maintenance responsibilities of either ODOT or the Oklahoma Turnpike Authority (OTA). The two agencies serve as the agencies responsible for intrastate travel within Oklahoma. ODOT is broken into eight field divisions that have maintenance and construction responsibilities in the respective jurisdictions. ODOT maintains the majority of the highway system, and OTA maintains the Oklahoma turnpike system. Figure 85 illustrates prestressed concrete girder bridges built between 1960 and 1979 by superstructure rating and ownership. During this timeframe, ODOT built 287 bridges while OTA built 164 bridges.
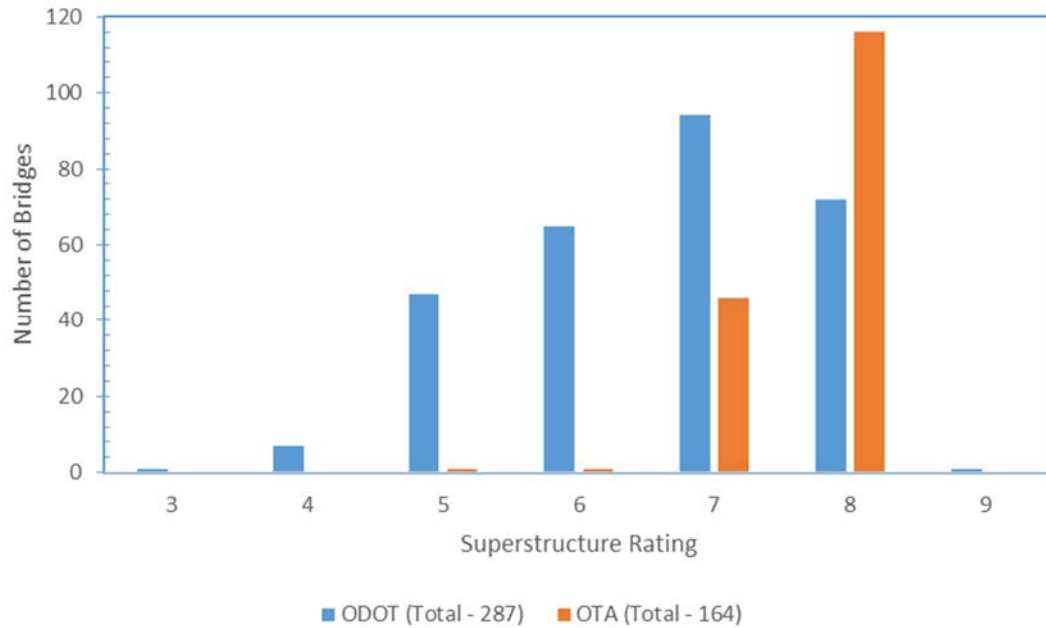
Figure 85. Oklahoma Prestressed Concrete Girder Bridges (1960-1979) by Superstructure Rating and Ownership

Almost all of the applicable OTA bridges were rated in either good or very good condition. The ODOT bridges had more reasonable variability given the age of the bridges where many were considered good or very good, but also more reasonably rated as fair or satisfactory condition. Figure 86 illustrates the breakdown of ownership for applicable bridges built between 1960 and 1979. While having higher superstructure ratings, the OTA bridges were generally older than the ODOT bridges. Further research should consider the maintenance per bridge spent at OTA vs. ODOT, as a possible indicator to the varied success; or differences in inspection opinion.
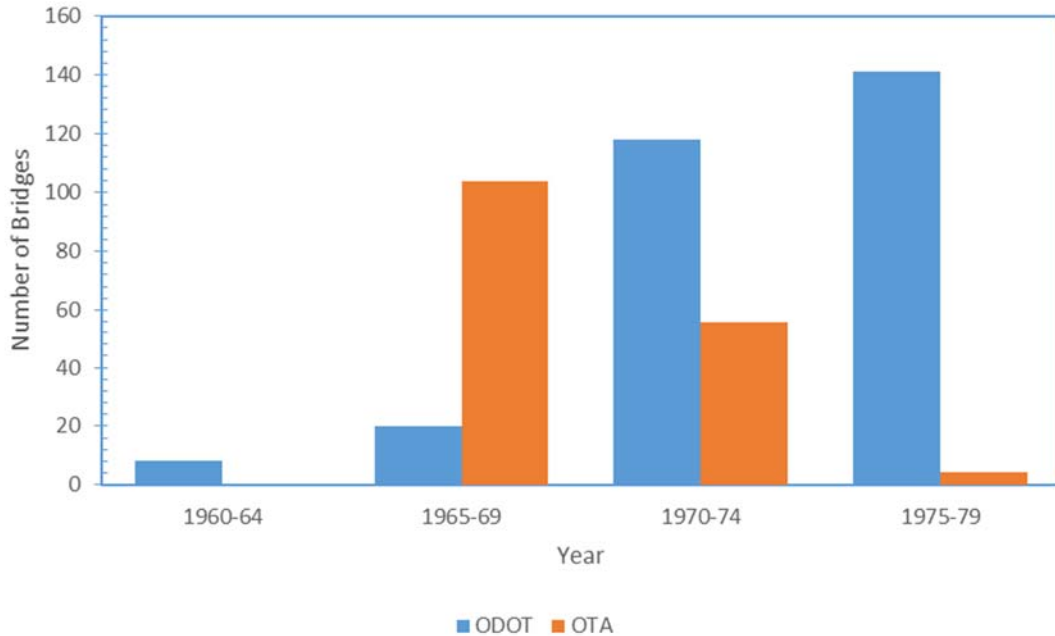
Figure 86. Oklahoma Prestressed Concrete Girder Bridges Ownership (1960-1979)

4.3.1.2.2 Field Divisions and Superstructure Ratings

As mentioned previously, ODOT is broken into eight field divisions that have

maintenance and construction responsibilities within their respective jurisdictions. For

the 1960 – 1979 timeframe, as Figure 87 shows, most of the prestressed concrete

bridges in Field Divisions 1, 2, 4, and 7 were considered in good or very good

condition. Field Division 8 had a reasonable distribution between poor and very good

condition. Field Divisions 1, 2, 4 and 7 had sharp drops in bridges that were considered

to be in fair condition or less. Funding and maintenance could play a part in why there

were greater proportions of the bridges in favorable conditions in those regions, or

potentially differences in inspections. Interestingly, OTA accounted for the majority of

the bridges constructed in 1960-1979 in Field Divisions 1 and 2, and approximately

50/50 with ODOT in Field Division 4.
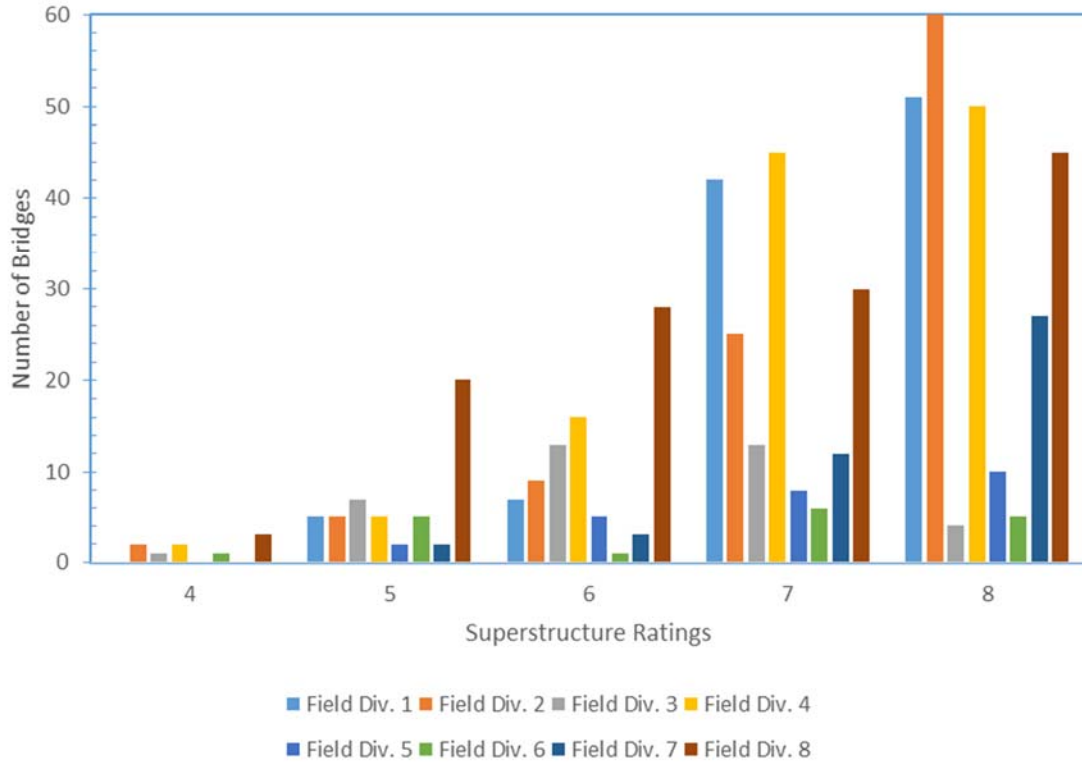
Figure 87. Oklahoma Prestressed Concrete Girder Bridges (1960-1979) by Superstructure Rating and Field Division

4.3.2 Visual Inspection

A total of 19 bridges were inspected through five site inspections to serve as a survey of

the prestressed concrete girder bridges constructed from 1960 – 1979 in Oklahoma. The

five site visits took place in five different ODOT Field Divisions. A thorough discussion

of each bridge visit can be found in the Appendix. During the inspections, various

deterioration characteristics were found at multiple sites. The following sections

summarize those characteristics and hypothesizes their origins.

4.3.2.1 Corroded Bearing Plates

Many of the bridges inspected had corroded bearing plates; the corrosion, however,

ranged from an initial stage to heavily corroded with expansion of the steel. Heavily

corroded bearing plates had a "flaky" appearance to them – likely providing little to no

structural support. The steel in the bearing plate had corroded to the point where a few layers were held together in the center, but no cohesion was provided at the edge. Figure 88 is an example of a corroded bearing plate.

The bearing plates rested right on the concrete abutment of the bridge. The location of the bearing plates, also coincide with the end of the beams, which allow for potential drainage from the deck to fall, and pool near the bearing plates. The bearing plates are also exposed to the elements and could be impacted by eroded materials introduced by wind or liquid flow. Of many of the features inspected, the bearing plates were aesthetically the most displeasing.

Figure 88. Example of corroded bearing plate

The anchor bolts and nuts for many of the bridges were also corroded. It was very likely

for a corroded anchor bolt to be found through a corroded bearing plate. The corroded

anchoring system, much like the bearing plates, hypothetically could not provide much

structural support due to the level of corrosion and deterioration of the members. The

anchor bolts may also have been subjected to ponding of water and other liquids, as

well as just the effects of being exposed to the elements. Figure 89 is an example of a

corroded anchor bolt.

Figure 89. Example of corroded anchor bolt

In one observed case, deteriorated and necking members were coated to prevent further

corrosion and damage (Figure 90). It was not immediately apparent the significance and

effect of coating the anchor bolts and nuts that had already suffered severe deterioration without replacing them.

Figure 90. Example of coated, damaged anchor bolt and nut

4.3.2.3 Spalling above Support

The corroding bearing plates, almost always resulted in spalling of the concrete on the bottom of the girder directly above the bearing plate. The observed spalling correlated with the degree of corrosion exhibited on the bearing plates. The rusting coloration associated with corrosion could be found on much of the concrete that came in contact with the corroded bearing plates. Figure 91 is an example of spalling above the bearing support.

Figure 91. Example of spalling above bearing support

In many cases, the spalling also resulted in cracks emanating from the deteriorating

area.

Figure 92 is an example of cracking surrounding damage above a bearing support.

Figure 92. Example of crack from damage around the bearing plate

4.3.2.4   Exposed Rebar and Prestressing Strands

Deterioration of concrete typically leaves the embedded materials exposed to the

elements. This exposure provides an opportunity for further corrosion of the embedded

steel, and further deterioration of the concrete structure. Exposed steel that begins to

corrode, such as shown in Figure 93, likely does not have adequate bonding to provide

any actual strength to the member at hand. Figure 94 is an example of exposed

prestressing strands.

Figure 93. Example of exposed steel

Figure 94. Example of exposed prestressing strands

4.3.2.5   Diagonal Crack at Back Corner of Girder

At the back corner of many of the prestressed girders visited, there was a diagonal crack that often resulted in a considerable amount of concrete missing from this area. This commonly noted deterioration characteristic is not immediately explainable like many of the previous characteristics. The common "back diagonal crack" typically led to insufficient concrete cover exposing the embedded steel materials to extreme environments. For most bridges where this characteristic was observed, many of the aforementioned deterioration characteristic were also present: corroding bearing plates, anchor bolts, and nuts; spalling above the support; and exposed steel. The "back diagonal crack" characteristic took many forms as Figure 95 and Figure 96 depict.

Figure 95. Example of back diagonal cracking/spalling

103

Figure 96. Example of back diagonal cracking

4.3.2.6   Vertical Cracking along Girder and Diaphragm Interface

Many of the prestressed girders were connected to a diaphragm that spanned multiple

girders at the ends of the spans. In many cases, there was a vertical separation

(cracking) between the diaphragm and girder, as shown in Figure 97. The separation

could likely be attributed to a weak point created during the construction process where

the elements were formed separately and cast at different times. Opposing movements

of the two structural elements may also have occurred due to temperature, shrinkage,

and creep effects causing cracking in that location. A crack at this location could

potentially allow water and chlorides to penetrate to the prestressing strand ends.

Figure 97. Example of vertical cracking along diaphragm and girder

4.3.2.7   Horizontal Cracking along Top Flange and Web Interface

Horizontal cracking was observed along the interface of the top flange and web many times, as shown in Figure 98 and Figure 99. The horizontal cracking may have occurred due to differential movement caused by shrinkage or high stresses resulting from the eccentric prestress force or release forces. The exact cause of these cracks was not explicitly apparent.

Figure 98. Example of horizontal cracking along the top flange and web interface

Figure 99. Example of horizontal cracking along the top flange and web interface

4.3.2.8 Diagonal Cracking from the Top Flange and Web Interface

Another frequently noted deterioration characteristic was diagonal cracking that

emanated from the top flange and web interface, shown in Figure 100 and Figure 101.

The cause of the diagonal cracking was not immediately apparent, but may be related to

stresses caused by the eccentric prestress. The cracks were generally small in width and

had varying lengths.

Figure 100. Example of diagonal cracking from the top flange and web interface

Figure 101. Example of diagonal cracking from the top flange and web interface

4.3.2.9   Diaphragm Deterioration

While not exactly pertinent to the structural health of the prestressed girders, it is worth

mentioning that many of the diaphragms spanning the girders were in a deteriorated

state. Many seemed to have insufficient concrete cover, leading to exposed rebar, and initiation of corrosion, as shown in Figure 102 and Figure 103.

Figure 102. Example of Diaphragm deterioration

Figure 103. Example of Diaphragm deterioration

Overall, the girders subjected to the corrosion accelerant process did not exhibit many of the common factors noticed in girders visited in the field. Those corroded ends exhibited the common rusting discoloration, as well as the initiation of corrosion impacting the prestressing strands. In general, the deterioration in the field was frequent, but visually seemed much worse.

5   Summary, Conclusions, and Recommendations

5.1   Summary

Over the course of this research, nine half-scale AASHTO Type II girders were designed, constructed, and exposed to varying levels of a corrosive environment through a corrosion accelerant process. The varying levels of exposure to the end zone of the girders replicated the various environmental conditions a bridge girder could be exposed to in the field. The girders were designed with two different reinforcement configurations (Girder A and Girder C design) to create similar stress states to a recently decommissioned prestressed concrete girder bridge in Oklahoma built within 1960-1979. Six of the half-scale girders were shear tested to determine what, if any effect the end zone deterioration has on the shear capacity of the girder. The remaining three half-scale girders that were exposed to the various environmental conditions will form the basis of additional research discussed later in this section. Of the six shear tests on the corroded end of the girders, four resulted in slip of the prestressing strands prior to the initial crack of the beam. For the control end of the girders, all six shear tests (both Girder A and Girder C designs) illustrated cracking of the girder prior to the initiation of slip. The control end of the girders cracking prior to slip shows that bonding was not affected in the same manner as the corroded end. The two most common failure mechanisms were: bond-shear failure (either cracking before slip or slip before cracking) and bond-shear/flexure failure where cracking occurred before slip and the flange deteriorated.

Shear tests resulted in measured shear values less than the design shear capacity for each girder in all cases (i.e., corroded and control end) when compared to the ACI and

AASHTO LRFD 2007 methods. The designed shear capacities were calculated using actual girder dimensions and measured compressive strengths. The a/d ratio used was 2 which is near the limiting value for the methods given by the codes which may have reduced the applicability of the code equations. All of the girder ends that had been exposed to the corrosive environment had a larger measured shear than the control end, except for one girder (Girder C2). Similar results were shown by Abosrra et al. (2011) for minor corrosion. The percent difference between the measured and design shear values ranged from 21–32% below expectation for the corroded ends not including Girder C2 which was 58% below expectation. For the control end, the percent difference had a much larger range – from 35–91% below expectation. These results may be due to several issues. The corroded ends may have sustained a larger load because the moisture from the corrosion accelerant process actually helped the girders cure longer. With the exception of Girder C2, the corroded end of the girders were tested first. The order of testing could have potentially impacted the condition of the beam and had an impact on the remaining end – resulting in less resistance available. While the measured compressive strengths were used to calculate the shear capacities, variation in the measured strengths could have caused transfer lengths greater than estimated during calculation of shear capacity.

Overall, the corroded ends of the girders with the Girder A design, sustained a larger failure load than those corroded ends of the girders with the Girder C design. Based on the results, the larger prestressing strands in the Girder C design could have been more susceptible to slip, causing the beam to fail sooner than the smaller prestressing strands used in the Girder A design. Larger diameters of reinforcement and prestressing strands

require larger anchorage lengths per the ACI and AASHTO LRFD codes, which supports this possibility. Further research would be necessary to prove if this indeed was the reason.

Concurrently with the lab experiments, a total of 19 bridges were inspected through five site inspections to serve as a survey of the prestressed concrete girder bridges constructed from 1960 – 1979 in Oklahoma. The five site visits took place in five different Oklahoma Department of Transportation (ODOT) Field Divisions. During the inspections, various deterioration characteristics were found at multiple sites. Those deterioration characteristics include: corroded bearing plates; corroded anchor bolts and nuts; spalling above the support; exposed rebar and prestressing strands; diagonal cracking of the back corner of the girder; vertical cracking along the girder and diaphragm interface; diagonal cracking from the top flange and web interface; and diaphragm deterioration. In reviewing the National Bridge Inventory data, there was variance in superstructure condition ratings between bridges owned by ODOT and those owned by the Oklahoma Turnpike Authority. It was not immediately clear if this variance was a result of deferred maintenance and lack of funding, or differences in inspector opinions among the entities.

Together, the observations from the field inspections and the lab experiments were used to analyze existing retrofit methods and determine recommendations for in-situ rehabilitation for varying levels of deterioration. Fiber reinforced polymer, such as carbon fiber reinforced polymer systems (e.g., sheets, U-wraps, and strips) were identified as a viable option for increasing strength of girders damaged in the field.

Available literature reviewed showed improved strength (flexural and shear) for repaired members in comparison to those unrepaired.

While this research effort has been largely inclusive in the data sought and presented, the results are expected to be similar only to the work performed during this analysis. Any differences in girder designs, concrete mix, bridge configurations, etc. could cause a variation from the results presented in this thesis.

5.2 Conclusions

The following conclusions can be drawn from the results obtained during the research discussed in this thesis:

- The corroded ends of the members exhibited larger measured shear strengths for the conditions tested.

- The difference in measured and design shear strengths could be attributed to: the variation in compressive strengths; an a/d ratio near the limit for the methods used; and potential variations in transfer length related to compressive strength.

- All of the shear failures included the effects of strand slip and the tests of corroded ends indicated that strand slip occurred prior to cracking, while the tests of the control ends indicated cracking occurred prior to strand slip.

- Common deterioration characteristics were observed at various bridges across the State of Oklahoma but did not appear to correlate with the superstructure ratings.

5.3 Recommendations

As a result of the work reported in this thesis, the following items are recommendations and topics for future research:

- Further analysis of the benefits associated with prestressed girders exposed to corrosive environments will take place as part of a larger research effort that this thesis does not discuss. The remaining three half-scale girders that were exposed to the various environmental conditions will be repaired on the corroded end and then shear tested on both ends. The shear tests will provide an opportunity to analyze the benefit of the exposed, repaired end to the unrepaired, control end of the girder.

- The effect of the order of testing of the corroded and control ends on the shear capacity should be investigated further.

- A larger number of specimens and more heavily corroded members should be tested to better understand the effects of corrosion on shear capacity.

- The effects of larger prestressing strands to be more susceptible to strand slip, causing the beam to potentially fail sooner than smaller prestressing strands should be investigated further.

- It is recommended that for end girders exposed to chloride-laden water that caution is taken to prevent the initiation of extreme deterioration though preventative maintenance of the metal bearing plates, anchor bolts and nuts such as use of a protective coating system. Those that have begun the deterioration process would benefit from repair to the member such as patching, coupled with

the use of a fiber reinforced polymer, particularly near the end of the girder to

increase the shear strength.

6 References

Abosrra, I., Ashour, A., & Youseffi, M. (2011, May 23). Corrosion of Steel Reinforcement in Concrete of Differenct Compressive Strengths. *Construction and Building Materials*.

Almusallam, A. A. (2001, January 5). Effect of degree of corrosion on the properties of reinforcing steel bars. *Construction and Building Materials*, 361-368.

Basham, K. (2015, March 16). Delve Into Two Theories Related to Cracks and Rebar Corrosion. *Concrete Contractor*. Retrieved March 20, 2015, from ForConstructionPros.com: http://www.forconstructionpros.com/article/12039769/delve-into-two-theories-related-to-cracks-and-rebar-corrosion

Bruce, S. M., McCarten, P. S., Freitag, S. A., & Hasson, L. M. (2008). *Deteoriation of Prestressed Concrete Bridge Beams.* Land Transport New Zealand Research Report 337.

Cai, C., & Miao, X. (2015). *Repairing/Strengthening of Bridges with Post-tensioned FRP materials and Performance Evaluation.* Louisiana State University. Louisiana Transportation Research Center.

Chou, G. K., & Hover, K. C. (1987, January). Cathodic Protection for Prestressed Structures. *Concrete International*, pp. 26-30.

Coggins, F. B., & French, C. W. (1990, September - October). Chloride Ion Distribution in Twenty-Year-Old Prestressed Bridge Girders. *ACI Materials Journal, 87*(5), 479-488.

Cranor, B. (2015). *Analysis and Experimental Testing for Shear Behavior of an AASHTO Type II Girder in Service for Several Decades.* MS Thesis.

Darwin , D., Browning, J., Van Nguyen, T., & Locke, Jr. , C. (2002). *Mechanical and Corrosion Properties of a High-Strength, High Chromium Reinforcing Steel for Concrete.* University of Kansas Center for Research, Inc.

Dinges, T. (2009). *The History of Prestressed Concrete: 1888 to 1963.* Kansas State University, College of Engineering, Manhattan.

ElBatanouny, M. K., Mangual, J., Ziehl, P. H., & Matta, F. (2014, March 1). Early Corrosion Detection in Prestressed Concrete Girders Using Acoustic Emission. (ASCE, Ed.) *Journal of Materials in Civil Engineering, 26*(3), 504-511.

ElSafty, A. (2013, April). Getting Clearance: CFRP U-wrapping shows promise as a repair option. *Roads & Bridges*, pp. 22-27.

Fasl, J., Larosche, C. J., & Fraczek, J. (2016, April 1). Ductility Behavior of Corroded Bars in Concrete Slabs. *Concrete International*, pp. 55-61.

Federal Highway Administration. (1995). *Recording and Coding Guide for the Structure Inventory and Appraisal of the Nation's Bridges.* Washington, D.C.

Higgins, C., Williams, G., Mitchell, M., Dawson, M., & Howell, D. (2012, November-December). Shear Strength of Reinforced Concrete Girders with Carbon Fiber-Reinforced polymer: Experimental Results. *ACI Structural Journal, 109*(6), 805-814.

International Federation for Structural Concrete. (2001). *Design and Use of Externally Bonded Fibre Reinforced Polymer Reinforcement (FRP EBR) for Reinforced Concrete Structures.* Lausanne: International Federation for Structural Concrete.

Merrill, B. D., Keske, S., & McGormley, J. (2015). *Girder Anchorage Zone Crack Investigation - Interim (Phase 1) Report.* Oklahoma City: Oklahoma Department of Transportation.

MIT OpenCourseWare. (2008, November 21). *Reinforced and Prestressed Concrete.* Retrieved from Flickr.com: https://www.flickr.com/photos/mitopencourseware/3048302726/

Mukherjee, A., & Rai, G. (2009). Performance of Reinforced Concrete Beams Externally Prestressed with Fiber Composites. *Construction and Building Materials, 23*(2), 822-828.

Nawy, E. G. (2010). *Prestressed Concrete: A Fundamental Approach.* Upper Saddle River, New Jersey: Prentice Hall.

Novokshchenov, V. (1989, September). Condition Survey of Prestressed Concrete Bridges. *Concrete International*, pp. 60-68.

Pape, T. M., & Melchers, R. E. (2013, November). Performance of 45-year-old corrdoed prestressed concrete beams. *Structures and Buildings, 166*(SB10), 547-559. doi:http://dx.doi.org/10.1680/stbu.11.00016

Pritzl, M. D., Tabatabai, H., & Ghorbanpoor, A. (2014, September). Laboratory Evaluation of Select Methods of Corrosion Prevention in Reinforced Concrete Bridges. *International Journal of Concrete Structures and Materials, 8*(3), 201-212.

Ray, I., Parish, G. C., Davalos, J. F., & Chen, A. (2011, April 1). Effect of Concrete Substrate Repair Methods for Beams Aged by Accelerated Corrosion and Strengthened with CFRP. *Journal of Aerospace Engineering, 24*(2), 227-239.

Rogers, R. A., Wotherspoon, L., Scott, A., & Ingham, J. M. (2012). Residual strength assessment and destructive testing of decommissioned concrete bridge beams

with corroded pretensioned reinforcement. *PCI Journal*(Summer 2012), 100-118.

Smith, J. L., & Virmani, Y. P. (2000). *Materials and Methods for Corrosion Control of Reinforced and Prestressed Concrete Structures in New Construction (FHWA-RD-00-081).* McLean: U.S. Department of Transportation, Federal Highway Administration.

Song, G., & Shayan, A. (1998). *Corrosion of steel in concrete: causes, detection and prediction: a state-of-the-art review.* ARRB Transport Research Ltd. Review Report 4.

Szilard, R. (1969, January). Corrosion and Corrosion Protection of Tendons in Prestressed Concrete Bridges. *ACI Journal*, 42-59.

Transportation Research Board. (2016). *TRID Database*. Retrieved from Transportation Research Board Website: https://trid.trb.org/view.aspx?id=1329302

Vu, K., Stewart, M. G., & Mullard, J. (2005, September-October). Corrosion-Induced Cracking: Experimental Data and Predictive Models. *ACI Structural Journal, 102*(5), 719-726.

7 Appendix

7.1 Beam "A" and Beam "C" Drawings

From "Sections Prestressed Concrete Girders FAP 244-2(134)093, Sheet No. 44, Revision #6" Drawing
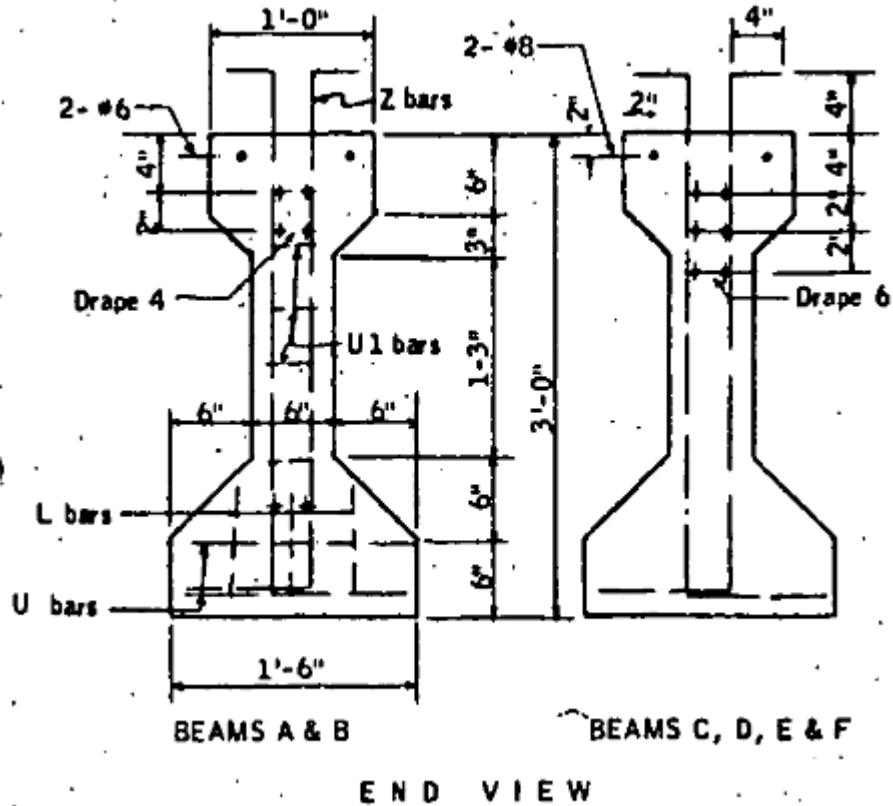
Figure 104. End view of Beam "A" and Beam "C"
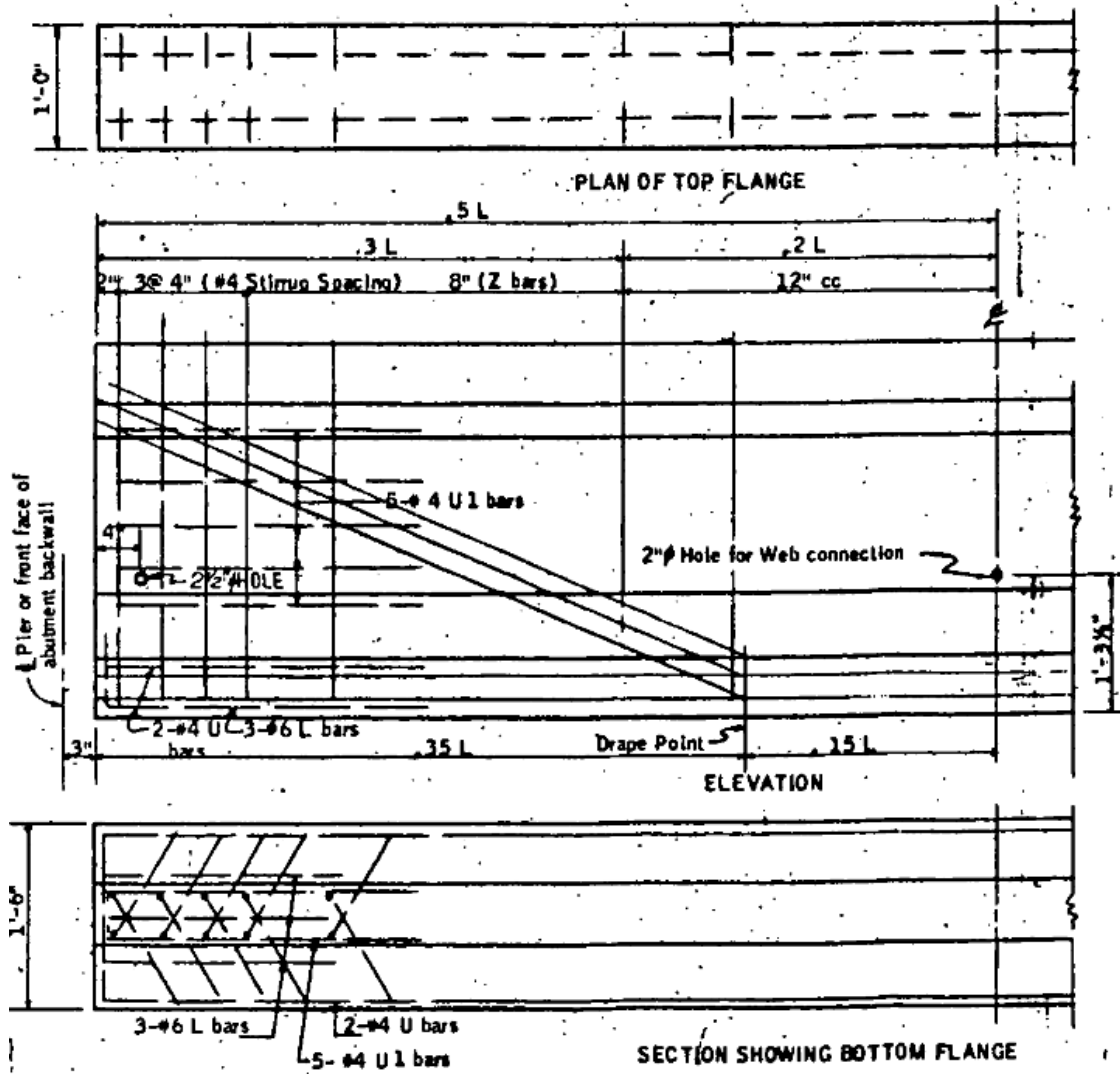
Figure 105. Span of Beam "A" and Beam "C"
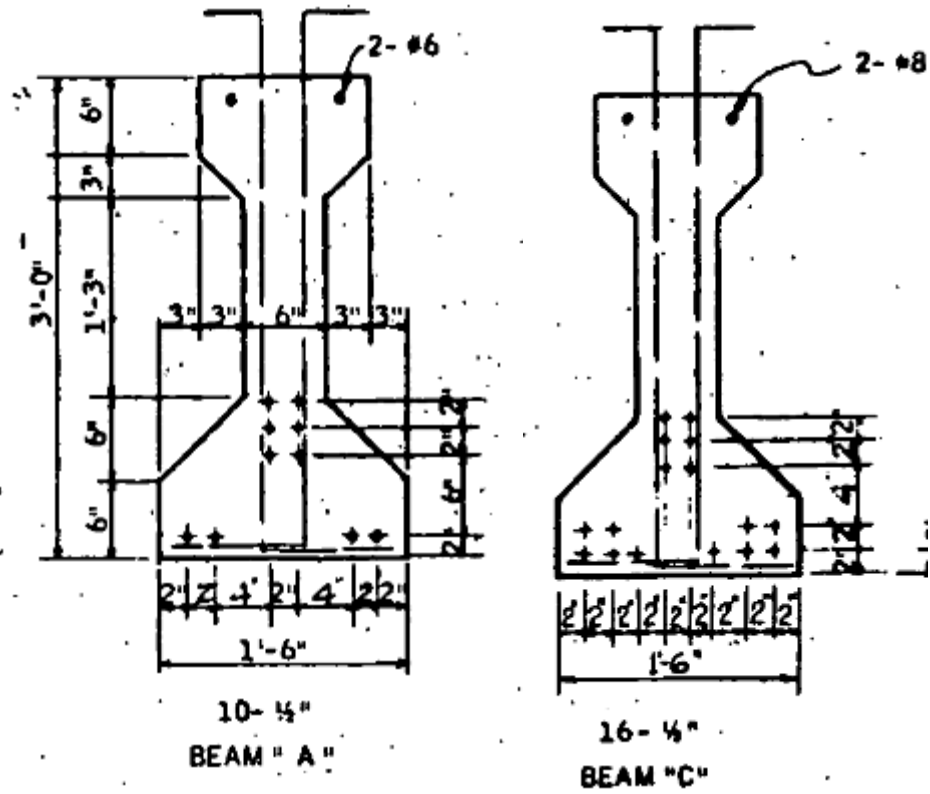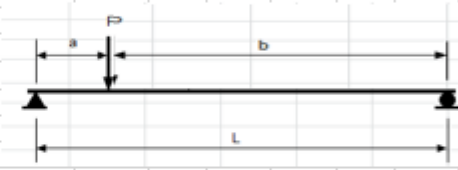
Figure 106. Midspan view of Beam "A" and Beam "C"

122

7.2   Girder Design

Girder A

Type	2	1=Type 2 AASHTO Girder, 2= Type 2 AASHTO Girder (1/2 scale), 3=46' Girder, 4
Length	18	

Pretension or Post-tension?	Pretension	if Post-tension, time after moist	
Low Relaxation Strands?	No	cure to prestress application?	
Tendon Type	1		

Dimensions (inches)

TYPE	Girder	D1	D2	D4	D5	D6	D7	B1	B2	B3	B4	B6
2	AASHTO Type II (half-scale) w/o Deck	22.5	3	1.5	3	3	12	6	9	3	1.5	3

Additional Loads

w_d (lb/ft)	0.00	
P_l (kips)	0.00	
Distance between supports (ft	9.000	
Tributary width of girders (ft)	0	

Stirrup Spacing

Location (ft)	0	0	0.667	5.4	9
Spacing (in)		1	2	4	6
A_v (in²)	0.11				

Prestress Draping Strands

Drape Length (ft)	0
Drape Height (in.)	0
Strands Draped (#)	0

*Location from bottom of girder

Strand Location at Ends

Row (in.)	2	4	6	8	10	12	14	16	18	20	22	24
# Strands	0	2	0	0	0	0	0	0	0	0	0	0

Strand Location at Mid Span

Row (in.)	2	4	6	8	10	12	14	16	18	20	22	24
# Strands	0	2	0	0	0	0	0	0	0	0	0	0

Concrete Properties	
f'_{ci} (psi)	4000
f'_c (psi)	6000
Unit Weight (pcf)	150
Lightweight Coefficent, λ	1.00

Mild Steel Properties	
d' (in)	2
f_y (ksi)	60
A's (in2)	0.88

Prestress Properties	
Loss Method	Gross
f_{pu}	270
f_{py}	229.5
f_{pi}	186
Strand Type	0.52
Relative Humidity	70
E_{ps} (ksi)	28500

	Tendon Type
1	Gr. 270 Stress-Relieved Strand or Wire
2	Gr. 250 Stress-Relieved Strand or Wire
3	Gr. 240 or 235 Stress Relieved Wire
4	Gr. 270 Low-Relaxation Strand
5	Gr. 250 Low-Relaxation Wire
6	Gr. 240 or 235 Low-Relaxation Wire
7	Gr. 145 or 160 Stress Relieved Bar

ACI Shear Capacity Calculation				
Properties				**Loadings**
Type	2			
cgs (in.)	4			
h (in.)	22.5			
d_p (in.)	18.50			
d' (in.)	2.00			
b_w (in.)	3			
w_d (k/ft)	0.110			
w_l (k/ft)	0.000			
P (kips)	62.365	62.365		
A_g (in^2)	105.75			
A_{ps} (in^2)	0.33			
L (ft) supports	9		**Simplified Shear**	
l_c (ft)	3.083333333		V_c (kips)	41.43
a (ft)	3.083333333		V_{min} (kips)	8.60
b (ft)	5.92		V_{max} (kips)	21.50
V_{de} (kips)	0		**Detailed Shear**	
$V_{d(-support)}$ (kips)	0.99140625		V_{ci} (kips)	26.14
$V_{d(+support)}$ (kips)	0.991		$V_{ci,min}$ (kips)	7
V_{dc} (kips)	-0.340		V_{cw} (kips)	23.7
M_{dc} (k-ft)	-0.523624674		**Final**	
V_{ue} 1 (kips)	40.99921296		V_c (kips)	23.66
V_{ue} 2 (kips)	21.36578704		V_s (kips)	30.525
V_{uc} (kips)	40.65956452546		V_n (kips	54.18
M_{cu} (k-ft)	125.8906153		ϕV_n (kips)	40.63522
V_i (kips)	40.999		M_n (k-ft)	126.4149
M_{max} (k-ft)	126.41424			

Girder C

Type	2	1=Type 2 AASHTO Girder, 2=Type 2 AASHTO Girder (1/2 scale), 3=46' Girder, 4
Length	18	

Pretension or Post-tension?	Pretension	if Post-tension, time after moist
Low Relaxation Strands?	No	cure to prestress application?
Tendon Type	1	

Dimensions (inches)

TYPE	Girder	D1	D2	D4	D5	D6	D7	B1	B2	B3	B4	B6
2	AASHTO Type II (half-scale) w/o Deck	22.5	3	1.5	3	3	12	6	9	3	1.5	3

Additional Loads

w_d (lb/ft)	0.00
P_1 (kips)	0.00
Distance between supports (ft	9.000
Tributary width of girders (ft)	0

Stirrup Spacing

Location (ft)	0	0	0.667	5.4	9
Spacing (in)		1	2	4	6
A_v (in^2)	0.11				

Prestress Draping Strands

Drape Length (ft)	0
Drape Height (in.)	0
Strands Draped (#)	0

*Location from bottom of girder

Strand Location at Ends

Row (in.)	2	4	6	8	10	12	14	16	18	20	22	24
# Strands	0	2	0	0	0	0	0	0	0	0	0	0

Strand Location at Mid Span

Row (in.)	2	4	6	8	10	12	14	16	18	20	22	24
# Strands	0	2	0	0	0	0	0	0	0	0	0	0

127

Concrete Properties			
f'_{ci} (psi)	4000		
f'_c (psi)	6000		
Unit Weight (pcf)	150		
Lightweight Coefficent, λ	1.00		

Mild Steel Properties			
d' (in)	2		
f_y (ksi)	60		
A'_s (in2)	0.88		

Prestress Properties			
Loss Method	Gross		
f_{pu}	270		
f_{py}	229.5		
f_{pi}	202.5		
Strand Type	0.6		
Relative Humidity	70		
E_{ps} (ksi)	28500		

Time			
Days when prestress strands are released			1
Days when curing stops			1
Days from release that deck was placed			28
Days since girder batched			17155

ACI Shear Capacity Calculation					
Properties					**Loadings**
Type	2				
cgs (in.)	4				
h (in.)	22.5				
d_p (in.)	18.50				
d' (in.)	2.00				
b_w (in.)	3				
w_d (k/ft)	0.110				
w_l (k/ft)	0.000				
P (kips)	80.730	80.730			
A_g (in^2)	105.75				
A_{ps} (in^2)	0.434				
L (ft) supports	9		**Simplified Shear**		
l_c (ft)	3.083333333		V_c (kips)	41.43	
a (ft)	3.083333333		V_{min} (kips)	8.60	
b (ft)	5.92		V_{max} (kips)	21.50	
V_{de} (kips)	0		**Detailed Shear**		
$V_{d(-support)}$ (kips)	0.99140625		V_{ci} (kips)	33.02	
$V_{d(+support)}$ (kips)	0.991		$V_{ci,min}$ (kips)	7	
V_{dc} (kips)	-0.340		V_{cw} (kips)	27.1	
M_{dc} (k-ft)	-0.523624674		**Final**		
V_{ue} 1 (kips)	53.0725		V_c (kips)	27.13	
V_{ue} 2 (kips)	27.6575		V_s (kips)	30.525	
V_{uc} (kips)	52.73285156250		V_n (kips	57.65	
M_{cu} (k-ft)	163.1165837		ϕV_n (kips)	43.23984	
V_i (kips)	53.073		M_n (k-ft)	163.6411	
M_{max} (k-ft)	163.6402083				

7.3   Bridge Site Visits

The following sections provide a detailed discussion of each site visit, and photos representative of observations for each entire bridge. Each photo includes a reference location within the bridge based on the numbering system described in the Methodology section. The bridges are listed in order of superstructure rating, from best to worst, and organized by ODOT field division.

7.3.1 Field Division No. 1

Field Division No. 1 (Figure 107), located in eastern Oklahoma, includes Adair,

Cherokee, Haskell, McIntosh, Muskogee, Okmulgee, and Wagoner counties. The

Division's headquarters is in Muskogee, and as of

January 30, 2016, Mr. Darren A. Saliba is the

Division Engineer.
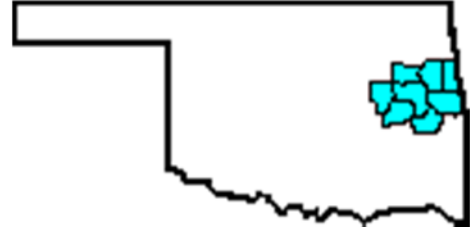
Figure 107. Field Division 1 Jurisdiction[2]

On April 17, 2015, four bridges were visited in Field Division No. 1, as detailed below.

7.3.1.1 NBI# 24219, Indian Nation Turnpike & Co. Rd. E1095, Okmulgee County

This bridge was built in 1965, and is maintained by the Oklahoma Turnpike Authority.

For this bridge, located at Indian Nation Turnpike (under[3]) & Co. Rd. E1095, the

superstructure rating is 8, or very good condition.

The following highlights some key findings at this site:

- Bearing plates are expanding, and corroding (Figure 108 and Figure 109)

---

[2] http://www.odot.org/flddiv1/images/flddiv1.gif
[3] For future reference, the first descriptor in the bridge's location, is the feature that is "under."

Figure 108. Example of corroding bearing plate (2W-S)

Figure 109. Another example of a corroding bearing plate (3W-S)

- Horizontal crack at 4W-S flange/web interface; and vertical crack (Figure 110 and Figure 111)
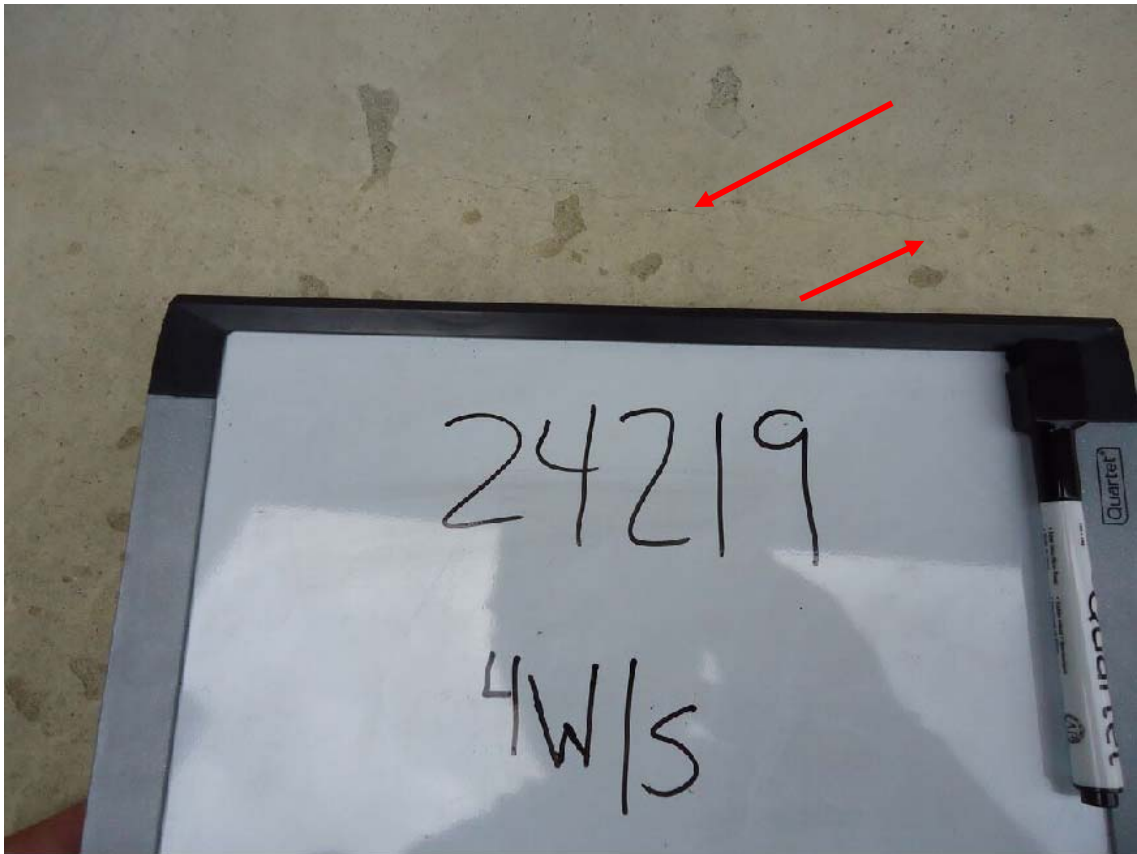
Figure 110. Horizontal Crack at Flange/Web Interface[4](4W-S)

---

[4] Some pictures will be exaggerated in size to clearly show the small feature of interest, that otherwise would likely be unnoticeable.
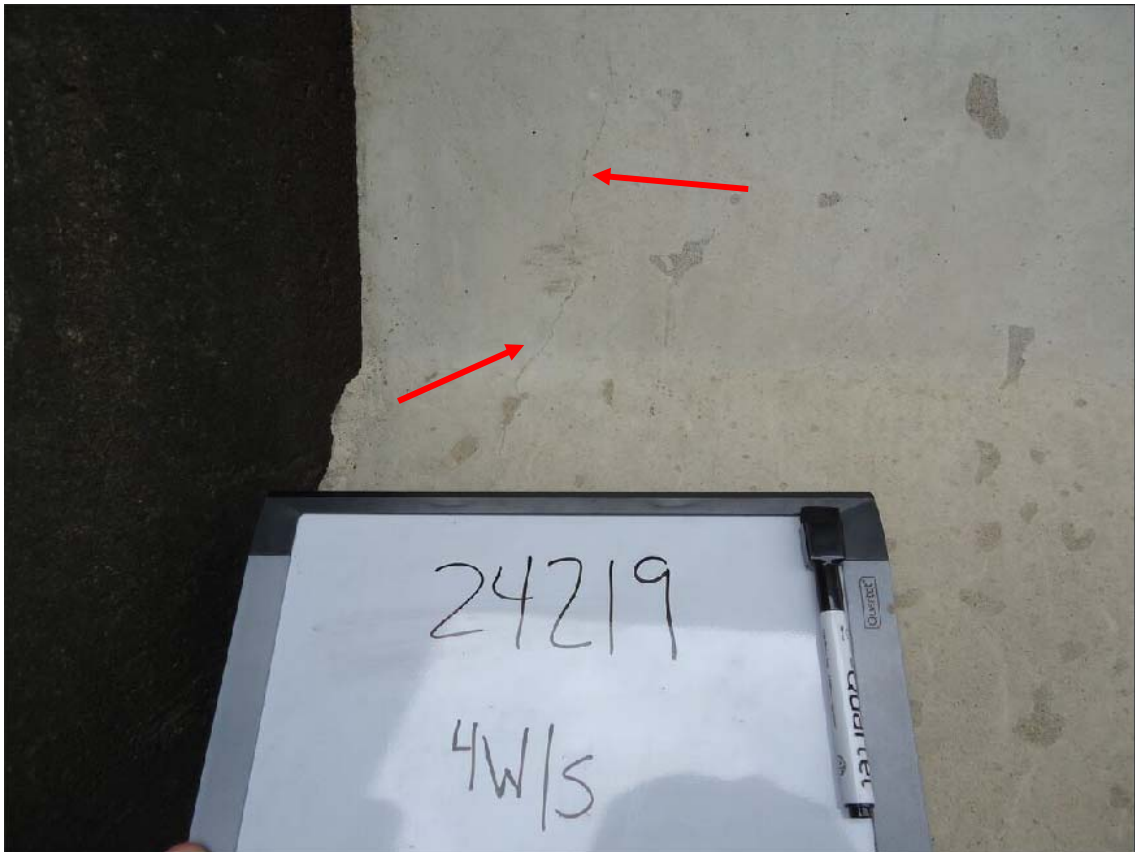
Figure 111. Vertical Crack from web through flange (4W-S)

7.3.1.2   NBI# 19214, S.H. 150 & U.S. 69 SB, McIntosh County

This bridge was built in 1976, and is maintained by ODOT. The superstructure rating is

7, or good condition. The following highlights some key findings at this site:

- Corroded anchor bolts (Figure 112)

Figure 112. Corroded anchor bolt (1S-W)

- Underside of bridge deck corroded with exposed rebar (Figure 113)

Figure 113. Exposed rebar, showing insufficient concrete cover at end of bridge deck (1N-W)

- Example of concrete repair work likely to prevent further spalling of the

  concrete (Figure 114). The repair seems to consist of mortar added to the surface

  of the existing girder end.

Figure 114. Repaired concrete on girder end and corroded bolt (1S-W)

7.3.1.3   NBI# 19215, S.H. 150 & U.S. 69 NB, McIntosh County

The bridge was built in 1976, and is maintained by ODOT. The superstructure rating is
7, or good condition. The following highlights some key findings at this site:

- Diagonal cracking on the web of the beam (Figure 115 and Figure 116)

Figure 115. Diagonal cracking on the web of the beam (3N-W)

Figure 116. Diagonal cracking on the web of the beam, heading towards the bottom flange (1S-W)

- Repair to spalled back corner likely to prevent further spalling of the girder end (Figure 117).

Figure 117. Repair to spalled back corner (6N-W)

7.3.1.4   NBI# 15804, I-40 & Lotahwatah Rd. N41, McIntosh County

The bridge was built in 1963, and is maintained by ODOT. The superstructure rating is 5, or fair condition. The following highlights some key findings at this site:

- Back concrete diagonal crack in the beam (Figure 118)

Figure 118. Back diagonal crack in the beam end (3N-E)

- Separation at diaphragm and girder (Figure 119)

Figure 119. Separation at the diaphragm and girder end (1N-W)

7.3.2 Field Division No. 2

Field Division No. 2 (Figure 120), located in southeastern Oklahoma, includes Atoka,

Bryan, Choctaw, Latimer, Le Flore, McCurtain, Marshall, Pittsburg, and Pushmataha

counties. The Division's headquarters is in

Antlers, and as of January 30, 2016, Mr. Anthony

Echelle is the Division Engineer.
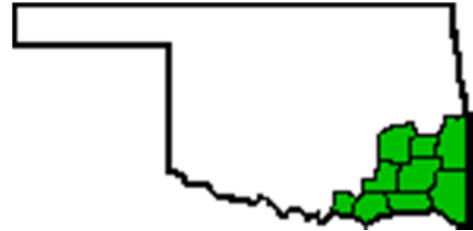
Figure 120. Field Division 2 Jurisdiction[5]

On March 21, 2015, four bridges were visited in Field Division No. 2, as detailed

below.

7.3.2.1   NBI# 18554, S.H. 78 & U.S. 69 SB, Bryan County

The bridge was built in 1973, and is maintained by ODOT. The superstructure rating is

8, or very good condition. The following highlights some key findings at this site:

- Diagonal back corner cracking/spalling in the beam (Figure 121 and Figure 122)

Figure 121. Spalled back corner of beam end (1W-S)

---

[5] http://www.odot.org/flddiv2/images/flddiv2.gif

Figure 122. Spalled back corner of beam end (4E-N)

- Cracking and spalling at pipe interface with exterior of concrete girder (Figure
  123). It was not immediately clear the purpose of the pipe (e.g., drainage pipe,
  hole for diaphragm connection).

Figure 123. Crack from interior pipe that runs through web of beam (4E-N)

- Diaphragm deterioration, exposed rebar showing corrosion (Figure 124)

Figure 124. Deterioration of an interior diaphragm (6W-N); the diaphragm connects two interior beam ends

7.3.2.2   NBI# 18555, S.H. 78 & U.S. 69 NB, Bryan County

This bridge was built in 1973, and is maintained by ODOT. The superstructure rating is 8, or very good condition. The following highlights some key findings at this site:

- Spalling at pipe interface with exterior of concrete girder (Figure 125)

Figure 125. Spalling around pipe interface with exterior of concrete girder (3E-N)

- Heavily deteriorated anchor bolts (Figure 126 and Figure 127)

Figure 126. Anchor bolt with extreme deterioration, with necking of the anchor bolt at the top (4E-S)

Figure 127. Close-up of deterioration of anchor bolt, with necking at the top (4E-S). The pen is shown in the picture to illustrate the amount of necking occurring to the steel member.

- Diagonal cracks from top flange/web interface towards pipe (Figure 128)

Figure 128. Diagonal cracks from top flange/web interface towards pipe on interior beam (5W-N)

- Back corner diagonal cracking in beam (Figure 129)

Figure 129. Back corner diagonal cracking of beam end (5W-S)

7.3.2.3 NBI# 17536, U.S. 271 & Indian Nation Turnpike, Pushmataha County

The bridge was built in 1969, and is maintained by the Oklahoma Turnpike Authority.

The superstructure rating is 7, or good condition. The following highlights some key

findings at this site:

- Spalling above support of corroding bearing plate, minor spalling horizontally

    along base of girder, and cracking emanating from spalling location (Figure 130,

    Figure 131, and Figure 132)

Figure 130. Spalling above corroded support of exposed, exterior girder (1E-N)

Figure 131. Corroded bearing plate (1E-S)

Figure 132. Diagonal crack in bottom flange of beam from corroding support (10W-N)

146

- Spalled back corner of girder and exposed prestressing strand ends (Figure 133)

Figure 133. Spalled back corner and exposed prestressing strands

This bridge was built in 1965, and is maintained by the Oklahoma Turnpike Authority. The superstructure rating is 5, or fair condition. The following highlights some key findings at this site:

- Bottom of girders with exposed and deteriorating rebar and/or prestressing strands (Figure 134 and Figure 135)

Figure 134. Exposed rebar due to spalled concrete on the bottom of an exposed, exterior girder (1N-E)

Figure 135. Exposed rebar due to spalled concrete (1N-W)

- Horizontal cracking along top flange/web interface (Figure 136)

Figure 136. Crack along intersection of the top flange and web

- Extremely corroded bearing plates (Figure 137)

Figure 137. Corroded, and deteriorated bearing plate (8N-E)

- Cracking near concrete/corroded bearing plate interface (Figure 138)

Figure 138. Cracking from corroded bearing plate into bottom flange (10S-W)

7.3.3   Field Division No. 3

Field Division No. 3 (Figure 139), located in central Oklahoma, includes Cleveland,

Coal, Garvin, Hughes, Johnston, Lincoln, McClain, Okfuskee, Pontotoc, Pottawatomie,

and Seminole counties. The Division's

headquarters is in Ada, and as of January 30,

2016, Mr. Kevin Bloss is the Division Engineer.
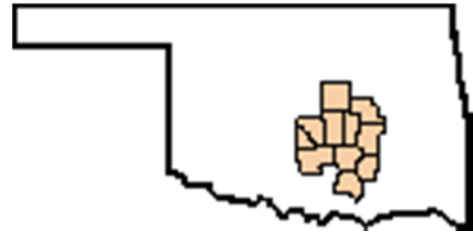
Figure 139. Field Division 3 Jurisdiction[6]

There was only one bridge that fell within the specified criteria, and that bridge was not

inspected.

---

[6] http://www.odot.org/flddiv3/images/flddiv3.gif

7.3.4   Field Division No. 4

Field Division No. 4 (Figure 140), located in northcentral Oklahoma, includes

Canadian, Garfield, Grant, Kay, Kingfisher, Logan, Noble, Oklahoma, and Payne

counties. The Division's headquarters is in Perry,

and as of January 30, 2016, Mr. Brian Taylor is

the Division Engineer.

Figure 140. Field Division 4 Jurisdiction[7]

On October 24, 2015, three bridges were visited in Field Division No. 4, as detailed

below.

7.3.4.1   NBI# 18497, Cimarron Turnpike & Co. Rd N3340, Pawnee County

This bridge was built in 1973, and is maintained by the Oklahoma Turnpike Authority.

The superstructure rating is 7, or good condition. The following highlights some key

findings at this site:

- Corroded bearing plate and resulting spalling above the support (Figure 141)

---

[7] http://www.odot.org/flddiv4/images/flddiv4.gif

Figure 141. Corroded bearing plate, and spalling along bottom of girder and back of girder end (3S-W)

- Spalling above the support and at back of girder (Figure 142)

Figure 142. Corroded anchor bolt and spalling along bottom of girder and girder end (5N-E)

This bridge was built in 1975, and is maintained by the Oklahoma Turnpike Authority.

The superstructure rating is 7, or good condition. The following highlights some key

findings at this site:

- Serious deterioration of girder and back wall due to moisture/water (Figure 143

   and Figure 144)

Figure 143. Extreme deterioration of back wall and girder end due to moisture/water (1E-N). The exposed, exterior girder has a corroded bearing plate and spalling occurring at the girder end.

Figure 144. Vertical cracking with visible corrosion on exterior, exposed girder (12E-S)

- Back corner spalled and prestressing strands exposed (Figure 145 and Figure 146)

Figure 145. Exposed prestressing strands of an exposed, exterior girder (1W-N)

Figure 146. Exposed prestressing strands (10W-N)

- Exposed prestressing strands and expanded, ("flaky") bearing plates (Figure 147)

Figure 147. Corroded and flaky bearing plate, not providing much functionality as original designed (1W-S)

- Heavily corroded and broken anchor bolt (Figure 148)

Figure 148. Corrosion at cavity of abutment and bolt interface (7E-S)

157

- Spalling above corroded bearing plates and missing anchor bolts (Figure 149)

Figure 149. Spalling above corroded bearing plate, missing anchor bolt (10E-S)

- Back corner diagonal cracking of beam end (Figure 150)

Figure 150. Back corner diagonally cracked on beam end (11W-S)

This bridge was built in 1978, and is maintained by ODOT. The superstructure rating is 6, or satisfactory condition. The following highlights some key findings at this site:

- Spalling and cracking at pipe in the web (Figure 151)

Figure 151. Spalling and cracking above pipe in web (1N-E)

- Diagonal crack in web towards bottom of girder from top of beam (Figure 152)

Figure 152. Diagonal crack in web from top flange towards bottom of beam (1N-W)

- Corroding anchor bolts (Figure 153)

Figure 153. Corroding anchor bolt (4S-E)

7.3.5　Field Division No. 5

Field Division No. 5 (Figure 154), located in southwestern Oklahoma, includes

Beckham, Blaine, Custer, Dewey, Greer, Harmon, Jackson, Kiowa, Roger Mills,

Tillman, and Washita counties. The Division's

headquarters is in Clinton, and as of January 30,

2016, Mr. Brent Almquist is the Division

Engineer.
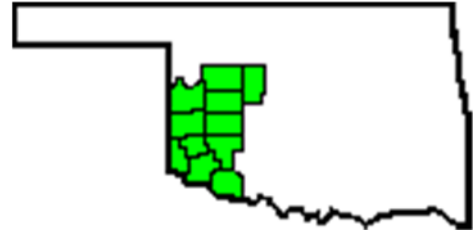
Figure 154. Field Division 5 Jurisdiction[8]

There was only one bridge that fell within the specified criteria, and that bridge was not

inspected.

7.3.6　Field Division No. 6

Field Division No. 6 (Figure 155), located in northwestern Oklahoma (the Panhandle),

includes Alfalfa, Beaver, Cimarron, Ellis, Harper, Major, Texas, Woods, and

Woodward counties. The Division's headquarters

is in Buffalo, and as of January 30, 2016, Mr. Ron

McDaniel is the Division Engineer.

Figure 155. Field Division 6 Jurisdiction[9]

There were no bridges that fell within the specified criteria. Interestingly, the vast

majority of bridges on the western side of the state (Divisions No. 5 and 6) were steel

bridges, as opposed to concrete bridges.

---

[8] http://www.odot.org/flddiv5/images/flddiv5.gif
[9] http://www.odot.org/flddiv6/images/flddiv6.gif

7.3.7 Field Division No. 7

Field Division No. 7 (Figure 156), located in southcentral Oklahoma, includes Caddo,

Carter, Comanche, Cotton, Grady, Jefferson, Love, Murray, and Stephens counties. The

Division's headquarters is in Duncan, and as of

January 30, 2016, Mr. Jay Earp is the Division

Engineer.

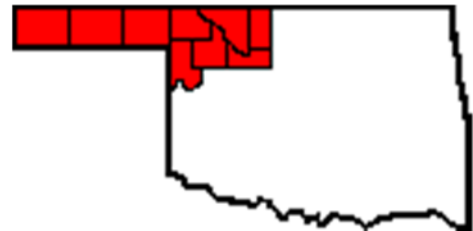*Figure 156. Field Division 7 Jurisdiction[10]*

On February 21, 2015, five bridges were visited in Field Division No. 7, as detailed

below.

7.3.7.1   NBI# 18793, UP R.R. & U.S. 62, Grady County

This bridge was built in 1963, and is maintained by ODOT. The superstructure rating is

8, or very good condition. The following highlights some key findings at this site:

- Back corner diagonal cracking (Figure 157)

Figure 157. Back corner diagonal crack of exposed, exterior beam (1E-N)

- Spalling above corroding bearing plate (Figure 158)

Figure 158. Corroded bearing plate and anchor bolt, with spalling above the support (5E-S)

- Back corner spalling (Figure 159)

Figure 159. Back corner spalling of girder (9E-S)

7.3.7.2 NBI# 18494, U.S. 81 & S.H. 7 EB, Stephens County

This bridge was built in 1973, and is maintained by ODOT. The superstructure rating is 8, or very good condition. The following highlights some key findings at this site:

- Back corner diagonal cracking (Figure 160 and Figure 161)

Figure 160. Back corner diagonal cracking of exterior beam (1E-S)

Figure 161. Similar back corner cracking (deformation) (2E-S)

- Spalling above corroded bearing plates (Figure 162)

Figure 162. Spalling above the corroded bearing plate (1W-N)

- Separation at diaphragm and girder interface (Figure 163)

Figure 163. Vertical separation of diaphragm and girder at interface (5E-S)

165

- Spalling and cracking at corroded bearing plate (Figure 164 and Figure 165)

Figure 164. Corroded bearing plate and anchor bolt, with spalling and cracking above the corroded bearing plate (5W-N)

Figure 165. Spalling girder end and corroded bearing plate (5W-S)

This bridge was built in 1963, and is maintained by ODOT. The superstructure rating is 7, or good condition. The following highlights some key findings at this site:

- Back corner spalled and exposed vertical rebar (Figure 166)

Figure 166. Exposed vertical rebar due to spalled girder end of exposed, exterior beam (1W-N)

- Concrete spalled off at diagonal crack on back corner (Figure 167)

Figure 167. Back corner diagonal crack with a width at the base of approximately three inches (2E-N)

- Spalling at diaphragm and girder interface (Figure 168)

Figure 168. Spalling at diaphragm and girder interface (3W-N)

The bridge was built in 1973, and is maintained by ODOT. The superstructure rating is 7, or good condition. The following highlights some key findings at this site:

- Heavily corroded bearing plate, anchor bolt, and nut; with spalling above support (Figure 169)

Figure 169. Corroded bearing plate, bolt, and nut along with spalling above the support of an exposed, exterior girder (1E-N)

- Corroded bearing plate and diagonal cracking at back corner (Figure 170 and Figure 171)

Figure 170. Corroded bearing plate and diagonal back corner crack with a maximum width of approx. four inches

Figure 171. Corroded bearing plate and diagonal back corner crack with a maximum width of approx. five inches (2W-N)

- Corroded, flaky bearing plate (Figure 172 and Figure 173)

Figure 172. Corroded, flaky bearing plate

Figure 173. Corroded, flaky bearing plate

- Vertical crack at back corner of girder and diaphragm interface (Figure 174)

Figure 174. Vertical crack along interface of girder end and diaphragm (1W-S)

7.3.7.5   NBI# 18582, U.P. R.R./7th St. & S.H. 7 EB, Stephens County

This bridge was built in 1973, and is maintained by ODOT. The superstructure rating is 7, or good condition. The following highlights some key findings at this site:

- Exposed rebar and corroded bearing plate (Figure 175)

Figure 175. Exposed rebar, corroded, flaky bearing plate, and spalling of concrete (5E-N)

- Vertical cracks near the top flange and web intersection in the beam (Figure 176)

Figure 176. Crack along the web of girder (5E-S)

- Diagonal back corner spalling and exposed, corroded prestressing strands

  (Figure 177)

Figure 177. Diagonal back corner spalling and exposed prestressing strands (5W-S)

- Corroded bearing plate and spalling back corner (Figure 178)

Figure 178. Corroded bearing plate, exposed rebar, and spalled back corner of girder (5W-S)

7.3.8 Field Division No. 8

Field Division No. 8 (Figure 179), located in northeastern Oklahoma, includes Craig,

Creek, Delaware, Mayes, Nowata, Osage, Ottawa, Pawnee, Rogers, Tulsa, and

Washington counties. The Division's headquarters

is in Tulsa, and as of January 30, 2016, Mr.

Randle White is the Division Engineer.

Figure 179. Field Division 8 Jurisdiction[11]

On October 17, 2015, three bridges were visited in Field Division No. 8, as detailed

below.

7.3.8.1   NBI# 18768, BNSF R.R./Co Rd & S.H. 167, Rogers County

This bridge was built in 1974, and is maintained by ODOT. The superstructure rating is

8, or very good condition. The following highlights some key findings at this site:

- Horizontal crack at top flange and web intersection for about a foot from beam
  and diaphragm interface (Figure 180 and Figure 181)

---

[11] http://www.odot.org/flddiv8/images/flddiv8.gif

Figure 180. Horizontal crack at top flange and web interface for about one foot into the beam (1S-E)

Figure 181. Horizontal crack at top flange and web interface for about one foot into the beam (5S-E)

- Corroded and necking anchor bolt and bearing plate covered with a protective coating (i.e. paint coating) (Figure 182 and Figure 183)

Figure 182. Anchor bolt and bearing plate coated (1S-E)

Figure 183. Necked anchor bolt and bearing plate both deteriorated and coated (2S-E)

- Crack at girder and diaphragm intersection (Figure 184)

Figure 184. Crack at girder and diaphragm intersection (1S-W)

- Cracking in the back corner of the diaphragm (Figure 185, Figure 186, and

  Figure 187)

Figure 185. Back diagonal and vertical crack in girder end (2N-W)

Figure 186. Diagonal crack at back corner of girder end (2S-W)

Figure 187. Diagonal crack in back corner of girder end (4N-E)

7.3.8.2 NBI# 18076, S.H. 20 & U.S. 75 SB, Tulsa County

This bridge was built in 1971, and is maintained by ODOT. The superstructure rating is 5, or fair condition. The following highlights some key findings at this site:

- Vertical crack at girder/diaphragm intersection (Figure 188 and Figure 189)

Figure 188. Vertical crack at girder/diaphragm interface (1N-W)

Figure 189. Vertical crack at bottom flange and diaphragm interface (3N-E)

- Spalling at girder/diaphragm intersection (Figure 190)

Figure 190. Exposed rebar, back corner spalled (2S-W)

- Diagonal cracking from top flange/web intersection towards end of the beam (Figure 191 and Figure 192)

Figure 191. Diagonal crack from top flange and web interface (2S-W)

Figure 192. Diagonal crack from top flange and web interface

- Underside corrosion on diaphragm between girders (Figure 193 and Figure 194)

Figure 193. Corrosion and deterioration of underside of diaphragm

Figure 194. Similar corrosive underside of diaphragm, with exposed rebar cage

7.3.8.3   NBI# 18077, S.H. 20 & U.S. 75 NB, Tulsa County

This bridge was built in 1971, and is maintained by ODOT. The superstructure rating is 5, or fair condition. The following highlights some key findings at this site:

- Cracking along top flange/web intersection, as well as cracks emanating from this region and going towards the flange of the beam (Figure 195 and Figure 196)
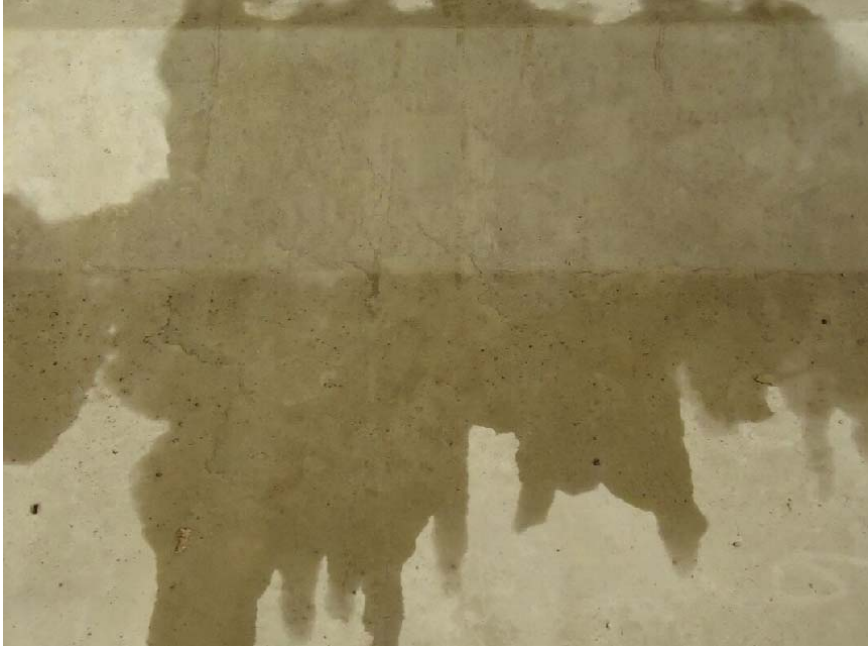
Figure 195. Horizontal crack along top flange and web interface (3N-E)

Figure 196. Diagonal crack from top flange and web intersection going further into the web (5N-W)

- Diagonal back corner spalling and exposed prestressing strands (Figure 197)

Figure 197. Diagonal back corner spalling of diaphragm and exposed prestressing strands (5S-W)

7.4 FHWA's Recording and Coding Guide for the Structure Inventory and Appraisal of the Nation's Bridges

Superstructure Condition Ratings

N   NOT APPLICABLE

9   EXCELLENT CONDITION

8   VERY GOOD CONDITION - no problems noted.

7   GOOD CONDITION - some minor problems.

6   SATISFACTORY CONDITION - structural elements show some minor deterioration.

5   FAIR CONDITION - all primary structural elements are sound but may have minor section loss, cracking, spalling or scour.

4   POOR CONDITION - advanced section loss, deterioration, spalling or scour.

3   SERIOUS CONDITION - loss of section, deterioration of primary structural elements. Fatigue cracks in steel or shear cracks in concrete may be present.

2   CRITICAL CONDITION - advanced deterioration of primary structural elements. Fatigue cracks in steel or shear cracks in concrete may be present or scour may have removed substructure support. Unless closely monitored it may be necessary to close the bridge until corrective action is taken.

1   "IMMINANT" FAILURE CONDITION - major deterioration or section loss present in critical structural components or obvious vertical or horizontal movement affecting structure stability. Bridge is closed to traffic but corrective action may put it back in light service.

0   FAILED CONDITION - out of service; beyond corrective action.

99 Miscoded Data